A TEST OF HOST-TAXON, ENVIRONMENT, AND DISTANCE EFFECTS ON LEAF FUNGAL ENDOPHYTES IN *METROSIDEROS* ON THE ISLAND OF O‘AHU

A THESIS SUBMITTED TO THE GRADUATE DIVISION OF THE UNIVERSITY OF HAWAI‘I AT HILO IN PARTIAL FULFILLMENT OF THE REQUIREMENTS FOR THE DEGREE OF

MASTER OF SCIENCE

IN

TROPICAL CONSERVATION BIOLOGY AND ENVIRONMENTAL SCIENCE

DECEMBER 2019

By

Gary L. Sur

Thesis Committee:

Dr. Rebecca Ostertag, Chairperson
Dr. Jolene Sutton, Primary Advisor
Dr. Scott Geib
Dr. Elizabeth Stacy

Acknowledgments

First and foremost, I want to thank my primary advisor, Dr. Elizabeth Stacy, for her steadfast guidance, inspiration, and support throughout the course of this project. Her tireless efforts helped me overcome many seemingly insurmountable challenges, and encouraged me to become a better researcher. Additionally, I thank the members of my thesis committee Dr. Rebecca Ostertag, Dr. Jolene Sutton, and Dr. Scott Geib for their contributions in developing this project, providing lab supplies, equipment, and recommendations that were vital for this project. I thank the National Science Foundation CREST (Centers of Research Excellence in Science and Technology) grant and University of Hawai‘i at Hilo for funding this project. I also thank Doreen Koizumi for her assistance in procuring supplies, reagents, and sequencing services. Special thanks are owed to Dr. Stacy, Jennifer Johansen, and Tomoko Sakishima for collecting and storing all *Metrosideros* leaf samples from O‘ahu and to Anne Veillet, Renee Corpuz, and Tomoko Sakishima for their invaluable help towards completing my DNA extractions, PCRs, and library preparation. I am grateful to Audra McKinzie of ThermoFisher Scientific, and DC3 Therapeutics LLC for their Ion Torrent sequencing service. Demultiplexing and filtering of the DNA sequences and bioinformatic analyses would not have been possible without the significant efforts and patience of Dr. Geoffrey Zahn, to whom I am extremely grateful. Thanks are also owed to Dr. Naupaka Zimmerman, Dr. Karla McDermid, Deborah Beirne, Erin Datlof, Blaine Luiz, Chris Yakym, and Ron Kittle for their helpful advice with lab methods or bioinformatics and to Dr. Anthony Amend for his correspondence on factors that can influence leaf fungal communities. Finally, I thank the TCBES program, the UH Hilo Core Genetics Facility, and the U.S. Pacific Basin Agricultural Research Center for providing resources and equipment for this project.

Abstract

Tree fungal endophyte (FE) communities may be influenced not only by abiotic environmental conditions, but also by varying degrees of affinity to their host plants. The landscape-dominant woody genus *Metrosideros* (Myrtaceae) comprises many morphologically distinct taxa that occupy different habitats throughout the Hawaiian Islands. This study used *Metrosideros* on O‘ahu to test the relative importance of environment versus host taxon on FE composition and diversity. Variation in FE communities due to geographic distance (across and within sites) was also examined. From each of four elevation gradients (sites), leaves were collected from four *Metrosideros* taxa, two sympatric taxa occurring at high elevations, representing a wetter and slightly cooler environment, and two sympatric taxa occurring at lower elevations, representing a drier and slightly warmer environment (11 trees/taxon/gradient, n = 176 trees). DNA was extracted from surface-sterilized leaf samples. Fungal DNA was amplified using barcoded internal transcribed spacer (ITS) forward and reverse primers, and the barcoded amplicons underwent next-generation sequencing (IonTorrent). The sequences were filtered in R, using RStudio and bioinformatically processed with the *vegan* and *dada2* packages. The remaining samples (n = 113 trees) yielded 1,637 unique ESVs (exact sequence variants). Permutation tests, diversity indices, and Akaike information criterion models revealed that variation in FE diversity was significantly explained by *Metrosideros* taxon, site, and geographic distance. Non-metric multidimensional scaling (NMDS) plots showed considerable overlap in FE communities among host taxa and among sites, however, and evidence for host-specificity of leaf FEs was weak and restricted to 700-1,000 m above sea level. FE communities did not vary with elevation (environment); however, the elevation ranges examined may be too narrow for the detection of elevation/environmental effects. Lastly, a significant pattern of isolation by distance on FE

community composition was detected across the island as well as within each of the four sites. These results suggest that within O‘ahu *Metrosideros*, leaf FE communities vary in diversity and composition across space, some of this variation is associated with host taxonomic effects and distance, and very little is associated with environmental variation across the island`s elevation gradients.

Table of Contents

Acknowledgements ..... **i**

Abstract ..... **ii**

List of Tables ..... **vii**

List of Figures ..... **viii**

INTRODUCTION **1**

Host-Specificity **3**

Leaf Pubescence and Fungal Communities **4**

Environmental Effects on Leaf FEs **5**

Isolation by Distance in FE Communities **7**

DNA Barcoding of FEs **7**

Shift to Exact Sequence Variants **8**

Tree Genus *Metrosideros* **10**

Hawaiian *Metrosideros* **10**

Leaf FEs in Hawaiian *Metrosideros* **12**

HYPOTHESES **15**

METHODS **17**

Study System **17**

Sample Collection **17**

Surface Sterilization **18**

DNA Extraction **19**

Amplification and Sequencing **19**

Polymerase Chain Reaction (PCR) 20

PCR Purification and Dilution 20
Library Synthesis and Sequencing 21
Bioinformatics 22
Raw Sequence Demultiplexing 22
ITSxpress 22
ESV Filtering and Statistical Analyses 23
FE Richness and Relative Abundance (H_{1A}, H_{1B}, H_3) 24
FE Community Dissimilarity (H_{1A}, H_2, H_3) 25
Isolation by Distance (H_3) 25
Shannon Diversity (H_{1A}, H_{1B}, H_2, H_3) 26
Host-Specificity (H_{1A}) 26
RESULTS 28
Amplification and Sequencing 28
Bioinformatics 29
Taxonomy and Richness of FEs 29
Beta Diversity (H_{1A}, H_2, H_3) 30
Isolation by Distance (H_3) 31
Alpha Diversity (H_{1A}, H_{1B}, H_2, H_3) 32
Detection of Host-Specific FEs (H_{1A}) 32
DISCUSSION 34
Composition of FE Taxa in Oʻahu *Metrosideros* 34
Host-Taxon Effects on FE Composition (H_{1A}) 36
Host-Specificity of FEs (H_{1A}) 38

Leaf Type Effects on FE Composition (H_{1B}) 39

Site and Isolation-by-Distance Effects on FE Composition (H_3) 40

Environmental Effects on FE Composition (H_2) 42

Unknown Functions of *Metrosideros* FEs 44

CONCLUSIONS 46

TABLES & FIGURES 47

APPENDIX A: Kruskal-Wallis Test (H_{1A}) 79

APPENDIX B: Supplementary Figures 80

LITERATURE CITED 85

List of Tables

Table 1. Traits of eight *Metrosideros* taxa on O‘ahu 47

Table 2. Barcoded forward ITS-1F primers and reverse ITS-2R primers 48

Table 3. Sampling details, taxon code, site, and primers 49

Table 4. Quantity of successfully amplified and bioanalyzed samples 54

Table 5. Quality-control trimming of demultiplexed samples 55

Table 6. PermANOVA for Bray-Curtis dissimilarity 56

Table 7. Best-fit AICs of Shannon diversity 56

Table 8. Shannon diversity model selections with elevation and host taxon 56

Table 9. Shannon diversity model selections with leaf type, host taxon, and site 56

Table 10. Shannon diversity model selections without taxon 57

Table 11. Shannon diversity ANOVA 57

Table 12. Prevalence of host-specific fungi ANOVA 57

Table 13. List of five fungal phyla 57

Table 14. List of 20 fungal classes 58

Table 15. List of 58 fungal orders 59

List of Figures

Figure 1. Sampling sites on the Island of O‘ahu 61

Figure 2. Mean annual rain map of the Island of O‘ahu 62

Figure 3. Internal transcribed spacer 63

Figure 4. BluePippin electropherogram of purified samples 63

Figure 5. Bioanalyzer electropherogram of library 64

Figure 6. Location of samples at Mt. Ka‘ala and ‘Aiea Ridge 65

Figure 7. Elevation profiles of all sites 66

Figure 8. PCA biplot of FE relative abundance for each sample 67

Figure 9. Rarefaction curves of FE absolute abundance for each sample 68

Figure 10. Comparison of FE relative abundance at high or low elevation 69

Figure 11. Comparison of FE relative abundance among sites 70

Figure 12. Comparison of FE relative abundance among host taxa 71

Figure 13. Relative abundance of FE phyla and classes among four sites 72

Figure 14. Relative abundance of FE phyla and classes among host taxa 73

Figure 15. Mantel test histograms for each site and among all sites 74

Figure 16. NMDS plot of leaf type and host taxon 75

Figure 17. NMDS plot of leaf type and site 76

Figure 18. Shannon diversity box plots for each host taxon 77

Figure 19. Host-specificity and elevation 78

Figure S1. FE richness among eight *Metrosideros* taxa on O‘ahu 80

Figure S2. Mean FE richness/adult/site on O‘ahu Island 81

Figure S3. Shannon diversity values per site 82

Figure S4. Relationship between elevation and Shannon diversity 83

Figure S5. Relationship between mean annual rainfall and Shannon diversity..... 84

INTRODUCTION

FEs are microbial fungi that dwell within plant tissues (Griffin & Carson 2018), and they have been found in every plant species examined (Sieber 2007; Rodriguez et al. 2009). Modern FEs originated from terrestrial fungi that emerged about 720 million years ago (Ma) among the first land embryophytes (Pirozynski & Malloch 1975; Lutzoni et al. 2018), with the first true FEs appearing 590-467 Ma (Lutzoni et al. 2018). Having evolved 595-558 Ma (Lutzoni et al. 2018), over 95% of FEs belong to the oldest phylum Ascomycota (Arnold et al. 2009). The other major FE phylum Basidiomycota may have emerged 481-452 Ma as embryophytic diversity increased (Lutzoni et al. 2018). After the appearance of more complex angiosperms (300 Ma) (Sieber 2007), FEs further diversified into taxa that had greater tolerance of, or became more pathogenic to, their host plants (Saikkonen et al. 2004; Saikkonen 2007; Pumplin & Voinnet 2013).

FEs may be host-specific or generalists, pathogens or mutualists (Zhou & Hyde 2001; Saikkonen 2007). Often considered harmless or beneficial to plants (Petrini 1991; Zhou & Hyde 2001; Arnold et al. 2003; Saikkonen 2007; Porras-Alfaro & Bayman 2011), FEs in fact exist along a spectrum of mutualism/pathogenicity in relation to their plant hosts (Wilson 1995). Single mutations (Redman et al. 1999), interactions between endemic plants and nonnative FEs (Sieber 2007; Cleary et al. 2016), and climatic changes (Morrica & Ragazzi 2008) can convert previously benign FEs into pathogenic fungi. Moreover, within a single tree species, cohabiting benign and pathogenic FEs can contribute to different outcomes. *Theobroma cacao* trees inoculated with host-specific FEs suffered 7.1% less leaf loss from a pathogenic *Phytophora* mold than sterilized endophyte-free plants (Arnold et al. 2003). However, Christian et al. (2019) observed in *T. cacao* trees that nitrogen uptake and biomass were highest when the trees were coinfected with the beneficial FE *Collectotrichum tropicale* and the pathogenic FE *Phyotphora*

palmivora. Hence, labeling FEs as simply beneficial might wrongly conceal their full impact upon forest health (Griffin & Carson 2018).

There are about 120,000 named fungal operational taxonomic units (OTUs) (Hawksworth & Lücking 2017). The OTU concept of clustering DNA sequences together by a chosen similarity threshold (usually at 97% similarity) to define individual species compensates for the frequent absence of other biological information (e.g., morphology, life cycle, host-interactions) in fungi identified only through sequencing (Schloss et al. 2009; Lanzén 2013; Westcott & Schloss 2015; Callahan et al. 2017; Raja et al. 2017; Knight et al. 2018). Still, global estimates for the number of fungal OTUs remain controversial. A long-held conservative estimate of 1.5 million fungal OTUs (Hawksworth 1991; Hawksworth 2001) led to an estimate of ~1.3 million OTUs based on an anticipated ratio of host-specific fungal OTUs to plants 1.6:1 (Dreyfuss & Chapela 1994). Hawksworth (2001) later reset the ratio of host-specific fungal OTUs to plants from 1.6:1 to 186:1, but avoided altering the richness estimates in the absence of general agreement from other studies. However, since the advent of next-generation sequencing (NGS) to document unculturable fungi (Hawksworth 2012), current consensus supports a higher global richness estimate of 5.1 million fungal OTUs (O'Brien et al. 2005; Blackwell 2011; Hawksworth 2012). In a subsequent analysis of studies that split species complexes into multiple cryptic species, used newer ratios of plant to fungal taxa, used updated sequencing and field-based databases, or estimated the richness of unknown fungi from poorly studied biomes or biodiversity hotspots, Hawksworth and Lücking (2017) revised the global estimation downward to 2.2-3.8 million fungal OTUs. All of these competing estimates assume that <10% of all fungal OTUs have been named (Hawksworth & Lücking 2017), suggesting that the vast majority of fungal taxa (including FEs) on Earth remains unclassified.

Compared to fungi that inhabit grasses (i.e., clavicipitaceous FEs), less is known about non-clavicipitaceous leaf FEs in forest trees (Arnold et al. 2003; Rodriguez et al. 2009; Dickie et al. 2013; Griffin & Carson 2018; Terhonen et al. 2019). Leaf FEs may comprise a major fraction of unstudied fungal taxa (Porras-Alfaro & Bayman 2011), especially in tropical forests (Arnold & Lutzoni 2007; Porras-Alfaro & Bayman 2011; Suryanarayanan 2011). Yet some studies suggest that FE diversity is lower in tropical forests than in temperate forests (Cannon & Simmons 2002; Suryanarayanan et al. 2003). Regardless, recent studies of FE diversity in trees, especially studies of variation in FE community structure across host taxa and environments, are revealing nuanced mutualistic relationships.

Host-specificity

Evidence supports the presence of host-specific FEs in some tree species. Cuttings of Balsam poplar (*Populus balsamifera*) collected from seven geographically separate Alaskan regions maintained their native endophyte communities despite growing in the same common garden for several years (Bálint et al. 2013). Additionally, *Coffea arabica* growing in Hawai‘i, Puerto Rico, and Mexico kept the same two FE taxa transferred from their parent populations in Columbia (Vega et al. 2010). In Iran, four geographically distant mandarin (*Citrus reticulata*) populations were primarily colonized by the fungal orders Dothideomycetes and Sordariomycetes (Sadeghi et al. 2019). That *Citrus limon* is also dominated by the same fungal orders (Durán et al. 2005; Douanla-Meli et al. 2013) suggests that notable host-specificity has developed among certain FEs within the genus *Citrus* (Sadeghi et al. 2019). Host effects were insignificant, however, in a study of FE community composition in three pine species (*Pinus*

taeda, *P. virginiana*, and *P. echinata*) in the Eastern United States (Oono et al. 2014). Thus, host-specificity and host-taxonomic effects on FE diversity may be common, but not universal.

Different phytochemicals found in different plant species may selectively promote the growth of highly host-specific FEs over less host-specific FEs (Arnold et al. 2003; Christian et al. 2019). Arnold et al. (2003) studied FEs grown *in vitro* in *T. cacao* leaf extracts, finding that nine FEs commonly found in *T. cacao* leaves outcompeted other FEs. However, when those same nine FEs were transferred to other media besides that of *T. cacao*, they were less dominant than other FEs.

Host-specificity is also evident in the sharply contrasting relationships that individual FEs can have with closely related host species. The saprotrophic Manchurian FE *Hymenoscyphus fraxineus* is normally dormant within the healthy tissues of Manchurian ash trees (*Fraxineus mandshurica*), only expressing strong growth within senescing or dead leaves (Cleary et al. 2016). European ash (*F. excelsior*), however, suffers fatal *H. fraxineus* infections that develop into severe necrotic defoliation and bark cankers (Cleary et al. 2016). Similarly, the 19th and 20th centuries saw the introduction of Japanese chestnut trees (*Castanea crenata*) to North America (Anagnostakis & Hillman 1992). Asymptomatic *C. crenata* trees also introduced the FE *Cryphonectria parasitica*, the same chestnut blight that killed most endemic American chestnut (*C. dentata*) populations (Anagnostakis & Hillman 1992). Opportunistic infections highlight how closely related plant taxa may not only harbor different FE communities, but may also experience drastically dissimilar mortality rates with the same FEs.

Leaf Pubescence and Fungal Communities

High leaf trichome density as well as the secretion of antifungal compounds by glandular trichomes strongly influence epidermal fungal communities (Valkama et al. 2005). For instance, the high trichome densities in *Phaseolus vulgaris* trapped and prevented 60% to 80% of pathogenic rust spores from infecting its foliar epidermis (Mmbaga & Steadman 1992). By comparison, a glabrous variety of *P. vulgaris* generally had higher epidermal spore densities than pubescent varieties (Mmbaga & Steadman 1992). Similarly, in comparison with trees with lower trichome densities, birches with greater trichome densities had significantly less pathogenic rust infections (Valkama et al. 2005). Increasing concentrations of secreted antifungal compounds corresponding with greater densities of glandular trichomes of *Betula pendula* also decreased the abundance of the benign FE *Fusicladium* (Valkama et al. 2005). In Hawai‘i, herbivorous epidermal grazers such as the endangered endemic tree snails (*Achatinella mustelina*) on the Island of O‘ahu can alter epiphytic fungal communities (O'Rorke et al. 2014). *A. mustelina* appears to favor glabrous surfaces over pubescent leaves (A. Amend, pers. comm.).

Despite the influence of leaf pubescence on epidermal fungi, its impact on FE communities is not clear. A study involving 28 species of Panamanian trees and shrubs revealed that while innate leaf terpenoids influenced FE richness, the presence or absence of pubescence did not influence infection rates (Arnold 2002). Microscopic examination revealed FEs in the mostly glabrous-leafed Atlas pistachio (*Pistacia atlantica*) (Zareb et al. 2016). However, the same study found that FEs were absent around the bases of specialized trichomes, suggesting that these trichomes can physically block the entrance of FEs into nearby leaf tissue (Zareb et al. 2016). The influence of leaf trichomes on foliar FE communities merits further study.

Environmental Effects on Leaf FEs

FE communities may vary more across environmental gradients or ecotones than across host plant genotypes or taxa (Arnold & Lutzoni 2007; Cordier et al. 2012; Zimmerman & Vitousek 2012). In northern Alaska, FE communities in White spruce (*Picea glauca*) were primarily affected by local climatic conditions (e.g., temperature, solar intensity, humidity) instead of host genotypes (Eusemann et al. 2016). On the Island of Hawai‘i, lower elevation and higher precipitation as well as warmer temperatures were associated with higher FE diversity across populations of *M. polymorpha* (Zimmerman & Vitousek 2012).

The dominance of generalist FEs in tropical forests may stem from the low population densities characteristic of tropical wet forest trees (Peay 2008). Unlike the vertical transmission (i.e., maternal plant to seeds) of FEs in grasses, most FE communities in forest trees are horizontally transmitted via contact with adjacent trees (Rodriguez et al. 2009; Eusemann et al. 2016; Griffin & Carson 2018; Terhonen et al. 2019). Compared to higher latitudes, the tropics have greater plant species richness (Gentry 1988; Reynolds et al. 2003) as well as greater richness of forest FE generalists (i.e., non-host specific FEs) (Cannon & Simmons 2002; Arnold & Lutzoni 2007). In most lowland tropical wet forests, high tree species richness corresponds with low densities of individual tree species (e.g., <1 individual/ha) (Pitman et al. 2001). It could thus be evolutionarily disadvantageous for FEs to form strong affinities with rare plant hosts (Peay et al. 2008). The relative rarity of conspecific individuals may partially explain the observed absence of tropical FE host-specificity (Cannon & Simmons 2002; Suryanarayanan et al. 2003) and the commonly observed sharing of similar FE communities among sympatric tree species (Cannon & Simmons 2002).

The high relative abundance of common tree taxa in tropical forests, however, may partially counteract this trend towards generalist FEs. The tree genus *Theobroma*, for instance, is

commonly found throughout the Amazon across thousands of square kilometers (Pitman et al. 2001), and *T. cacao* was found to harbor host-specific FEs (Arnold et al. 2003). Whether host-specific FEs are a feature of other relatively abundant tropical tree species remains to be seen.

Isolation by Distance in FE Communities

Isolation by distance (IBD) caused by distance-dependent dispersal may shape the distribution of FEs in some plant communities. Since the IBD model was first described by Wright (1943), its application to FEs has shifted towards finding how strongly IBD influences FE community composition rather than genetic distance within individual FE taxa. Dissimilarity in FE community composition can increase with geographic distance (Saucedo-Garcia et al. 2014; Datlof et al. 2017; Ghasemi et al. 2019). Among several geographically distant southern Californian pine populations, each population had different strains of the FE *Diplodia scrobiculata* (Burgess et al. 2004). Even when host-taxonomic effects were not significant, isolated pine forests across 500 km in the eastern half of the continental United States developed their own unique FE strains (Oono et al. 2014). Across the Island of Hawai‘i, however, geographic distance failed to explain variation in FE composition within the dominant tree, *Metrosideros polymorpha* (Zimmerman & Vitousek 2012).

DNA Barcoding of FEs

Traditional methods of taxonomic classification through morphology of laboratory-cultured strains fail to identify most FEs. Only 1% to 10% of all microbes are culturable in laboratories (Staley & Konopka 1985; Rondon et al. 1999). Furthermore, phenotypic plasticity influenced by substrate (e.g. petri dish or host plant) can limit the taxonomic utility of cultured FE specimens

(Hebert et al. 2003; Sieber 2007).

DNA barcoding can be used to identify otherwise indecipherable taxa (Hebert et al. 2003). DNA barcoding uses short DNA sequences that have accumulated neutral substitutions as the result of random genetic drift (Stoeckle 2003). DNA barcoding of fungi employs fungal-specific primers that target nuclear ribosomal DNA (nrDNA) internal transcribed spacer (ITS) regions (Fig. 3) (Schoch et al. 2012; Zimmerman & Vitousek 2012). Compared to nuclear RNA cistrons and protein-coding genes, ITS regions identify broader ranges of fungal taxa and show the clearest barcode gaps (Schoch et al. 2012). A barcode gap is the genetic distance between intraspecific and interspecific taxa, and the presence of barcode gaps significantly aids the delineation of taxa (Meyer & Paulay 2005). Lastly, ITS sequences are more amenable to PCR amplification than are protein-coding genes (Schoch et al. 2012).

Shift to Exact Sequence Variants

There has been increasingly strong advocacy of late to cease OTU-clustering protocols for microbial sequencing and shift to exact sequence variants (ESVs) (Callahan et al. 2017; Knight et al. 2018). The similarity thresholds cluster sequence variants into OTUs by grouping similar sequences as one OTU (Schloss et al. 2009; Knight et al. 2018), with 97% being most commonly used similarity threshold (Westcott & Schloss 2015; Callahan et al. 2017). There is controversy, however, about the most appropriate similarity threshold to use for ITS-amplified fungal sequences (Blaalid et al. 2012) with suggested thresholds ranging from 90% to 99% (e.g., Ryberg et al. 2009; Amend et al. 2010; Lim et al. 2010; Tedersoo et al. 2010; Lentendu et al. 2011). One concern is that higher OTU similarity thresholds can inflate FE richness. For example, Gazis et al. (2011) found that raising the similarity threshold from 95% to 100%

increased OTU richness from 31 to 50 OTUs. Alternatively, at lower similarity thresholds, OTU clusters risk losing information on actual biological sequence variations such as single nucleotide polymorphisms, or risk combining functionally disparate taxa (Peay et al. 2016; Callahan et al. 2017; Knight et al. 2018). The popular 97% similarity threshold, for instance, clusters the pathogen *H. fraxineus* with the benign saprotroph *H. albidus* as one OTU (Kõljalg et al. 2013).

De novo, and closed-reference clustering methods usually create OTUs that are incomparable to OTUs from other studies, and require additional processing for meta-analyses (Rideout et al. 2014; Callahan et al. 2017). Instead of using reference databases, de novo OTU clusters rely solely on the collection of sequences within the given dataset (Rideout et al. 2014). Individual datasets likely have unequal collections of sequences, FE relative abundances, and errors, and the de novo OTUs from two datasets can be incomparable (Callahan et al. 2017). Furthermore, applying de novo OTU meta-analyses and replicated studies requires recompiling and pooling raw sequence data for combined analyses. In contrast, closed-reference OTUs rely on external reference databases to cluster and compare OTUs from multiple datasets. In the latter case, biological differences or sequences not recorded in the latest reference database are discarded without further investigation (Rideout et al. 2014). As fungal DNA databases are continually updated with new sequences (Callahan et al. 2017; Nilsson et al. 2018), closed-referenced studies have increasingly limited usability with each new update (Callahan et al. 2017). Hence, the impossible reproducibility of de novo OTUs, and the gradually increasing irrelevance of closed-reference OTUs may hinder subsequent diversity studies (Callahan et al. 2017).

ESVs, in contrast, are the actual DNA sequences that do not rely on arbitrary similarity thresholds (Callahan et al. 2017). Unlike de novo OTUs, ESVs from different studies can be compared directly in meta-analyses. The ESVs are deduced in a de novo process (Callahan et al.

2017) based on the verified assumption that among datasets erroneous sequences are rarer than actual ESVs and are thus removed along with rare sequences as part of the quality control steps (Callahan et al. 2016a). Like closed-reference OTUs, the DNA sequences of the ESVs can be identified using existing reference databases (Callahan et al. 2017). ESVs that remain unidentified are kept for later identification in future updated reference databases (Callahan et al. 2017).

Tree Genus *Metrosideros*

The widespread distribution of the tree genus *Metrosideros* may stem from Eocenic to Miocenic (40-16 Ma) Tasmania (Tarran et al. 2016; Tarran et al. 2017). Although *Metrosideros* is now completely extinct in Australia, the oldest *M. leunigii* fossils had identifiable traits present in extant *Metrosideros* taxa (Tarran et al. 2016; Tarran et al. 2017). After possibly landing on Eocenic New Zealand (Wilson 1996; Lee et al. 2012), genus *Metrosideros* diverged into two subgenera: *Metrosideros*, and *Mearnsia* (Dawson 1984). The current geographic range of *Metrosideros* subgenus *Metrosideros* includes the sub-Antarctica islands of New Zealand, the Bonin islands of Japan, and the Hawaiian archipelago (Tarran et al. 2016). In the current study, all mentions of *Metrosideros* strictly refers to the subgenus *Metrosideros*. As early as 3.9 (2.6-6.3) MYA (Percy et al. 2008), but likely closer to 3.1 MYA (Dupuis et al. 2019), *Metrosideros* colonized the Hawaiian Islands, landing on either Kauaʻi or Oʻahu.

Hawaiian *Metrosideros*

Metrosideros is the dominant woody species complex in the Hawaiian Islands, where it comprises five species, including the abundant *M. polymorpha*, for which eight infraspecific taxa

are named (Dawson & Stemmerman 1990), but several additional morphotypes have been recognized (Stacy & Sakishima 2019) and described (Stacy et al. 2020). These taxa and morphotypes are distinguished by leaf and other vegetative traits, which are strikingly diverse (Tsujii et al. 2015, Sur et al. 2018), and common-garden studies demonstrate that the differences among forms are heritable (Stemmermann 1983; Cordell et al. 1998; Stacy et al. 2016; Stacy et al. unpub. data). Collectively, the many forms of *Metrosideros* span an exceptional range of environments, including deserts, montane and subalpine forests, wind-swept ridges, bogs, rivers, and new lava flows (Mueller-Dombois 1987; Dawson & Stemmermann 1990; Mueller-Dombois 1992; Cordell et al. 2000). This exceptional ecological diversity can be attributed to significant ecological, physiological, and/or anatomical divergence among taxa (Cordell et al. 2000; Morrison & Stacy 2014; Ekar et al. 2019). Lastly, the observed ecological differences among taxa correspond with a range of genetic distances among taxa (DeBoer & Stacy 2013; Stacy et al. 2014; Stacy & Sakishima 2019; Stacy et al. 2020).

The 3.7-million-year-old island of Oʻahu (Carson & Clague 1995) has the highest richness of *Metrosideros* taxa of any Hawaiian Island (Stacy & Sakishima 2019). Oʻahu hosts four endemic species, including many infraspecific taxa of the abundant *M. polymorpha*, that are distinguishable by macromorphological (Dawson & Stemmermann 1990) and micromorphological traits (Sur et al. 2018). *Metrosideros* is a dominant taxon on both the Koʻolau (945 m elevation) and Waiʻanae Volcanoes (1,227 m elevation), where it comprises multiple taxa or morphotypes distributed with overlap in a predictable sequence from 250 m elevation to the volcano peaks along predominantly leeward ridges (Stacy et al. 2020). Increasing exposure to the northeast trade winds with increasing elevation results in a dramatic range of climates along the leeward elevation gradients of Oʻahu. On Koʻolau Volcano, for

instance, taxa occurring at low elevations experience an average of 1,000 mm/year of rainfall and low winds (Fig. 2) (Giambelluca et al. 2013; Giambelluca et al. 2014). In contrast, taxa restricted to the highest elevations on Koʻolau experience considerably wetter (>6,000 mm/year) (Giambelluca et al. 2013; Giambelluca et al. 2014) and windier conditions (>44.7 m/s) (Chock et al. 2005). Waiʻanae Volcano experiences an analogous, yet less extreme, increase in precipitation with elevation from about 1,200 mm/year (lower elevation) to 2,200 mm/year (highest elevation) (Giambelluca et al. 2013; Giambelluca et al. 2014). The occurrence of morphologically distinct, sympatric *Metrosideros* taxa at both low and high elevations on Oʻahu offers the opportunity to examine simultaneously how host taxon and climate impact FE composition.

Leaf FEs in Hawaiian *Metrosideros*

Only a few studies have examined leaf FE diversity in Hawaiian *Metrosideros*. Zimmerman and Vitousek (2012) concluded that leaf FE diversity in populations of *M. polymorpha* on Hawaiʻi Island is strongly influenced by elevation, temperature, and precipitation. In contrast, Cobian et al. (2019) concluded that elevation (i.e., at 1,000-2,000 m) had no impact on leaf FE richness, diversity, or composition within each of three abundant native plants on Mauna Loa Volcano, including *Metrosideros*. The smaller geographic scale of sampling done by Cobian et al. (2019), however, relative to Zimmerman and Vitousek (2012) may have contributed to their contrasting results. Cobian et al. (2019) did find, however, that FE communities differed across plant genera at all elevations and that the strength of host-specificity varied with elevation. Elevation explained 46% of the variation in FE host-specificity, with the greatest host-specificity observed at middle elevations (1,400-1,500 m) (Cobian et al. 2019). Darcy et al. (2019) included

Metrosideros as one of 80 genera of trees and shrubs across five main Hawaiian Islands (n = 119 trees, or 11% of all samples) in their study of abiotic and biotic factors that affect leaf FE community composition. All FE genera showed significant, albeit weak, associations with a number of variables, including evapotranspiration (10%), elevation (8%), host-plant phylogenetic distance (6%), seasonality (2%), cloud cover (2%), precipitation (2%), relative humidity (2%), solar radiation (2%), and geographic distance (0.2%) (Darcy et al. 2019). Combined, these studies suggest that climatic variables may strongly influence FE community composition in Hawaiian *Metrosideros*, but variation in FE communities among *Metrosideros* taxa remains unexplored.

Notably, the *Metrosideros* communities on Hawai‘i Island examined by Zimmerman and Vitousek (2012) and Cobian et al. (2019) comprise just 2-3 infraspecific taxa of the widespread *M. polymorpha*: var. *polymorpha*, var. *incana*, and var. *glaberrima* (Dawson & Stemmermann 1990; DeBoer & Stacy 2013; Stacy et al. 2014), and sampled trees were not assigned to variety in these studies. The sampling in Darcy et al. (2019) from O‘ahu likely contained multiple *Metrosideros* species and infraspecific taxa of *M. polymorpha* (Dawson & Stemmermann 1990; Sur et al. 2018; Stacy & Sakishima 2019; Stacy et al. 2020), yet the final sampling (n = 9) was insufficient for taxon-level analyses even if trees had been designated to taxa. As other studies have detected different FE communities (and dissimilar responses to the same FEs) in closely related tree species, it is possible that FE communities vary across the many taxa of Hawaiian *Metrosideros*. Intriguingly, a comparison of culturable FE communities grown from the leaves of two common-garden trees of *M. polymorpha* derived from low- (105 m) and high- (2,470 m) elevation populations on Hawai‘i Island revealed nearly distinct communities in spite of the proximity of the trees in the garden (B. Perry, unpub. data). To better understand what

determines leaf FE composition in this dominant woody species complex, I used NGS metagenomics to examine how FE communities vary across *Metrosideros* host taxa, elevations, and geographic distance on the Island of Oʻahu.

HYPOTHESES

Hypothesis 1A (H_{1A}): FE communities vary across *Metrosideros* taxa.

The many forms of *Metrosideros* on O‘ahu, both species and infraspecific taxa, may harbor largely host-specific FE communities, suggesting symbiotic relationships between these trees and their endophytes. The co-occurrence of sympatric taxa at both the low and high ends of *Metrosideros*’ elevation range on the island will allow determination of the relative strength of host-specificity among FEs sharing a common environment.

Hypothesis 1B (H_{1B}): FE communities differ between glabrous- and pubescent-leaved taxa.

In population genetic analyses of *Metrosideros* on both Hawai‘i Island (Stacy et al. 2014) and O‘ahu (Stacy & Sakishima 2019), glabrous- and pubescent-leaved taxa (i.e., leaf type) cluster into two partially but significantly isolated groups, suggesting greater phylogenetic affinity within each group relative to that between groups. If FE communities have coevolved with *Metrosideros* in O‘ahu, and if host-specificity is broad, then I expect to observe differences in FE composition between pubescent and glabrous-leaved taxa.

Hypothesis 2 (H_2): FE communities vary across environments.

Metrosideros populations on the Island of O‘ahu occur continuously from roughly 250 m above sea level to the summits of the Ko‘olau (960 m) and Wai‘anae (1,237 m) Volcanoes. Among montane Hawai‘i Island *Metrosideros* populations, FE diversity increased in regions with higher precipitation (Zimmerman & Vitousek 2012). If precipitation is an important determinant of FE diversity, I predict that FE diversity will rise with elevation towards the wetter volcanic summits of O‘ahu.

Hypothesis 3 (H_3): FE communities vary with geographic distance.

Instead of being influenced by environment or host taxon, FE communities may be determined by dispersal alone, varying simply as a function of geographic distance between host plants (Burgess et al. 2004; Oono et al. 2014; Datlof et al. 2017). If true, I expect to observe a negative relationship between similarity indices and geographic distance among FE communities (individual trees or populations) sampled across the island.

Null Hypothesis: FE composition is random with respect to elevation, taxon, leaf type, and geography.

This null hypothesis predicts no significant associations between FE composition and any of the examined factors.

METHODS

Study System—Eight *Metrosideros* taxa were sampled, including three of the four species on the island of O‘ahu: *M. polymorpha*, *M. rugosa*, and *M. tremuloides* (Table 1). The fourth species, *M. macropus*, was not suitable for this study due to its low population density and broad elevation range. The sampled taxa of *M. polymorpha* included three named taxa (var. *incana*, var. *glaberrima*, and race *prostrata*) and three unnamed morphotypes (race B, race F, and race L) described in Stacy et al. (2020). Of the six *M. polymorpha* infraspecific taxa sampled, var. *incana* and var. *glaberrima* typically occur at relatively lower elevations (e.g., < 600 m on Ko’olau) and the other four taxa are restricted to relatively higher elevations (e.g., > 600 m on Ko’olau; Table 1; Stacy et al. (2020)). The mature leaves of three taxa (*M. polymorpha* var. *incana* and race F, and *M. rugosa*) are pubescent; all others have glabrous adult leaves. Whole-plant morphology varies widely across the sampled taxa from the mat-like form of *M. polymorpha* race *prostrata* to the shrub-like adults of *M. rugosa*, and *M. polymorpha* race B and race L and the tall trees of *M. tremuloides*, *M. polymorpha* var. *incana* var. *glaberrima*, and race F and (Stacy & Sakishima 2019; Stacy et al. 2020).

Sample Collection—From November 2010 to September 2012, young leaf and leaf bud samples were collected from adult plants in 16 *Metrosideros* populations on the leeward ridges and backbone or summit of Ko‘olau and Wai‘anae Volcanoes on O‘ahu (Fig. 1). The three sites on Ko‘olau were ‘Aiea Ridge, Konahuanui ridge, and the closely situated Wiliwilinui and Kuliou‘ou (WWNKOO) ridges, which are treated as a single, combined site in this study. Individually, neither Kuliou‘ou or Wiliwilinui had enough host-taxon richness nor abundance of samples to satisfy the collection protocol, and closely adjacent WWNKOO ridges share a

relatively small area with similar environmental conditions. The single site on Wai‘anae was Mt. Ka‘ala. From each site four taxa were sampled, including a pair of sympatric low-elevation taxa and a pair of sympatric high-elevation taxa; seven of the eight pairs included both glabrous and pubescent taxa (Table 1). Waypoints were recorded for all sampled adults, or clusters in the case of adults spaced < ~2 m apart, and absolute elevations were derived from the geographic position data. Due to variation in the composition of the *Metrosideros* community across ridges, the taxa selected for study varied across the four sites. Leaf and bud samples were collected from 11 adults/taxon/site for a total of 176 adults and were cryopreserved at -80 °C within two days of collection.

Surface Sterilization—The protocol of Zimmerman and Vitousek (2012) was modified to clean cryopreserved leaves as well as to minimize DNA-shearing in thawing samples. All sterilants and water rinses were cooled to near freezing, and kept on ice during the sterilization procedure. Glassware, pipet tips, empty teabags, and other materials were autoclaved to prevent contamination.

First, the frozen samples were manually fragmented with tweezers. Omitting the petiole and midrib, the leaf fragments were placed into one autoclaved teabag/sample. The teabags were dipped in 95% ethanol (EtOH) for five seconds, immersed in 0.5% sodium hypochlorite for 30 seconds, bathed in 70% EtOH for 60 seconds, and finally rinsed in three baths of 500 ml ultrapure Milli-Q (Merck Millipore, Birmingham, MA) water for 60 seconds/bath. The sterilized samples were dabbed dry with autoclaved paper towels. Water from the third rinse was saved to check for contamination by epiphytic fungi using PCR.

DNA Extraction—Genomic DNA (gDNA) was extracted from surface-sterilized samples using a modified protocol for Macherey-Nagel NucleoSpin® Plant II kit (Macherey-Nagel GmbH & Co. KG, Düren, Germany). An equal mass of leaf tissue per extraction was collected for glabrous and pubescent samples, but pubescent leaves had double the volumes of the RNase A and PL2 reagents to improve their DNA quality. All extractions generated 100 µl of DNA per sample.

Amplification and Sequencing

Polymerase Chain Reaction (PCR)—The Ion 16S™ Metagenomics Kit User Guide (Pub. No. MAN0010799, Rev. C.0; ThermoFisher Scientific, Waltham, MA) was used with additional modifications. The fungal gDNA samples were amplified with the ITS-1 forward primer (ITS-1F, CTTGGTCATTTAGAGGAAGTAA) (Bohs 2007; Zimmerman & Vitousek 2012; Bazzicalupo et al. 2013), and the ITS-2 reverse primer (ITS-2R, GCTGCGTTCTTCATCGATGC) (Bohs 2007; Zimmerman & Vitousek 2012; Bazzicalupo et al. 2013). To later determine the origin of the fungal ESVs, each sample was assigned a unique pairing of one ITS-1F barcode and one ITS-2R barcode (Integrated DNA Technologies, Coralville, IA) (Table 2, and Table 3).

The 30.0-µl PCR reactions included 8.1 µl Milli-Q water, 2.5 µl gDNA, and 1.5 µl tween-20 (ThermoFisher Scientific, Waltham, MA), as well as final concentrations of 1X buffer (ProMega, Madison, WI), 0.2mM dNTPs (ProMega, Madison, WI), 0.4 µM $MgCl_2$ (ProMega, Madison, WI), 5.0 µg/µl bovine serum albumin (New England Biolabs, Ipswich, MA; ProMega, Madison, WI), 0.3 units/µl taq polymerase (ProMega, Madison, WI), 0.3 µM ITS-1F barcoded primer (Sigma-Aldrich, St. Louis, OH), and 0.3 µM ITS-2R barcoded primer (Sigma-Aldrich, St. Louis,

OH). The PCR program, with samples and negative controls, comprised 180 seconds at 95.0 °C followed by 24 cycles of denaturing at 95.0 °C (30 seconds), annealing at 52 °C (30 seconds), and extension at 72 °C (30 seconds), and one final extension at 72 °C for 7 minutes.

A mixture of 4.0 µl/PCR and 1.0 µl loading-dye 6X (ThermoFisher Scientific, Waltham, MA) was pipetted into each well of a 1.5% agarose electrophoresis gel, which was run at 90 volts for 40 minutes and stained with GelRed dye (Biotium, Fremont, CA). The gels were visualized under an ultraviolet lamp (UVP PhotoDoc-It Imaging System; Alpha Innotech Corp., San Leandro, CA). A 100-base-pair (bp) DNA ladder, and a negative-control PCR product were included in each gel. Successful amplification was indicated by a visible band of 200-600 bp; blank lanes indicated non-amplification. PCR products were stored at -20 °C.

PCR Purification and Dilution—Preceding library preparation, the PCR products were partially purified and then evaluated with a Bioanalyzer 2100 (Agilent Technologies, Santa Clara, CA). AmPure XP beads (ThermoFisher Scientific, Waltham, MA) were used at 0.8X concentration to remove most primer dimers. The Agilent High-Sensitivity DNA Kit (Agilent Technologies, Santa Clara, CA) was used to evaluate the results and to establish the double-stranded DNA (dsDNA) picomolarity (pM) of each targeted amplicon that ranges between 200 and 400 bp.

Limited dilutions were done to roughly equalize concentrations across samples while avoiding over-dilution of samples to undetectable concentrations. Dilutions were performed in 0.1X Tris-EDTA solution as follows: 1:10 for samples with initial concentrations of at least 100,000 pM DNA, 1:2 for samples with initial concentrations of 1,000 pM to less than 100,000 pM DNA, and no dilutions for samples with less than 1,000 pM DNA. The final products

(diluted or undiluted) with their unique barcoded primers were pooled into a single library, and a BluePippin size-selection gel (Sage Science, Inc., Beverly, CA) was used to isolate the desired 200-400-bp fragments from PCR artifacts and any remaining primer dimers <200 bp from the pooled library. Despite this filtering, however, amplicon fragments up to 788 bp remained in the library (Fig. 4) (see Results). The molar concentration of the library was determined in a fragment analysis electropherogram (Advanced Analytical, Ankeny, IA).

Library Synthesis and Sequencing—Amplification of ITS regions using next-generation sequencing (NGS) platforms is the best approach to characterizing the abundance and diversity of FE communities in natural systems. For this study, the Ion Torrent Ext sequencer (Thermo Fisher Scientific 2018) was chosen over other available sequencing platforms, due to greater read length possible using the Ion Torrent (600 bp max). Ion Torrent sequencers can handle amplicons that are 200–600 bp long (Thermo Fisher Scientific 2016; Thermo Fisher Sckientific 2018). Illumina Miseq sequencers are less error prone in base-calling than Ion Torrent sequencers (i.e., 99.9% accuracy vs. 99% accuracy, respectively), and the Miseq platform has lower false-positive rates of non-existent single nucleotide polymorphisms (Quail et al. 2012). However, the length of amplified ITS sequences frequently exceeds the 150-bp limit of Miseq (Porter & Golding 2011; Quail et al. 2012). Because of these sequencing limitations and the expected sizes of the FE amplicons, the Ion Torrent sequencer was chosen for this project.

The libraries were prepared following the Ion 16S™ Metagenomics Kit User Guide. An Ion Xpress Barcode with the Ion P1 adaptor (ThermoFisher Scientific, Waltham, MA) was ligated onto the barcoded ITS primers, and a Bioanalyzer 2100 (Agilent Technologies, Santa Clara, CA) was used to determine the final library concentration.

The undiluted library was shipped to DC3 Therapeutics LLC, San Francisco, CA. The library was template-barcoded and quantified using their 520/530 ExT Chef Kit (ThermoFisher Scientific, Waltham, MA; Thermo Fisher 2018) and subsequently sequenced on a 530-chip in the Ion S5 XL sequencer (ThermoFisher Scientific, Waltham, MA). The resulting sequences were returned as two fastq files.

Bioinformatics

Raw Sequence Demultiplexing—The two fastq files were merged into one fastq file in Mothur (Schloss et al., 2009). The merged fastq file was then demultiplexed with an oligo file containing every individual-diagnostic combination of the ITS-1F and ITS-2R primer barcodes (Table 2, and Table 3). All sequences that did not exactly match any pair of primer barcodes were discarded. Every demultiplexed fastq dataset represented one sample, and each sample was identifiable by its respective sample ID number (e.g., o51). All downstream bioinformatics procedures were completed in RStudio (R Core Team 2018), and used ESVs (Callahan et al. 2017).

ITSxpress—ITSxpress (Rivers et al. 2018) was used to extract the ITS1 region of fungal rDNA from all demultiplexed fastq datasets. While most protocols follow similarity-threshold clustering for ESV analyses, ITSxpress prepares the raw sequences for downstream filtering into ESVs (Bengtsson-Palme et al. 2013; Callahan et al. 2017; Rivers et al. 2018). Although the high variability of the ITS region may be useful for fine-scale taxonomic classification, this variability makes alignment for phylogenetic analysis impossible (Bengtsson-Palme et al. 2013). Instead, the ITSxpress software runs Hidden Markov Models (HMM) to evaluate many sequence

alignments for slight positional sequence-variations and to discard reads without ITS sequences (Durbin et al. 1998; Eddy 1998; Nilsson et al; 2010; Bengtsson-Palme et al. 2013) and flanking regions such as 18S and 5.8S. The ITSxpress software has a true-positive detection rate coupled with very low false-positive rate, making it well suited for ESV filtering (Bengtsson-Palme et al. 2013). The ITSxpress software also removed sequence replicates from all demultiplexed fastq files (Rivers et al. 2018). After the HMMSearch program identified the stop and start sites, the results were analyzed, ITSxpress removed the flanking 18S and 5.8S reads as well as the primers and barcodes (Rivers et al. 2018). The trimmed fastq files for each sample were then ready for downstream ESV filtering.

ESV Filtering and Statistical Analyses—The newest version of the R-package Divisive Amplicon Denoising Algorithm (DADA), DADA2, removes sequencing errors from the ESVs (Callahan et al. 2016a). After demultiplexing was completed, amplicon quality plots were created for each sample to determine the trimming cutoffs of low-quality sequences (Callahan et al. 2016a). In lieu of phred scores (Ewing & Green 1998), the sequences were filtered by the following quality control cut-offs (Callahan et al. 2016a): no ambiguous bases, a maximum of two estimated errors per read, truncation after finding the first base with a quality-control score of ≤ 2 (i.e., defines the end of a good quality sequence), and removal the average amount of low-quality base pairs (i.e., 15 bp) from all sequences (Callahan et al. 2016a). Any reads with ambiguous bases (i.e., unmatched bases), and/or more than two estimated errors were discarded (Callahan et al. 2016a). Additional filtering was done to remove chimeric sequences and any sequence with <100 nucleotides. Fungal taxa were assigned to the sequence table using a custom-made RDP_UNITE_with_Outgroups.fasta file (Zahn 2020). Subsequent R commands

converted this sequence table for statistical analyses and graphs (McMurdie & Holmes 2013; Callahan et al. 2016b).

Sequences with <3 copies, and non-fungal sequences were removed from the dataset. Groups (i.e., for taxon and site) showed clear asymptotes, but data were not rarefied to avoid losing information, and data were not plotted to avoid potential biases (McMurdie & Holmes 2014). Instead of using rarefaction curves, the data were converted into FE ESVs, and the relative abundances of the FE ESVs were used (Zahn 2020).

The statistical analyses were completed in RStudio using functions from the R packages *vegan*, and *stats* (Oksanen et al. 2018; R Core Team 2018). The *vegan* package includes multivariate tools for dissimilarity analysis, diversity analysis, and community ordination and is often used for descriptive community ecology (Oksanen et al. 2018). The *stats* package runs general statistical functions and generates graphs (R Core Team 2018).

FE Richness and Relative Abundance (H_{1A}, H_{1B}, H_3)—Bar plots with ± 1 standard-error bars were made to illustrate the variation in mean FE richness among *Metrosideros* taxa, and among sites. Defined as the proportion of each FE in relation to other FE taxa within a sample, the relative abundance of FE ESVs was examined using non-metric multidimensional scaling (NMDS). NMDS (*vegan* package) ordination plots were made using Euclidean distances (Kruskal 1964; Lefcheck 2012). In this process, multiple community dimensions are simplified and compacted into two dimensions for easier visualization of patterns (Lefcheck 2012). The NMDS plots revealed if individual host taxa, leaf type (i.e., pubescent vs. glabrous), and/or sites contained discernible groups of FE ESVs (Table 1). Relative abundance data were used to

generate a Bray-Curtis distance matrix, which was then used in PermANOVA tests and Mantel tests of isolation by distance.

FE Community Dissimilarity (H_{1A}, H_2, H_3)—PermANOVAs (Permutational multivariate analysis of variance) are used to evaluate how strongly unrestrained covariates influence a dependent variable (Oksanen et al. 2018) and are comparable to multivariate analysis of variance (Anderson 2001; McArdle & Anderson 2001) and redundancy analysis (Legendre & Anderson 1999).

In this study, PermANOVAs (999 permutations) were used to test if the explanatory variables (i.e., host taxon, site, relative elevation, absolute elevation, and the interaction of the host taxon with site) significantly influenced observed FE community composition. Additionally, PermANOVAs were used to test if sample outliers among the explanatory variables significantly influenced these results. For instance, if some samples had unusually high or low FE relative abundance, this could influence the downstream analyses of all samples.

Isolation by Distance (H_3)—Mantel tests were done on FE dissimilarity across the four sites as well as within each site. The Mantel test (*vegan* package) is a permutation test that examines the strength of the correlation between two distance matrices (Mantel 1967; Legendre and Fortin 1989; Oksanen et al. 2018), with the null hypothesis of no correlation (Mantel 1967; Legendre and Fortin 1989). Exactly 9,999 permutations of Euclidean geographic distance matrices were processed among sites (and among host plants within sites) to determine if more distant sites (or hosts) have more dissimilar FE communities.

Shannon Diversity (H_{1A}, H_{1B}, H_2, H_3)—The diversity of FE communities was estimated using the Shannon Diversity Index, which measures the quantity and evenness of taxa (Magurran 1988; Rosenzweig 1995; Begon et al. 1996; Oksanen et al. 2018). Model evaluation was done using the Akaike Information Criterion (AIC), such that the best-fit models include the strongest explanatory variables and produce the lowest AIC values, and models that differ by AIC values of ≤ 2 are considered equivalent (Logan 2011). While the AIC best-fit models only suggest which of the explanatory variables were likely most influential, the ANOVAs tested the actual significance of the following explanatory variables on FE diversity: host taxon, site, elevation, leaf type, and relative elevation (i.e., high- vs. low-elevation). The ANOVAs also assessed the importance of interactions between variables: host taxon with site, host taxon with absolute elevation, leaf type with site, leaf type with absolute elevation, and leaf type with site and absolute elevation. The results of the ANOVAs were interpreted by their F-statistics, and p-values of <0.05 were considered significant (i.e., the probability of the null hypothesis being true is less than 5%) (Logan 2011). Lastly, Kruskal-Wallis post-hoc tests were done to compare three high-elevation *Metrosideros* taxa (
): *M. polymorpha* race *prostrata*, *M. polymorpha* race B, and *M. rugosa.*

Host-Specificity (H_{1A})—To test for host-specificity, specnumber (*vegan* package) was used to remove ESVs with less than 1,000 sequences, and the remaining ESVs were evaluated based on their relative abundance within each host taxon. While ESVs may occur within multiple host taxa in low relative abundance, an ESV was designated as host-specific if it had $\geq 1\%$ relative abundance in only one host taxon (Zahn 2020 The resulting collection of purported host-specific ESVs was used to generate trend lines showing variation in host-specificity across host taxa and

elevations. ANOVAs were done to test if the explanatory variables (i.e., absolute elevation, host taxon, and interaction of absolute elevation with host taxon) influenced host-specificity.

RESULTS

Amplification and Sequencing

From the DNA extractions of 176 samples, 144 samples were amplified, and 132 samples were successfully quantified in a bioanalyzer for library preparation (Table 4). Most PCR products had electrophoresis gel bands of 200-400 bp, but some samples had bands >400 bp. An electropherogram evaluating the 132 purified samples pooled showed amplicon peaks of 200-788 bp with about half of the detected amplicons exceeding 400 bp (Fig. 4). Additionally, the electropherogram of the amplified library, with ligated Ion Adaptors and an Ion Xpress Barcode, had amplicon peaks >400 bp (Fig. 5). The final library of 132 pooled samples had a concentration of 7,801 pmol/l (Fig. 5).

Two chips were used for sequencing (ThermoFisher Scientific, Waltham, MA; ThermoFisher 2018), because the first chip was overloaded with too much library, and a second chip was needed to complete the sequencing. The loading density of the ion sphere particles (ISPs) in the first chip was 77.2% (29,233,092) of 37,851,934 available chip wells, and there were 28,924,972 library ISPs. Removal of polyclonals (54.9%), low-quality ISPs (33.0%), and adaptor dimers (1.1%) yielded a final library of 3,158,553 ISPs (10.9% of initial ISP library). The final ISP library of the first chip yielded 3,092,850 raw sequences. By comparison, the ISP loading density on the second chip was 82.8% (31,329,261) of 37,849,615 available chip wells, and there were 31,155,085 library ISPs. Removal of polyclonals (52.1%), low-quality ISPs (24.0%), and adaptor dimers (0.08%) yielded a final library of 7,203,142 ISPs (23.1% of the initial ISP library). The final ISP library of the second chip yielded 6,965,142 raw sequences. The two chips together yielded a total of 10,057,992 raw sequences among 132 samples.

Bioinformatics

Unrecoverable demultiplexing errors led to the removal of 17 samples amplified with the reverse primer H_ITS-2R (Table 2), resulting in 115 samples for downstream analyses (Table 5). The 115 samples had 1,183,085 demultiplexed raw sequences. DADA2 quality control reduced this count to 900,715 sequences. Removal of chimeric sequences further reduced this count to 900,353 sequences. Removal of all ESVs with less than three DNA copies yielded 1,691 ESVs among 114 samples (Table 5). Removal of non-fungal sequences yielded 1,637 fungal ESVs and further reduced the final sampling to 113 samples (Table 5; Fig. 6, and Fig. 7).

A PCA biplot (Fig. 8) of FE relative abundance across samples revealed 33 possible outliers. However, the PermANOVA of predicted explanatory variable outliers (see Methods) found these outliers had no significant ($df = 1$, $SS = 0.43$, $F = 0.90$, $p = 0.67$) influence on FE relative abundance. Rarefaction curves of FE absolute abundance for individual samples suggest many samples were asymptotic (Fig. 9).

Taxonomy and Richness of FEs

The remaining 113 samples collectively had a richness of 1,637 different FE ESVs. Of those 1,637 ESVs, the UNITE database matched 79.5% (1,301 ESVs) with five phyla, 71% (1,161 ESVs) with 20 classes, 64% (1,044 ESVs) with 58 orders, 52% (849 ESVs) with 133 families, 43% (700 ESVs) with 223 genera, and 27% (437 ESVs) with 200 species. Most FEs belonged to the phyla Ascomycota (77.0%) and Basidiomycota (22.4%), with far lower counts from each of the following phyla: Mucoromycota (0.5%), Chytridiomycota (0.1%), and Mortierellomycota (0.1%) (Table 13). The five most common FE classes were Dothideomycetes (38.0%), Sordariomycetes (14.7%), Eurotiomycetes (11.6%), Agaricomycetes (10.6%), and

Leotiomycetes (6.6%) (Table 14). Seventy-five percent of FEs were from the Pezizomycotina subphylum, and 25% of FEs belonged to other subphyla (Table 14) (Spatafora 2007). The asymptotic nature of the rarefaction curves of individual samples suggested that the 1,637 FE ESVs identified may be a reasonable estimate of true FE richness in these individuals (Fig. 9).

The 113 adults had a summed richness of 2,953 FE ESVs, or a mean of 26.1 FEs/tree. The eight *Metrosideros* taxa varied significantly in their respective richness of FE ESVs (Fig. S1): 501 in *M. polymorpha* var. *glaberrima*, 337 in *M. polymorpha* race F, 326 *M. rugosa*, 320 in *M. polymorpha* var. *incana*, 207 in *M. polymorpha* race B, 188 in *M. tremuloides*, 156 in *M. polymorpha* race L, and 116 *M. polymorpha* race *prostrata*. The four sites had similar mean FE richness per tree with overlapping standard-error bars (Fig. S2): Mt. Kaʻala (30.1 FEs/tree), ʻAiea Ridge (24.6 FEs/tree), Konahuanui (24.5 FEs/tree), WWNKOO (25.2 FEs/tree).

Beta Diversity (H_{1A}, H_2, H_3)

The PermANOVA tests of the Bray-Curtis dissimilarity values revealed significant effects of host taxon, site, an interaction between host taxon and site, and absolute elevation on FE community composition (Table 6). Sample outliers did not significantly influence the other PermANOVA results. The effect sizes were small, however. NMDS graphs of FE relative abundance showed little to no isolation by host taxon, site, or leaf type (Fig. 16, and Fig. 17). Altogether, the significant variables and interaction term explained only 23.5% of the variation in FE composition.

Host taxon had the strongest influence on FE composition, explaining 11.5% of the dissimilarity in FE community composition among samples (Table 6; Fig. 12, and Fig. 14); and variations in FE richness among host taxa as well as individual samples (Fig. S1). In fact, not all

fungal orders were recorded in all *Metrosideros* taxa (Fig. 12). Ascending towards FE phyla and classes, the differences across host taxa became even more pronounced (Fig. 14). Phylum Basidiomycota was most prominent *M. polymorpha* var. *incana*, *M. polymorpha* race B, and *M. polymorpha* race A, yet nearly absent in *M. tremuloides* and *M. polymorpha* race F (Fig. 14). Among classes, Dothideomycetes was most dominant in *M. polymorpha* race B and race F, but was less than half as abundant in *M. polymorpha* var. *incana* and *M. polymorpha* race L (Fig. 14). The proportion of unclassified fungal sequences also varied widely across host taxa from < 5% of ESVs in *M. polymorpha* var. *incana* to about 70% (i.e., 109) of ESVs in *M. polymorpha* race L (Fig. 14).

Site, in contrast, explained only 5.5% of the dissimilarity in FE composition (Table 6; Fig. 11, and Fig. 13). Not all fungal orders were documented at all sites (Fig. 11). The highest proportion of unclassified sequences (~40%) was observed at Mt. Ka‘ala, and the lowest (< 5%) was at ‘Aiea Ridge (Fig. 13). The interaction of host taxon with site explained another 5.4% of the variation in FE community dissimilarity across samples.

Elevation, whether included as a binary variable (low vs. high) or interval-scale variable (absolute elevation) had the weakest influence on FE community composition (Table 6; Fig. 10). FE communities did not differ between high- and low-elevation *Metrosideros* populations. Although FE communities did vary with absolute elevation of host plants, the relationship explained only 1.1% of the dissimilarities in FE composition.

Isolation by Distance (H_3)

Mantel tests (Fig. 15) revealed weak, but significant, correlations between geographic distance and FE composition dissimilarity across the four sites (beta-diversity; 9.3%), and within

each individual site (alpha-diversity; 12.4% at Mt. Ka‘ala, 19.3% at ‘Aiea Ridge, 10.3% at Konahuanui, and 22.6% at WWNKOO).

Alpha Diversity (H_{1A}, H_{1B}, H_2, H_3)

According to the AIC method, the better-fitting models of FE Shannon Diversity generally included elevation, host taxon, and/or site (Table 7). The best-fit model included host taxon, site, and elevation with no interaction terms (AIC = -38.40). Slightly less-fit models differed either by excluding site (AIC = -36.97) or by adding relative elevation (i.e., comparing high-elevation vs. low-elevation host taxa) (AIC = -36.87). Excluding host taxon (Table 10) yielded the least-fit model (AIC = -26.65; Table 7), further supporting host taxon as an important explanatory variable for FE composition (Table 8, and Table 9). Across host taxa, Shannon diversity estimates ranged from 0.59 (*M. polymorpha* race B) to 2.10 (*M. polymorpha* race *prostrata*) (Fig. 18). Across the four sites, mean Shannon diversity estimates ranged from 1.09 at WWNKOO to 1.41 at Mt. Ka‘ala (Fig. S3). Shannon diversity estimates did not vary with elevation (Table 8, and Table 11); however, a notably broad range of values was observed between 700 m and 800 m elevation (Fig. S4). A post-hoc test detected no correlation between mean annual rainfall and FE diversity ($t = -0.58$, $df = 111$, $p = 0.56$, adj. $r^2 = -0.04$) (Fig. S5). Lastly, the complete exclusion of leaf type from the better-fitting models suggests that FE diversity did not differ between glabrous and pubescent *Metrosideros* taxa. Among the three high-elevation taxa, a post-hoc Kruksal-Wallis test suggested only *M. polymorpha* race *prostrata* and *M. polymorpha* race B had significantly different Shannon diversity results ($p = 0.02$) (Appendix A).

Detection of Host-Specific FEs (H_{1A})

FE ESVs that had relative abundances of at least 1% within only one host taxon were designated as host-specific. Of the 1,637 unique FE ESVs observed, 17 FE ESVs met this criterion. Some of these 17 FE ESVs were present in other *Metrosideros* taxa but were below the 1% relative-abundance threshold. ANOVAs revealed that host-specificity did not vary among host taxa or across elevations; however, a significant interaction effect of host taxon with elevation was found (Table 12). Host-specificity of FEs increased with elevation until 700-1,000 m and then decreased at 1,200 m (i.e., the summit of Mt. Ka‘ala) (Fig. 19).

DISCUSSION

Leaf FEs occur throughout the plant kingdom (Rodriguez et al. 2009), yet the major drivers of the diversity and distribution of FEs among host plants and environments remain controversial. Leaf FE communities in trees have shown varying degrees of host affinity ranging from generalists to specialists (Rodriguez et al. 2009), and higher plant richness of tropical forests may select for generalist FEs that inhabit multiple hosts (Saikkonen 2007; Rodriguez et al. 2009). The importance of leaf pubescence as a physical or chemical barrier to FE infection has varying levels of support (Mmbaga & Steadman 1992; Arnold 2002; Zareb et al. 2016). FE composition and diversity can be influenced by local abiotic conditions such as temperature, elevation, and precipitation (Zimmerman & Vitousek 2012; Eusemann et al. 2016; Barge et al. 2019; Cobian et al. 2019; Darcy et al. 2019), as well as geographic distance (Wright 1943; Burgess et al. 2004; Helander et al. 2007; Saikkonen 2007; Oono et al. 2014; Datlof et al. 2017). This study sought to evaluate the importance of host taxon and environment for determining the composition and diversity of leaf FEs in the context of eight host taxa of the tree genus *Metrosideros* on the Island of O‘ahu.

Composition of FE Taxa in O’ahu *Metrosideros*

The dominant FE phyla across the eight host taxa were Ascomycota and Basidiomycota, comprising roughly 77% and 22.4% of observed ESVs, respectively. Of the previous leaf FE studies that included Hawaiian *Metrosideros* (Zimmerman & Vitousek 2012; Cobian et al. 2019; Darcy et al. 2019), only Zimmerman and Vitousek (2012) named the fungal phyla and classes observed. The FEs of *M. polymorpha* trees on Mauna Loa Volcano consisted of 99.1% Ascomycota and only 0.8% Basidiomycota (Zimmerman & Vitousek 2012). In contrast, Darcy

et al. (2019) noted only that the 5,239 ESVs retained after filtering belonged to the subphylum Pezizomycotina (phylum Ascomycota) and provided no additional details about fungal classifications or relative abundances. The dominance of subphylum Pezizomycota within phylum Ascomycota likely contributed to the dominance of these fungi in both the current study (80%) and Zimmerman and Vitousek (2012) (96.1%).

The 1,637 unique FE ESVs identified in O‘ahu *Metrosideros* represented 20 classes (71% of all FE ESVs), 58 orders (64%), and 200 species (27%). Conversely, this also means that 29%, 36%, and 73% of the ESVs for classes, orders, and species, respectively, were unidentified. This large percentage of unidentified ESVs is expected due to the limited number of named fungal taxa currently in genetic databases, especially as less than 10% of all fungal species on Earth have been identified (Hawksworth & Lücking 2017). For instance, the older version of GenBank used by Zimmerman and Vitousek (2012) may explain the lower FE diversity reported in that study. Almost 51% of their 665,155 sequences failed to match with either fungal or non-fungal taxa (Zimmerman & Vitousek 2012). Vandruff (2014) studied edaphic fungi collected around *M. polymorpha* trees at 10 sites on the Mauna Loa Volcano, and found that 21% to 47% of the fungal sequences per site failed to match with any fungal phylum. Of 1,780 leaf FE ESVs sequenced from eight species of the Hawaiian plant genus *Clermontia*, about 45% belonged to unknown fungal families (Datlof et al. 2017). Despite its limitations, the UNITE database is regularly updated with newly classified fungal sequences (Nilsson et al. 2018). Citing the mothur-compatible files of UNITE from the oldest available version (December 2013) to the most recent version (November 2018), the volume of confirmed fungal sequences grew from 2,441 to 9,407 (Nilsson et al. 2018). The accumulation of 6,966 new fungal sequences over five

years as well as the more recent FE studies suggest that future sequence-based surveys of fungal diversity will detect and identify greater fungal richness.

Host-Taxon Effects on FE Composition (H_{1A})

The most important explanatory variable for FE richness and diversity within O‘ahu *Metrosideros* was host taxon. Mean FE richness ranged from a low of 14 FEs/adult for *M. polymorpha* race L to a high of nearly 42 FEs/adult for *M. polymorpha* var. *glaberrima*. The absolute FE richness of *M. polymorpha* race L and var. *glaberrima* also differed at 156 FEs, and 501 FEs, respectively; however, this result is likely exaggerated by the greater sampling of *M. polymorpha* var. *glaberrima* populations in this study. Both of these hosts are glabrous, wet-forest taxa with relatively broad elevation ranges and high genetic diversity (Stacy et al. 2014; Stacy et al. 2020), and both taxa were sampled from both volcanoes in this study. These taxa differ strongly, however, in geographic distribution. *Metrosideros polymorpha* race L is a montane taxon endemic to O‘ahu at middle-to-high elevations. In contrast, *Metrosideros polymorpha* var. *glaberrima* spans all of the main Hawaiian Islands. *Metrosideros polymorpha* var. *incana,* another dominant taxon found on every Hawaiian Island except Kaua‘i (Stacy & Sakishima 2019), had the third-highest mean FE richness (33 FEs/adult). FE environmental studies (Saikkonen 2007; Vaz et al. 2014) as well geospatial studies (Poulin et al. 2011; Oono et al. 2014; Vaz et al. 2014) suggest that widespread host taxa tend to have greater FE richness. The results of the current study also suggest that FE richness may be greater in hosts with broad distributions.

The unexpectedly high mean FE richness of *M. polymorpha* race *prostrata* (34 FEs/adult) may suggest also that host habit influences FE richness. This taxon is restricted to seven high-

elevation montane sites on Ko‘olau Volcano (J. Lau, personal communication) that are impacted by extreme wind. Unlike any other Hawaiian *Metrosideros* taxon, *M. polymorpha* race *prostrata* is characterized by horizontal stems with only its leaves emerging from the moss-covered ground (Adee & Conrad 1990). In addition to the aforementioned routes of FE horizontal transmission to trees, this taxon may be more susceptible to colonization by soil-dwelling fungi, of which hundreds to thousands of taxa can occur per gram of soil (Fierer et al. 2007; Rousk et al. 2010; Griffin & Carson 2018). Exposure to both soil-dwelling and above-ground fungi may explain why the leaves of *M. polymorpha* race *prostrata* had among the highest mean FE richness observed, second only to that of the widespread *M. polymorpha* var. *glaberrima*.

The idea that host plants can significantly affect their FE composition and diversity is steadily gaining support (Arnold et al. 2003; Durán et al. 2005; Arnold & Lutzoni 2007; Saikkonen 2007; Vega et al. 2010; Kembel & Mueller 2014; Cobian et al. 2019; Darcy et al. 2019). Darcy et al. (2019) noted, however, that much of the literature ignores or minimizes the possible influence of host taxon by testing only one host (Arnold et al. 2003; Burgess et al. 2004; Cordier et al. 2012; Zimmerman & Vitousek 2012; Oono et al. 2014; Christian et al. 2019). In the current study, the host-taxon effect on FE community composition was surprisingly strong, considering the close evolutionary relationships among the eight host taxa. Host taxon explained 11.5% of FE diversity, exceeding the host-taxon effects of two recent studies of FE communities in Hawaiian plants at broader taxonomic scales. Cobian et al. (2019) found that host taxon explained 10% of FE composition among three plant genera (n = 120 samples, 40 samples/genus), including *Metrosideros*. In their study of 80 plant genera in Hawaii, including *Metrosideros*, Darcy et al. (2019) found host taxon explained just 6% of the variation in leaf FE composition. Given the recency of the *Metrosideros* radiation in Hawai‘i (i.e., roughly 3-4 MY;

Percy et al. 2008, Dupuis et al. 2019), the greater partitioning of leaf FEs among *Metrosideros* taxa on a single island relative to that among 80 plant genera across the entire archipelago is surprising.

Host-Specificity of FEs (H_{1A})

In consensus with previous studies of tropical forest FEs (Cannon & Simmons 2002; Suryanarayanan et al. 2003; Peay et al. 2008), it appears that an overwhelming majority of the 1,637 FE ESVs identified in this study were generalists. Host-specificity was weak overall, yet appeared to vary with elevation. At all four sites, signals of host-specificity peaked at approximately 700-1,000 m elevation. This finding may be consistent with the results of Cobian et al. (2019) who found that that elevation explained 46% of the variation in host-specific FEs (among three host genera) on Hawai‘i Island. They observed that host-specificity peaked at 1,400-1,500 m and then decreased at higher elevations on Mauna Loa Volcano (Cobian et al. 2019). In the current study, the range of Shannon diversity values was also notably broad at 700-800 m elevation, due to the presence of particularly high values. These high values of FE diversity may coincide with a relatively higher abundance of host-specific FEs at ~700-800 m elevation.

The signal of FE host-specificity among the eight O‘ahu *Metrosideros* taxa, however, was modest, and further studies are needed to characterize the strength of host-FE relationships. It is possible that some of these host-specific FE candidates could be newly evolved taxa that may simply require more time to disperse to other *Metrosideros* taxa (Poulin et al. 2011; Oono et al. 2014). One test of host-specificity could involve culturing FEs on *Metrosideros*-extract media that may establish how phytochemicals common in *Metrosideros* taxa influence FE community

development (Arnold et al. 2003). This approach is limited, however, by culturing biases, as only 1%-10% of all microbes are culturable (Staley & Konopka 1985; Rondon et al. 1999; Arnold et al. 2007; Rodriguez et al. 2009). An alternative approach could be a common-garden study with the eight *Metrosideros* host taxa. Common-garden studies of other plants (Bailey et al. 2005; Bálint et al. 2013) have revealed long-term persistence or dominance of specific FEs in individual host taxa. If, alternatively, the plants in the common garden develop the same FE communities and diversity, this result would support the position that most tropical forest trees exclusively harbor FE generalists (Cannon & Simmons 2002; Suryanarayanan et al. 2003; Peay et al. 2008).

Leaf-Type Effects on FE Composition (H_{1B})

In spite of the significant genetic divergence between pubescent and glabrous *Metrosideros* taxa on Oʻahu (Stacy & Sakishima 2019), there was no difference between the FE communities of pubescent- and glabrous-leaved hosts in this study. The idea that leaf pubescence may influence leaf FE communities originates from studies that show that dense leaf pubescence may physically or chemically inhibit epiphytic or endophytic fungal infections (Mmbaga & Steadman 1992; Valkama et al. 2005; Zareb et al. 2016). Moreover, within Hawaiʻi, endemic tree snails might alter epidermal fungal communities due to their preference for glabrous-leaved hosts (O'Rorke et al. 2014; A. Amend, pers. comm.).

The absence of an effect of pubescence on FE communities in this study may be due to the nature of leaf pubescence in *Metrosideros*. Although abaxial leaf pubescence varies substantially among the eight *Metrosideros* taxa from absent (glabrous leaves) to extremely dense, the adaxial surfaces of the leaves are almost always glabrous (Dawson & Stemmermann

1990; Sur et al. 2018; Stacy & Sakishima 2019). Horizontal transmission via direct contact of adjacent trees (Arnold & Lutzoni 2007) or from airborne (i.e., wind or animal-transmitted) (Brown & Hovmøller 2002; Gilbert & Reynolds 2005; Griffin & Carson 2018) fungal spores reaching the glabrous surfaces could cause strong overlap in the FE communities of glabrous and pubescent *Metrosideros* taxa. The glabrous leaves of *Theobroma cacao* seedlings, for instance, may be exposed to 36,000 airborne fungal spores/day (Arnold & Herre 2003; Gilbert & Reynolds 2005; Griffin & Carson 2018), and phytochemicals and epidermal thickness had insignificant effects on FE colonization (Arnold & Herre 2003). Across other tree genera, fungal hyphae can directly penetrate leaves in the spaces between epidermal cells or through stomata and other openings on the epidermis (Arnold & Herre 2003; Jones & Dangl 2006; Rodriguez et al. 2009).

Such epidermal openings may include secretory structures, which are common in Hawaiian *Metrosideros* (Corn 1979; Sur et al. 2018). Although the function of the secretory structures in Hawaiian *Metrosideros* is not yet determined, gland secretions in other plants are known to possess antimicrobial compounds that inhibit infection (Arnold 2002; Friedman et al. 2002). The secretion of antimicrobial compounds, if present, from secretory glands in O‘ahu *Metrosideros* might explain the apparent lack of leaf-pubescence effect on FE infection. Still, the possibility that secretory glands of *Metrosideros* may facilitate the entrance of FEs requires evaluation through future research.

Site and Isolation-by-Distance Effects on FE Composition (H_3)

The heavy overlap among sites in the bar plot and the NMDS plot indicated similar mean FE richness/tree/site and FE relative abundances among sites, respectively, and site explained just

5.5% of the dissimilarity of FE communities among samples. Nonetheless, there were some differences in FE communities among sites as indicated by unequal relative abundances of FE taxa. For instance, the less dominant phylum Basidiomycota varied greatly among sites. Mt. Kaʻala notably had the lowest abundance of Basidiomycota fungi as well as the highest abundance of unclassified fungal sequences. Perhaps this is related to Mt. Kaʻala being the highest-elevation site with the lowest mean annual precipitation (Giambelluca et al. 2013), or to being the most geographically isolated of the four sites. In contrast, the comparatively wetter and more closely spaced sites of ʻAiea Ridge, Konahuanui, and WWNKOO had at least triple the abundances of Basidiomycota compared to Mt. Kaʻala. The uneven distributions of FEs across sites is consistent with dispersal limitation and may be consistent with the broader scale observation by Darcy et al. (2019) of likely single-island-endemic FE taxa, as local variation in FE communities within islands would be expected to translate into significant differences among islands.

A weak but significant pattern of isolation by distance was observed across Oʻahu as well as within each of the four individual sites, further suggesting a role for dispersal limitation in the shaping of FE communities on Oʻahu. Across the 50-km distance that included the four sites, the correlation between FE community dissimilarity and distance was 9.3%. Within individual sites, the strength of isolation by distance increased with the total distance examined. In the final sampling of 113 samples, the distances between low- and high-elevation adults sampled at Konahuanui, Mt. Kaʻala, and ʻAiea Ridge were 1.6 km, 2.0 km, and 4.3 km, respectively, and the joint site WWNKOO covered an approximate area of 4.5 km^2. The two more narrowly sampled sites, Konahuanui and Mt. Kaʻala, showed the weakest correlations between geographic distance and FE community dissimilarity, 10.3% and 12.4%, respectively. By comparison, the longer

site, ʻAiea Ridge, had a stronger correlation of 19.3%, and the non-linear site of WWNKOO had the largest area and the strongest correlation (22.6%). The detection of isolation-by-distance effects at both global and local scales in this study is consistent with previous studies outside of Hawaiʻi of the influence of geographic distance on FE community composition over areas of 0.04-120,000 km^2 (Oono et al. 2014; Barge et al. 2019), or distances of 101-5,000 km (Vaz et al. 2014). In contrast, none of the three earlier studies of leaf FE communities in Hawaiian plants revealed significant isolation-by-distance effects, regardless of the spatial scale examined (Zimmerman & Vitousek 2012; Cobian et al. 2019; Darcy et al. 2019). The difference between the current results and those of prior studies of isolation by distance in FE communities in Hawaiʻi may be related to the greater host-taxon effect observed in this study and the variation in host-taxon composition across elevations and sites. More work is needed to establish how strongly geographic distance influences FE community composition within and across islands in Hawaiʻi.

Environmental Effects on FE Composition (H_2)

A limitation of tests of isolation by distance is that a positive correlation between geographic distance and FE community dissimilarity may be due in part to spatial heterogeneity in the environment. Among 10 North American populations of the tree *Populus trichocarpa* spanning 120,000 km^2, climate variation explained 8.1% of the variation in leaf fungal communities compared to just 1.4% for geographic distance (Barge et al. 2019). Environmental effects can also be influential over smaller spatial scales. In three Myrtaceous tree species dispersed across Argentina and Brazil, variation in FE community composition within 100 km was most strongly associated with abiotic environmental factors (i.e., elevation, precipitation, and temperature),

whereas isolation-by-distance effects were most pronounced at distances of 101 km to 5,000 km (Vaz et al. 2014). In Hawai‘i, elevation is associated with dramatic differences in temperature and precipitation over short distances (Cordell et al. 2000; Zimmerman & Vitousek 2012; Giambelluca et al. 2013). Across the main Hawaiian Islands, which span a distance of nearly 600 km, evapotranspiration, NDVI (Normalized Difference Vegetation Index), and elevation explained 10%, 10%, and 8% of the variation in FE composition, respectively (Darcy et al. 2019). At the scale of Hawai‘i Island across approximately 70 km on the slopes of the Mauna Loa Volcano, Zimmerman and Vitousek (2012) found that FE richness correlated with environmental conditions instead of geographic distance. Specifically, about 53% of the observed variation in FE composition across the island was associated with the combined effects of elevation and rainfall, which explained 93% and 95% of FE community similarity, respectively (Zimmerman & Vitousek 2012).

The current study and Cobian et al. (2019), however, suggest that environmental conditions may not affect FE communities in trees over small spatial scales in Hawai‘i. In the current study, elevation explained only 1% of the observed variation in FE composition, and FE diversity did not differ between high- and low-elevation communities of *Metrosideros* within sites despite the contrasting conditions at high (wetter) and low (drier) sites. Further, in the models of FE diversity, elevation was significant only when host taxon was excluded. The elevation ranges examined may have been too narrow for the detection of differences in FE communities. While the sampled plants occurred at 307-1,212 m elevation, the elevation range captured within individual sites spanned only 300 to 600 m, which represented just a fraction of the elevation range (~2,400 m) examined by Zimmerman and Vitousek (2012). Although the current study involved a greater range in mean annual rainfall (1,596-3,498 mm/yr; Giambelluca

et al. 2013) than that examined in Darcy et al. (2019) (13-550 mm/yr), it was still less than that included in Zimmerman and Vitousek (2012) (500-5,500 mm/yr). Lastly, the study by Cobian et al. (2019), which was most comparable to the current study in geographic scale (20 km) revealed no variation in FE community composition across the 1,000-m elevation gradient examined. The contrast among the findings of these four studies of Hawaiian FE communities to date, considered alongside results of FE communities in continental tree populations, suggest that environmental effects on FE communities may be weak at small spatial scales.

Unknown Functions of *Metrosideros* FEs

The functional roles of leaf FEs in Hawaiian *Metrosideros* remain unknown. *Neocoleroa metrosideri* is a fungal pathogen that causes minor leaf wilt in *M. excelsa* trees in New Zealand (Johnston & Park 2016). Since Hawaiian *Metrosideros* likely diverged from a lineage containing *M. excelsa* within the past few million years (Percy et al. 2008, Dupuis et al. 2019), its response to *N. metrosideri* may also have diverged. Different species of chestnut trees (genus *Castanea*) as well as ash trees (genus *Fraxinus*) experience starkly different survival rates when exposed to the same FE pathogens (Anagnostakis & Hillman 1992; Cleary et al. 2016). In short, how the 1,637 FE ESVs identified here influence the fitness of Hawaiian *Metrosideros* taxa is unknown.

Decoding the ecological roles of these FEs may lead to advances in protecting Hawaiian *Metrosideros* from current and future pathogens. Species of the pathogenic fungal genus *Ceratocystis* severely threaten the survival of *Metrosideros* in Hawai‘i (Heller et al. 2019). After infection, widespread blockage of the water-transporting xylem allows *Ceratocystis* to rapidly kill previously healthy trees within weeks or months (Luiz 2017; Heller et al. 2019). Studies in other trees reveal a role for some FEs in the defense against pathogens. In *T. cacao* trees,

dominant FEs may reduce the damage of pathogenic FEs that cause leaf wilt or seedpod loss (Arnold et al. 2003; Mejía et al. 2008). There may even be synergistic interactions between benign and pathogenic FEs that yielded greater net growth in affected individuals of *Theobroma cacao* (Christian et al. 2019). Given the variation in resistance to *Ceratocystis* observed among individuals of *Metrosideros* on Hawai‘i Island (Luiz 2017), characterization of the FE communities in resistant and susceptible trees would be a logical next step.

CONCLUSIONS

This study is the first to examine FE communities within and among multiple species and infraspecific taxa of Hawaiian *Metrosideros*. Results revealed that FE diversity and community composition varied significantly among some of the eight O‘ahu taxa examined, though the differences were relatively subtle. Evidence of modest FE host-specificity was also observed, but at higher elevations only. The presence of leaf pubescence had no influence on the diversity of FE communities, suggesting that unexamined micromorphological or chemical variation among *Metrosideros* taxa may influence FE diversity. FE communities varied significantly with distance both island wide and within individual sites. Elevation-associated environmental variation generally failed to explain FE diversity, which might be a consequence of the relatively small elevation ranges as well as the limited variation of environmental effects involved in our study. Further studies to characterize the strength of host-specificity, the fitness effects of FEs, and the spatial scale of environmental effects on FEs in Hawaiian *Metrosideros* should be done.

TABLES & FIGURES

Table 1. Traits of eight *Metrosideros* taxa that occur commonly across the leeward ridges and backbone of the Koʻolau and Waiʻanae Mountains, Oʻahu. *Metrosideros polymorpha* (*M. p.*) is the dominant species, and races L, F, and B are infraspecific morphotypes described in Stacy et al. (2020). Shown for each taxon is its relative elevation (high or low) within the full elevation range of *Metrosideros* forest, the elevation range of sampled adults, and abaxial leaf surface (glabrous or pubescent).

Site	Taxon	Taxon code	Relative elevation	Absolute elevation range (m)	Abaxial leaf surface
Mt. Kaʻala (Waiʻanae)	*M. p.* race L	L	High	1,199-1,233	Glabrous
	M. p. race F	F	High	1,205-1,231	Pubescent
	M. p. var. *glaberrima*	G	Low	653-817	Glabrous
	M. tremuloides	T	Low	935-975	Glabrous
ʻAiea Ridge (Koʻolau)	*M. p.* race L	L	High	588-615	Glabrous
	M. p. race *prostrata*	A	High	759-836	Glabrous
	M. p. var. *incana*	I	Low	476-533	Pubescent
	M. p. var. *glaberrima*	G	Low	501-589	Glabrous
Konahuanui (Koʻolau)	*M. p.* race B	B	High	924-953	Glabrous
	M. rugosa	R	High	788-897	Pubescent
	M. p. race F	F	Low	651-683	Pubescent
	M. tremuloides	T	Low	636-660	Glabrous
Wiliwilinui Kuliouʻou (Koʻolau)	*M. rugosa*	R	High	773-815	Pubescent
	M. p. race B	B	High	708-735	Glabrous
	M. p. var. *incana*	I	Low	486-514	Pubescent
	M. p. var. *glaberrima*	G	Low	486-498	Glabrous

Table 2. Barcoded forward ITS-1F primers and reverse ITS-2R primers used to amplify leaf FEs in O‘ahu *Metrosideros*.

Oligo	Barcoded Primer Sequences (5' - 3')
1_ITS1F	TTCAGTAGCTTGGTCATTTAGAGGAAGTAA
2_ITS1F	TTCAGATGCTTGGTCATTTAGAGGAAGTAA
3_ITS1F	TTCAGACGCTTGGTCATTTAGAGGAAGTAA
4_ITS1F	TTCAGCAGCTTGGTCATTTAGAGGAAGTAA
5_ITS1F	TTCAGCATCTTGGTCATTTAGAGGAAGTAA
6_ITS1F	TTCAGTATCTTGGTCATTTAGAGGAAGTAA
7_ITS1F	TTCAGTCTCTTGGTCATTTAGAGGAAGTAA
8_ITS1F	TTCAGTGTCTTGGTCATTTAGAGGAAGTAA
9_ITS1F	TTCGATAGCTTGGTCATTTAGAGGAAGTAA
10_ITS1F	TTCGACAGCTTGGTCATTTAGAGGAAGTAA
11_ITS1F	TTCGACATCTTGGTCATTTAGAGGAAGTAA
12_ITS1F	TTCGATCTCTTGGTCATTTAGAGGAAGTAA
13_ITS1F	TTCGAGATCTTGGTCATTTAGAGGAAGTAA
14_ITS1F	TTCGAGCTCTTGGTCATTTAGAGGAAGTAA
15_ITS1F	TTGACTAGCTTGGTCATTTAGAGGAAGTAA
16_ITS1F	TTGACGATCTTGGTCATTTAGAGGAAGTAA
17_ITS1F	TTGACATGCTTGGTCATTTAGAGGAAGTAA
18_ITS1F	TTGACAGTCTTGGTCATTTAGAGGAAGTAA
19_ITS1F	TTACGTAGCTTGGTCATTTAGAGGAAGTAA
20_ITS1F	TTACGATGCTTGGTCATTTAGAGGAAGTAA
21_ITS1F	TTACGATACTTGGTCATTTAGAGGAAGTAA
22_ITS1F	TTACATAGCTTGGTCATTTAGAGGAAGTAA
A_ITS2R	TTCTACTAGCTGCGTTCTTCATCGATGC
B_ITS2R	TTCTCATAGCTGCGTTCTTCATCGATGC
C_ITS2R	TTCTCTCAGCTGCGTTCTTCATCGATGC
D_ITS2R	TTCTCACAGCTGCGTTCTTCATCGATGC
E_ITS2R	TTCTCACTGCTGCGTTCTTCATCGATGC
F_ITS2R	TTCATACTGCTGCGTTCTTCATCGATGC
G_ITS2R	TTCAGACTGCTGCGTTCTTCATCGATGC
H_ITS2R	TTGCTGCGTTCTTCATCGATGC

Table 3. Sampled adults, including taxon code, site, and the individual-diagnostic combination of barcoded forward ITS-1F primer and barcoded reverse ITS-2R primer. The eight *Metrosideros* taxa are *M. polymorpha* (*M.p.*) var. *incana* (I), *M*.p.v. *glaberrima* (G), *M. tremuloides* (T), *M.p.* race L (L), *M.p.* race F (F), *M. p.* race B (B), *M. rugosa* (R), and *M. p.* race *prostrata* (A). Kuliou‘ou and Wiliwilinui were treated as one (combined) site because of their close proximity, similar environmental conditions, and limited sampling within sites.

Sample	Taxon	Site	ITS-1F	ITS-2R
O32	L	‘Aiea Ridge	1	A
O33	L	‘Aiea Ridge	1	B
O35	L	‘Aiea Ridge	1	C
O36	L	‘Aiea Ridge	1	D
O37	L	‘Aiea Ridge	1	E
O38	L	‘Aiea Ridge	1	F
O40	L	‘Aiea Ridge	1	G
O43	L	‘Aiea Ridge	1	H
O46	L	‘Aiea Ridge	2	A
O52	L	‘Aiea Ridge	2	B
O79	L	‘Aiea Ridge	2	C
O48	G	‘Aiea Ridge	2	D
O50	G	‘Aiea Ridge	2	E
O51	G	‘Aiea Ridge	2	F
O53	G	‘Aiea Ridge	2	G
O54	G	‘Aiea Ridge	2	H
O56	G	‘Aiea Ridge	3	A
O57	G	‘Aiea Ridge	3	B
O61	G	‘Aiea Ridge	3	C
O62	G	‘Aiea Ridge	3	D
O66	G	‘Aiea Ridge	3	E
O69	G	‘Aiea Ridge	3	F
O72	I	‘Aiea Ridge	3	G
O75	I	‘Aiea Ridge	3	H
O76	I	‘Aiea Ridge	4	A
O77	I	‘Aiea Ridge	4	B
O78	I	‘Aiea Ridge	4	C
O87	I	‘Aiea Ridge	4	D
O88	I	‘Aiea Ridge	4	E
O89	I	‘Aiea Ridge	4	F
O90	I	‘Aiea Ridge	4	G
O91	I	‘Aiea Ridge	4	H
O92	I	‘Aiea Ridge	5	A

Table 3. (Continued)

Sample	Taxon	Site	ITS-1F	ITS-2R
O98	R	Wiliwilinui	5	B
O99	R	Wiliwilinui	5	C
O100	R	Wiliwilinui	5	D
O101	R	Wiliwilinui	5	E
O102	R	Wiliwilinui	5	F
O103	R	Wiliwilinui	5	G
O104	R	Wiliwilinui	5	H
O105	R	Wiliwilinui	6	A
O106	R	Wiliwilinui	6	B
O107	R	Wiliwilinui	6	C
O108	R	Wiliwilinui	6	D
O119	F	Konahuanui	6	E
O120	F	Konahuanui	6	F
O122	F	Konahuanui	6	G
O125	F	Konahuanui	6	H
O127	F	Konahuanui	7	A
O128	F	Konahuanui	7	B
O131	F	Konahuanui	7	C
O134	F	Konahuanui	7	D
O138	F	Konahuanui	7	E
O141	F	Konahuanui	7	F
O142	F	Konahuanui	7	G
O132	T	Konahuanui	7	H
O137	T	Konahuanui	8	A
O139	T	Konahuanui	8	B
O143	T	Konahuanui	8	C
O145	T	Konahuanui	8	D
O146	T	Konahuanui	8	E
O148	T	Konahuanui	8	F
O151	T	Konahuanui	8	G
O154	T	Konahuanui	8	H
O155	T	Konahuanui	9	A
O156	T	Konahuanui	9	B
O175	L	Mt. Ka‘ala	9	C
O177	L	Mt. Ka‘ala	9	D
O179	L	Mt. Ka‘ala	9	E
O180	L	Mt. Ka‘ala	9	F

Table 3. (Continued)

Sample	Taxon	Site	ITS-1F	ITS-2R
O183	L	Mt. Ka‘ala	9	G
O185	L	Mt. Ka‘ala	9	H
O187	L	Mt. Ka‘ala	10	A
O189	L	Mt. Ka‘ala	10	B
O191	L	Mt. Ka‘ala	10	C
O194	L	Mt. Ka‘ala	10	D
O195	L	Mt. Ka‘ala	10	E
O176	F	Mt. Ka‘ala	10	F
O178	F	Mt. Ka‘ala	10	G
O181	F	Mt. Ka‘ala	10	H
O182	F	Mt. Ka‘ala	11	A
O184	F	Mt. Ka‘ala	11	B
O186	F	Mt. Ka‘ala	11	C
O188	F	Mt. Ka‘ala	11	D
O190	F	Mt. Ka‘ala	11	E
O192	F	Mt. Ka‘ala	11	F
O193	F	Mt. Ka‘ala	11	G
O197	F	Mt. Ka‘ala	11	H
O210	T	Mt. Ka‘ala	12	A
O211	T	Mt. Ka‘ala	12	B
O212	T	Mt. Ka‘ala	12	C
O213	T	Mt. Ka‘ala	12	D
O214	T	Mt. Ka‘ala	12	E
O215	T	Mt. Ka‘ala	12	F
O216	T	Mt. Ka‘ala	12	G
O217	T	Mt. Ka‘ala	12	H
O218	T	Mt. Ka‘ala	13	A
O219	T	Mt. Ka‘ala	13	B
O220	T	Mt. Ka‘ala	13	C
O225	G	Mt. Ka‘ala	13	D
O226	G	Mt. Ka‘ala	13	E
O227	G	Mt. Ka‘ala	13	F
O228	G	Mt. Ka‘ala	13	G
O229	G	Mt. Ka‘ala	13	H
O230	G	Mt. Ka‘ala	14	A
O231	G	Mt. Ka‘ala	14	B
O232	G	Mt. Ka‘ala	14	C

Table 3. (Continued)

Sample	Taxon	Site	ITS-1F	ITS-2R
O233	G	Mt. Ka‘ala	14	D
O234	G	Mt. Ka‘ala	14	E
O235	G	Mt. Ka‘ala	14	F
O296	B	Konahuanui	14	G
O297	B	Konahuanui	14	H
O298	B	Konahuanui	15	A
O299	B	Konahuanui	15	B
O300	B	Konahuanui	15	C
O301	B	Konahuanui	15	D
O302	B	Konahuanui	15	E
O303	B	Konahuanui	15	F
O304	B	Konahuanui	15	G
O305	B	Konahuanui	15	H
O306	B	Konahuanui	16	A
O295	R	Konahuanui	16	B
O311	R	Konahuanui	16	C
O312	R	Konahuanui	16	D
O313	R	Konahuanui	16	E
O314	R	Konahuanui	16	F
O315	R	Konahuanui	16	G
O316	R	Konahuanui	16	H
O317	R	Konahuanui	17	A
O318	R	Konahuanui	17	B
O319	R	Konahuanui	17	C
O320	R	Konahuanui	17	D
O322	I	Kuliou‘ou	17	E
O324	I	Wiliwilinui	17	F
O326	I	Wiliwilinui	17	G
O327	I	Wiliwilinui	17	H
O328	I	Wiliwilinui	18	A
O333	I	Wiliwilinui	18	B
O337	I	Wiliwilinui	18	C
O386	I	Kuliou‘ou	18	D
O387	I	Kuliou‘ou	18	E
O388	I	Kuliou‘ou	18	F
O389	I	Kuliou‘ou	18	G
O323	G	Wiliwilinui	18	H

Table 3. (Continued)

Sample	Taxon	Site	ITS-1F	ITS-2R
O325	G	Wiliwilinui	19	A
O329	G	Wiliwilinui	19	B
O330	G	Wiliwilinui	19	C
O331	G	Wiliwilinui	19	D
O332	G	Wiliwilinui	19	E
O334	G	Wiliwilinui	19	F
O335	G	Wiliwilinui	19	G
O336	G	Wiliwilinui	19	H
O338	G	Wiliwilinui	20	A
O390	G	Kuliou‘ou	20	B
O393	B	Kuliou‘ou	20	C
O394	B	Kuliou‘ou	20	D
O395	B	Kuliou‘ou	20	E
O404	B	Wiliwilinui	20	F
O405	B	Wiliwilinui	20	G
O406	B	Wiliwilinui	20	H
O407	B	Wiliwilinui	21	A
O408	B	Wiliwilinui	21	B
O409	B	Wiliwilinui	21	C
O410	B	Wiliwilinui	21	D
O411	B	Wiliwilinui	21	E
O500	A	‘Aiea Ridge	21	F
O501	A	‘Aiea Ridge	21	G
O502	A	‘Aiea Ridge	21	H
O503	A	‘Aiea Ridge	22	A
O504	A	‘Aiea Ridge	22	B
O505	A	‘Aiea Ridge	22	C
O506	A	‘Aiea Ridge	22	D
O507	A	‘Aiea Ridge	22	E
O508	A	‘Aiea Ridge	22	F
O509	A	‘Aiea Ridge	22	G
O510	A	‘Aiea Ridge	22	H

Table 4. Of the original sampling (n = 176 trees, 11 trees/taxon/site), the number of successful PCR products and number of amplified samples that were successfully quantified in the bioanalyzer for downstream reactions are shown for each sampled taxon at each site. *M. p.* is *M. polymorpha*. The four sites were Mt. Ka‘ala (MK), ‘Aiea Ridge (AR), Konahuanui (KHN), and the joint Wiliwilinui-Kuliou‘ou (WWNKOO) site.

Site	***Metrosideros* taxon**	**Successful PCRs (n = 144 trees)**	**Quantified (n = 132 trees)**
MK	*M. p.* race F	11	10
	M. p. var. *glaberrima*	8	8
	M. p. race L	11	11
	M. tremuloides	6	5
AR	*M. p.* race *prostrata*	8	5
	M. p. var. *glaberrima*	5	5
	M. p. var. *incana*	11	10
	M. p. race L	9	9
KHN	*M. p.* race B	9	9
	M. p. race F	11	11
	M. rugosa	8	8
	M. tremuloides	11	11
WWNKOO	*M. p.* race B	11	9
	M. p. var. *glaberrima*	7	5
	M. p. var. *incana*	8	6
	M. rugosa	10	10

Table 5. Post-sequencing quality-control trimming of demultiplexed samples. Initial number of trees per taxon per site before trimming, then removal of singletons, doublets, and non-fungal sequences, and lastly further trimming of other unmatched sequences (n = 113). The four sites were Mt. Ka‘ala (MK), ‘Aiea Ridge (AR), Konahuanui (KHN), and the joint Wiliwilinui-Kuliou‘ou (WWNKOO) site.

Site	**Sample taxon**	**Quality Controls (QC)**		
		Pre-QC tree count (n = 115 trees)	**Trees with non-doublets, non-singletons, fungal sequences (n = 114 trees)**	**Trees without other unmatched sequences (n = 113 trees)**
MK	*M. p.* race F	8	8	8
	M. p. race L	10	10	10
	M. p. var. *glaberrima*	7	7	7
	M. tremuloides	5	5	5
AR	*M. p.* race *prostrata*	4	4	4
	M. p. race L	8	8	7
	M. p. var. *glaberrima*	5	5	5
	M. p. var. *incana*	8	8	8
KHN	*M. p.* race B	7	7	7
	M. rugosa	7	7	7
	M. p. race F	10	10	10
	M. tremuloides	9	9	9
WWNKOO	*M. p.* race B	8	8	8
	M. rugosa	9	8	8
	M. p. var. *glaberrima*	4	4	4
	M. p. var. *incana*	6	6	6

Table 6. Permutation analysis of variance for Bray-Curtis dissimilarity. Tested explanatory variables were *Metrosideros* taxon (host taxon), site, an interaction (:) of taxon with site, relative elevation (high vs. low), absolute elevation, and sample outliers.

Variable	df	SS	F	r^2	P
Host taxon	7	6.15	2.069	0.115	**0.001**
Site	3	2.936	2.306	0.055	**0.001**
Host taxon : Site	5	2.907	1.370	0.054	**0.001**
Relative elevation	1	0.381	0.884	0.007	0.715
Absolute elevation	1	0.607	1.408	0.011	**0.031**
Sample outliers	1	0.430	0.905	0.008	0.655

Table 7. The best-fit models for Shannon diversity. In addition to the best-fit model are rival models differing by the inclusion (+), exclusion (-), or interaction (:) of other explanatory variables for FE diversity with *Metrosideros* taxon (host taxon), site, relative elevation (high vs. low), and absolute elevation. (RSS: Residual Sum of Squares)

AIC	df	RSS	AIC
Absolute elevation, Host taxon, Site (best model)		65.05	-38.40
- Site	3	69.47	-36.97
+ Relative elevation	1	64.78	-36.87
+ Host taxon : Site	7	59.01	-35.42
- Absolute elevation	1	69.47	-32.97
- Host taxon	7	81.70	-26.65

Table 8. ANOVA models for Shannon diversity with absolute elevation, *Metrosideros* taxon (Host taxon), site, relative elevation (high vs. low), and an interaction (:) of taxon with site.

Model	df	SS	F	P
Absolute elevation	1	1.12	1.78	0.19
Host taxon	7	21.77	4.95	**<0.001**
Site	3	4.42	2.35	0.07
Relative elevation	1	0.27	0.43	0.51
Host taxon : Site	6	5.77	1.53	0.18

Table 9. ANOVA models for Shannon diversity with leaf type, host taxon, and site.

Model	df	SS	F	P
Leaf type	1	0.06	0.09	0.77
Host taxon	6	22.50	5.51	**<0.01**
Site	3	0.33	0.16	0.92

Table 10. ANOVA models for Shannon diversity with leaf type, sites, absolute elevation as well as interactions (:) of leaf type with site, leaf type with absolute elevation, site with absolute elevation, and leaf type with site and absolute elevation.

Model	df	SS	F	P
Leaf type	1	0.06	0.09	0.76
Site	3	2.64	1.33	0.27
Absolute elevation	1	8.85	13.37	**<0.01**
Leaf type : Site	3	0.46	0.23	0.87
Leaf type : Absolute elevation	1	6.78	10.26	**<0.01**
Site : Absolute elevation	3	2.92	1.47	0.23
Leaf type : Site : Absolute elevation	3	6.48	3.26	0.02

Table 11. ANOVA models for Shannon diversity with *Metrosideros* taxon (host taxon), absolute elevation, outliers, and an interaction (:) of host taxon with absolute elevation.

Explanatory variable	df	SS	F	P
Host taxon	7	23.80	5.77	**<0.01**
Absolute elevation	1	0.58	0.99	0.32
Host taxon : Absolute elevation	7	0.50	0.86	0.55
Outliers	1	8.31	14.09	**<0.01**

Table 12. ANOVA models for host-specificity with *Metrosideros* taxon (host taxon), absolute elevation, and interactions (:) between explanatory variables.

Explanatory Variable	df	SS	F	P
Absolute elevation	1	0.06	0.06	0.81
Host taxon	7	9.80	1.53	0.17
Absolute elevation : Host taxon	7	18.89	2.95	**0.01**

Table 13. Five fungal phyla matched with 1,301 ESVs from 113 samples. Table shows frequencies and percentages.

Phylum	Freq	%
Ascomycota	1003	77.04
Basidiomycota	291	22.35
Mucoromycota	6	0.46
Chytridiomycota	1	0.08
Mortierellomycota	1	0.08

Table 14. Twenty fungal classes matched with 1,161 ESVs from 113 samples. Table shows frequencies and percentages. Classes marked with asterisk (*) belong to the subphylum Pezizomycotina.

Class	Freq	%
Dothideomycetes*	442	38.04
Sordariomycetes*	171	14.72
Eurotiomycetes*	135	11.62
Agaricomycetes	123	10.59
Leotiomycetes*	77	6.63
Tremellomycetes	70	6.02
Microbotryomycetes	44	3.79
Orbiliomycetes*	22	1.89
Lecanoromycetes*	19	1.64
Cystobasidiomycetes	18	1.55
Taphrinomycetes	12	1.03
Pucciniomycetes	8	0.69
Umbelopsidomycetes	6	0.52
Exobasidiomycetes	5	0.43
Saccharomycetes	4	0.34
Ustilaginomycetes	2	0.17
Agaricostilbomycetes	1	0.09
Mortierellomycetes	1	0.09
Pezizomycetes*	1	0.09
Spizellomycetes	1	0.09

Table 15. Fifty-eight fungal orders matched with 1,044 ESVs. Table shows frequencies and percentages.

Order	Freq	%
Capnodiales	250	23.92
Pleosporales	118	11.29
Chaetothyriales	84	8.04
Xylariales	77	7.37
Helotiales	75	7.18
Hypocreales	43	4.11
Tremellales	43	4.11
Microbotryomycetes_ord_Incertae_sedis	29	2.78
Agaricales	28	2.68
Polyporales	26	2.49
Orbiliales	21	2.01
Cantharellales	20	1.91
Botryosphaeriales	16	1.53
Coryneliales	16	1.53
Glomerellales	13	1.24
Phaeomoniellales	13	1.24
Taphrinales	12	1.15
Erythrobasidiales	10	0.96
Eurotiales	9	0.86
Filobasidiales	9	0.86
Auriculariales	8	0.77
Russulales	8	0.77
Sporidiobolales	8	0.77
Venturiales	8	0.77
Diaporthales	7	0.67
Myriangiales	6	0.57
Umbelopsidales	6	0.57
Hymenochaetales	5	0.48
Lecanorales	5	0.48
Ostropales	5	0.48
Sebacinales	5	0.48
Trechisporales	5	0.48
Trichosporonales	5	0.48
Chaetosphaeriales	4	0.38
Cystofilobasidiales	4	0.38

Table 15. (Continued)

Order	Freq	%
Dothideales	4	0.38
Saccharomycetales	4	0.38
Exobasidiales	3	0.29
Kriegeriales	3	0.29
Magnaporthales	3	0.29
Onygenales	3	0.29
Septobasidiales	3	0.29
Cystobasidiales	2	0.19
Cystobasidiomycetes_ord_Incertae_sedis	2	0.19
Microstromatales	2	0.19
Sordariales	2	0.19
Ustilaginales	2	0.19
Agaricostilbales	1	0.10
Caliciales	1	0.10
Hysteriales	1	0.10
Lecanoromycetes_ord_Incertae_sedis	1	0.10
Lecideales	1	0.10
Mortierellales	1	0.10
Patellariales	1	0.10
Pezizales	1	0.10
Pucciniales	1	0.10
Spizellomycetales	1	0.10
Trichosphaeriales	1	0.10

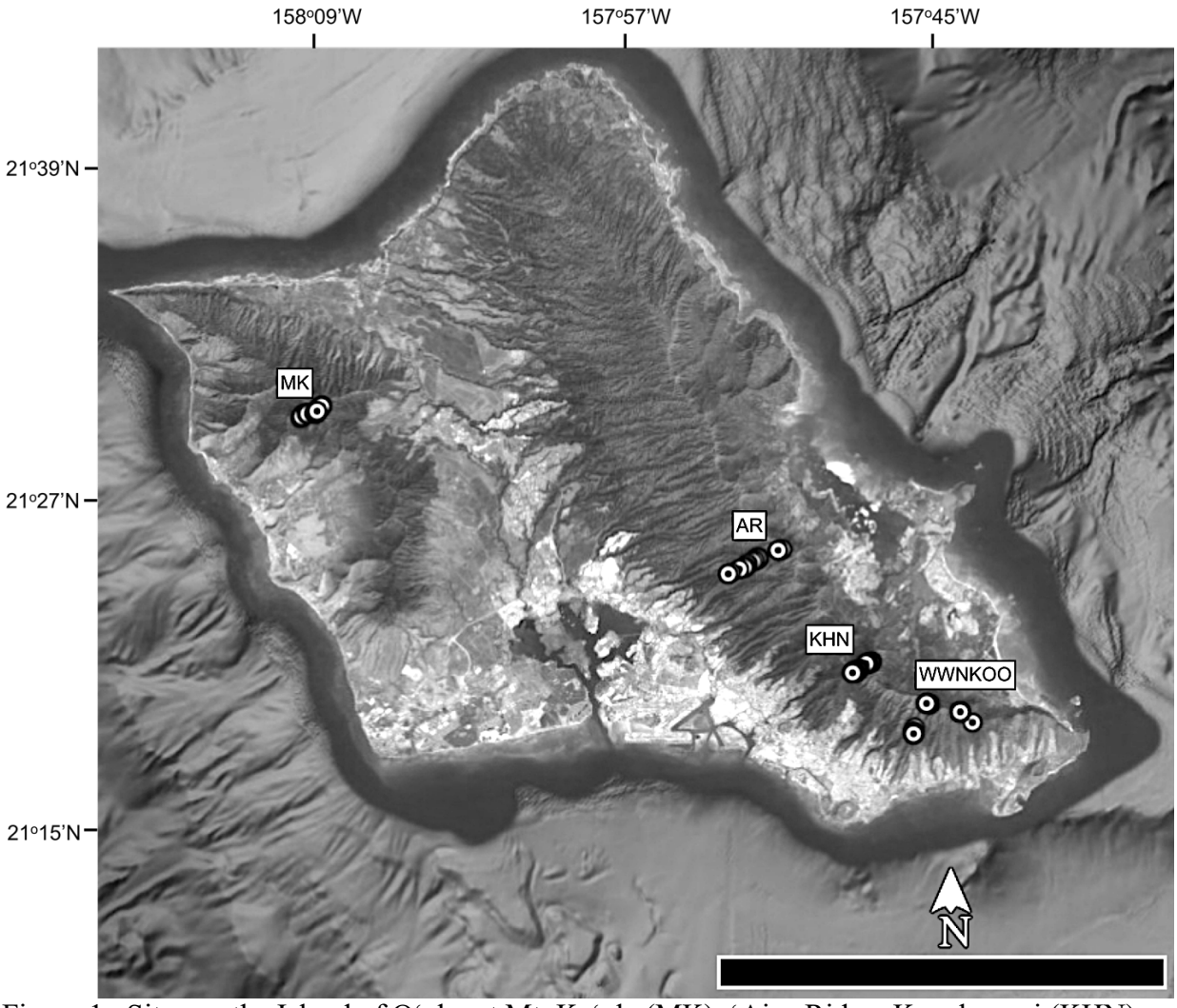

Figure 1. Sites on the Island of O‘ahu at Mt. Ka‘ala (MK), ‘Aiea Ridge, Konahuanui (KHN), and the joint Wiliwilinui-Kuliou‘ou (WWNKOO) site (Map data: Google Earth 2019a, Landsat/Copernicus; Data: SIO, NOAA, U.S. Navy, NGA, GEBCO; Data: LDEO-Columbia, NSF, NOAA). The dots indicate the locations of the sampled *Metrosideros* adults. (Scale bar = 30 km)

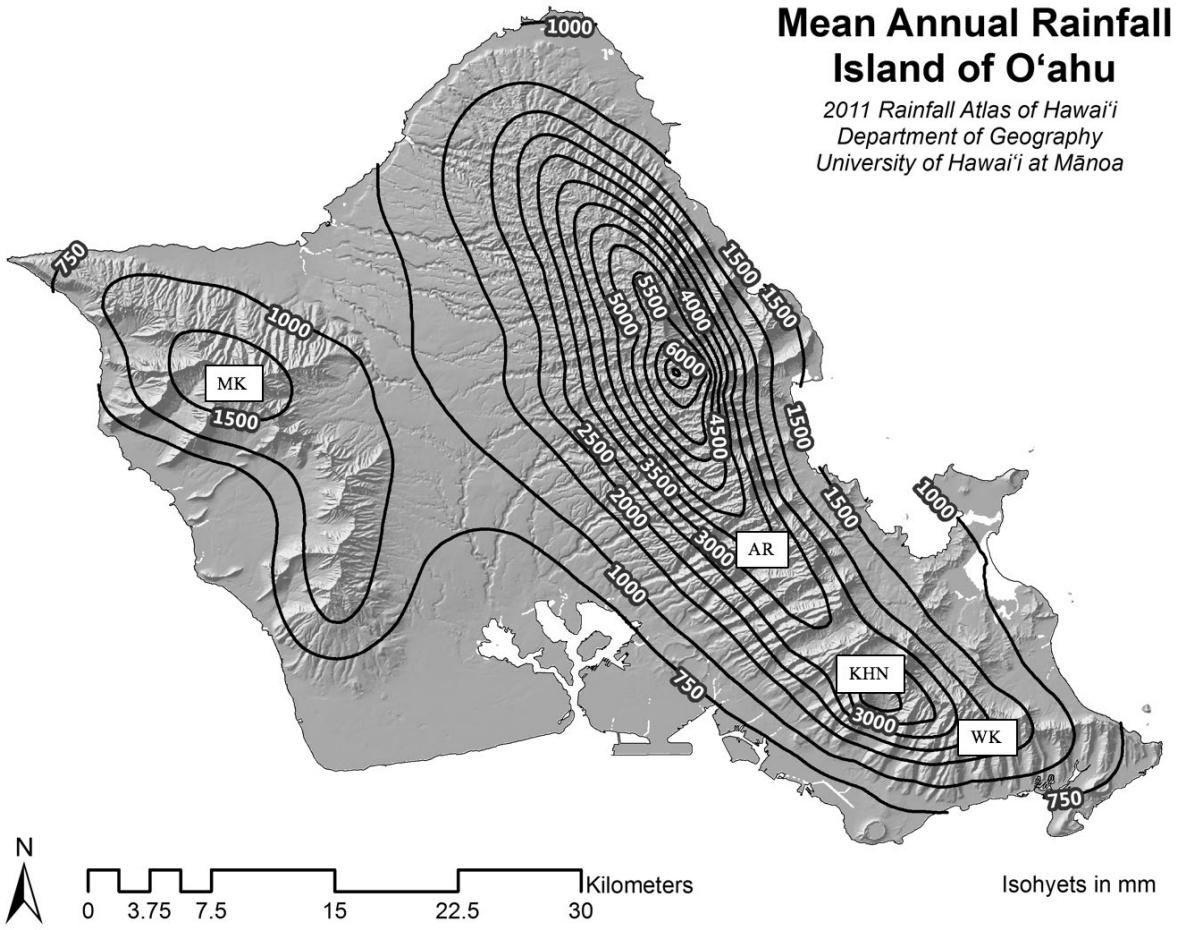

Figure 2. Mean annual rain map of the Island of O‘ahu with sites (Giambelluca et al. 2013): Mt. Ka‘ala (MK), ‘Aiea Ridge (AR), Konahuanui (KHN), and the joint Wiliwilinui-Kuliou‘ou (WK) site.

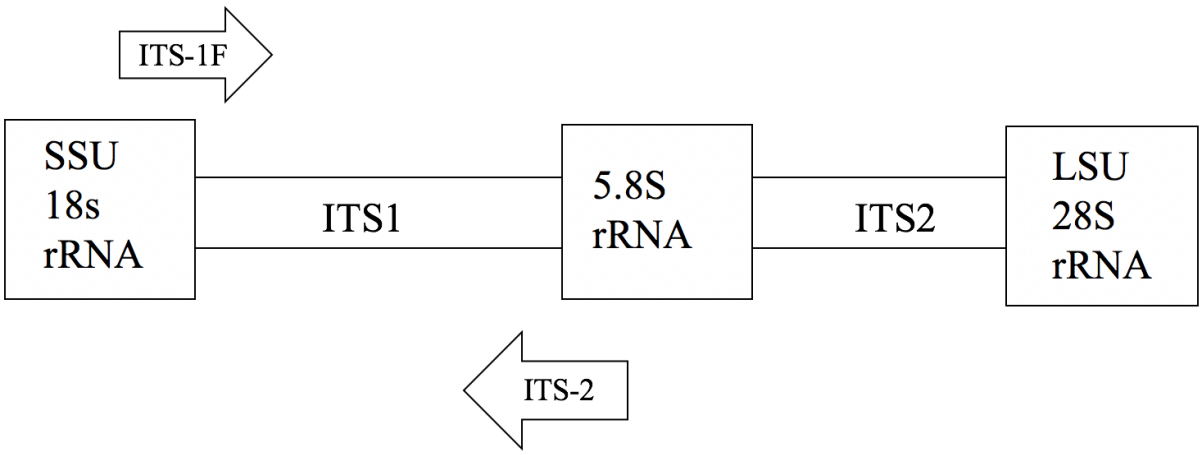

Figure 3. The two internal transcribed spacer (ITS) regions found between the 18S nuclear ribosomal small subunit (SSU) rRNA, and the 28S large subunit (LSU) rRNA. Forward and reverse primer used sequences from ITS-1F and ITS-2, respectively, from the ITS1 region (Bohs 2007).

.

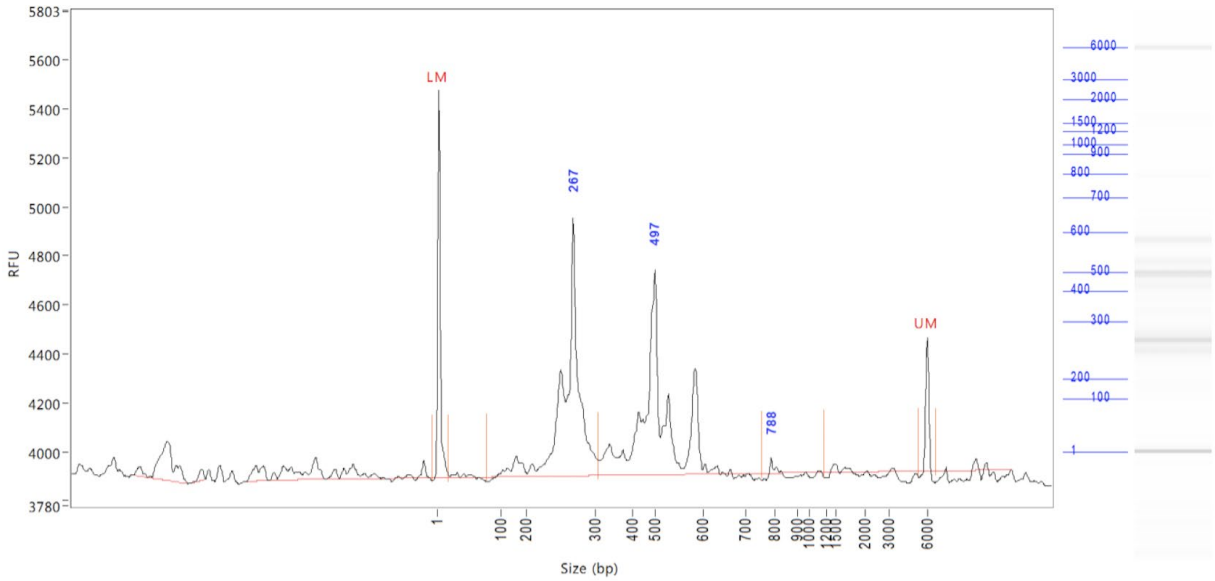

Figure 4. Electropherogram of 132 pooled samples after BluePippin purification.

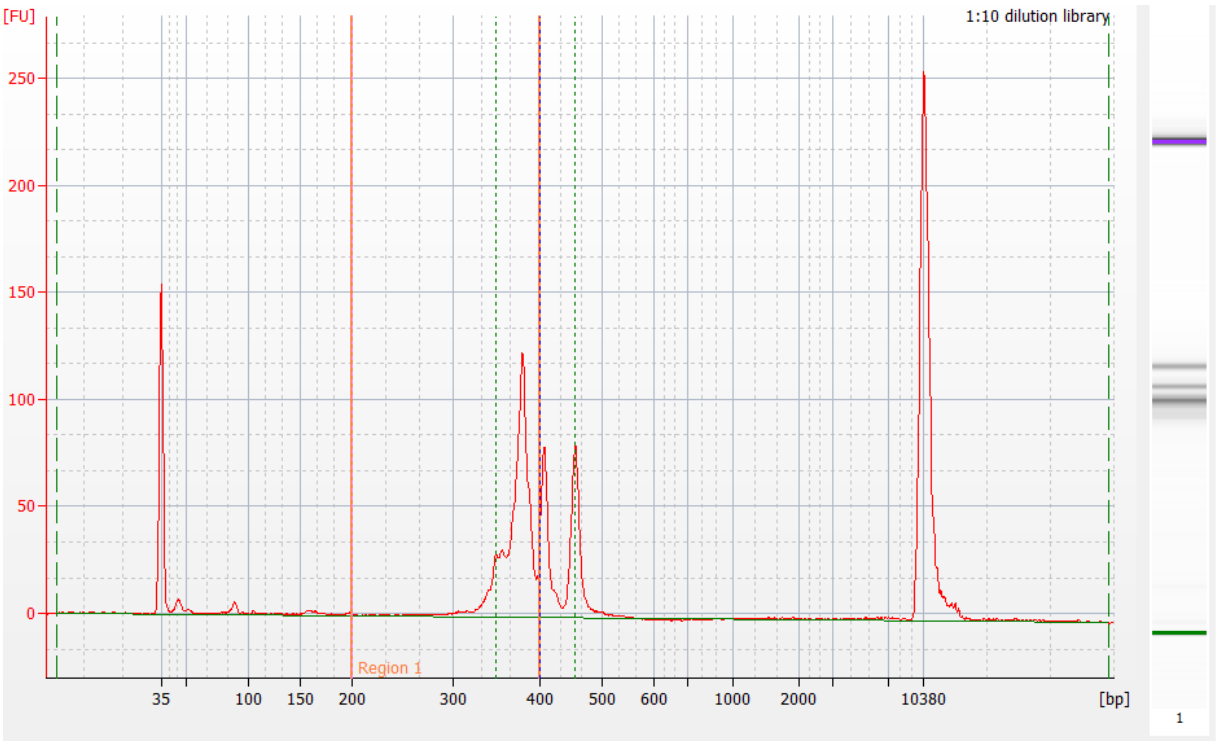

Figure 5. Bioanalyzer electropherogram of a diluted (1:10) amplified library with ligated Ion Adaptors, and Ion Xpress Barcode. At 200-600 bp, the undiluted library is 7081 pmol/l.

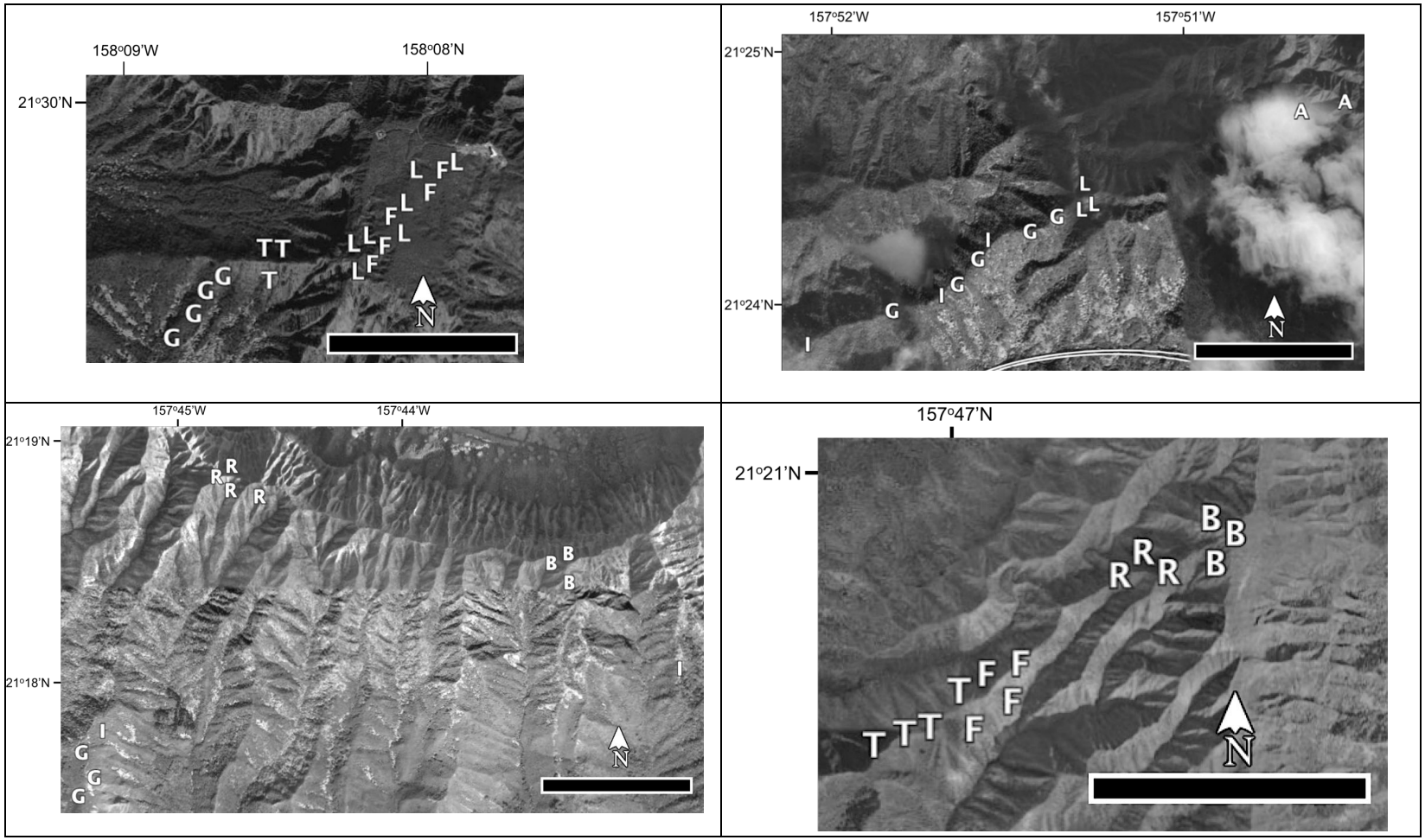

Figure 6. The distribution *Metrosideros* taxa showing the general locations final sampling (n = 113 adult plants) among sites. Clockwise from the top left: Mt. Kaʻala (Map data: Google Earth 2019b), ʻAiea Ridge (Map data: Google Earth 2019c), Konahuanui (Map data: Google Earth 2019d), and WWNKOO (Wiliwilinui and Kuliouʻou) (Map data: Google Earth 2019e). The eight *Metrosideros* taxa are *M. polymorpha* var. *incana* (I), *M. polymorpha* var. *glaberrima* (G), *M. tremuloides* (T), *M. polymorpha* race L (L), *M. polymorpha* race F (F), *M. polymorpha* race B (B), *M. rugosa* (R), and *M. polymorpha* race *prostrata* (A). (Scale bar = 1 km)

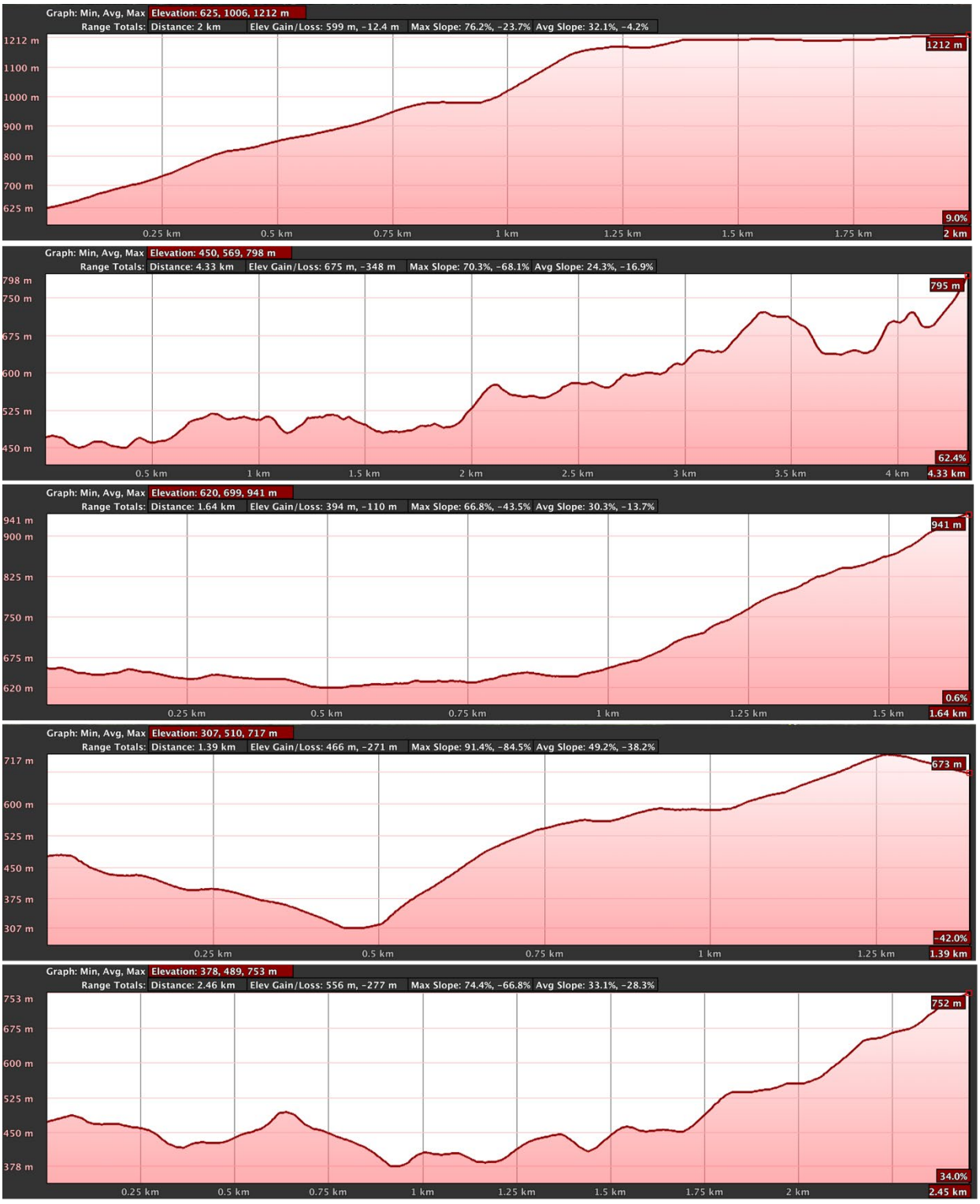

Figure 7. Elevation profiles of all sites of the final sampling (n = 113 adult plants). Top to bottom: Mt. Kaʻala, ʻAiea Ridge, Konahuanui, Wiliwilinui, and Kuliouʻou.

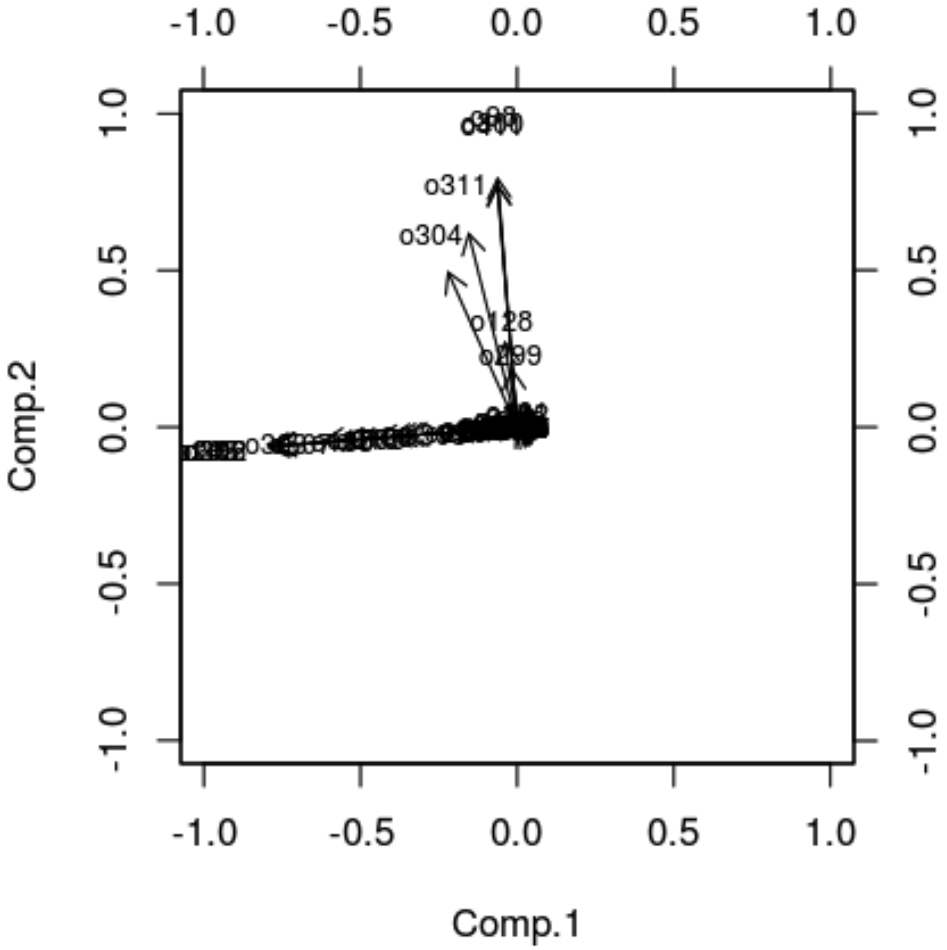

Figure 8. PCA biplot of FE relative abundance for individual samples, including 33 outliers.

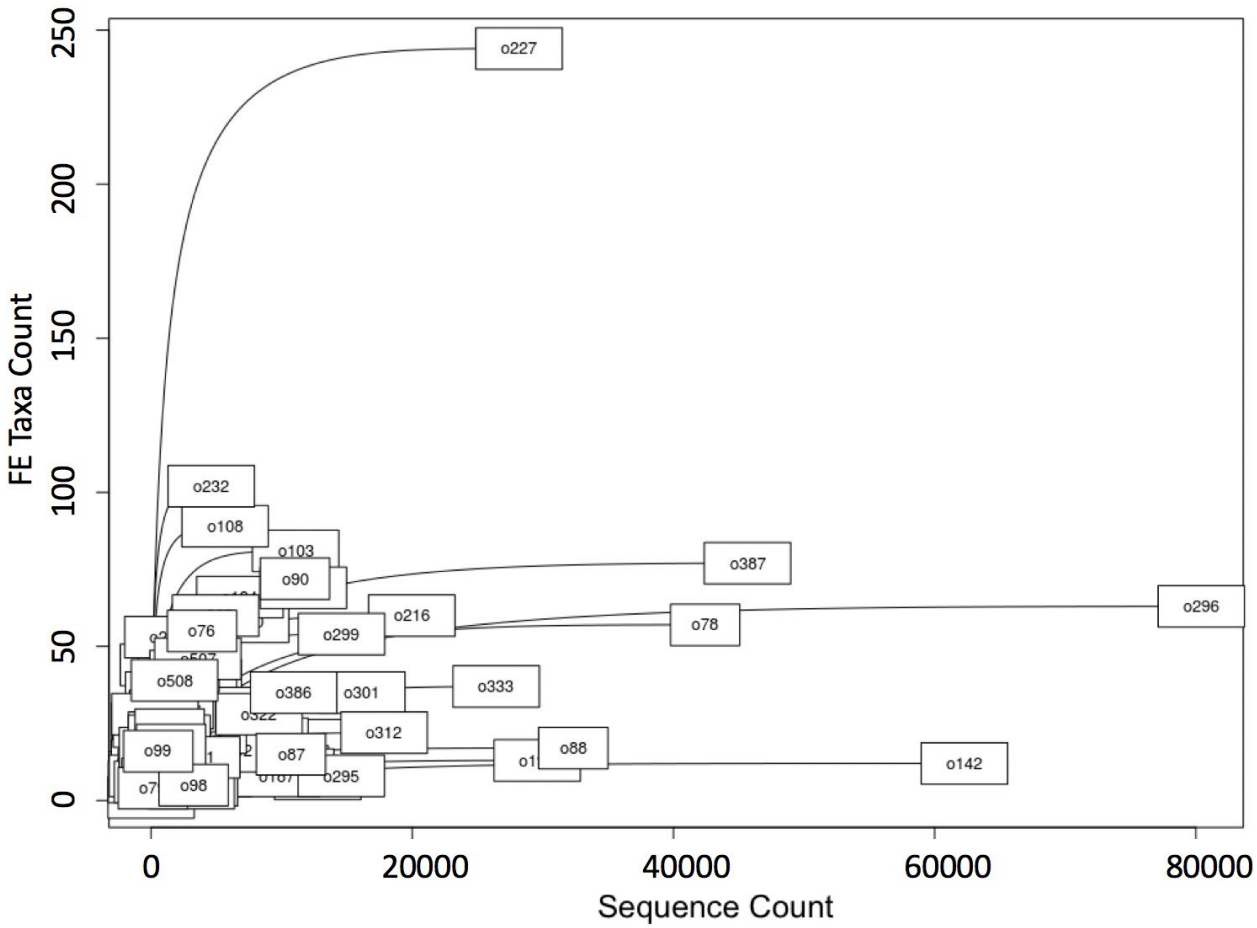

Figure 9. Rarefaction curves of FE absolute abundance for each sample (adult) with respect to the number of FE sequence reads.

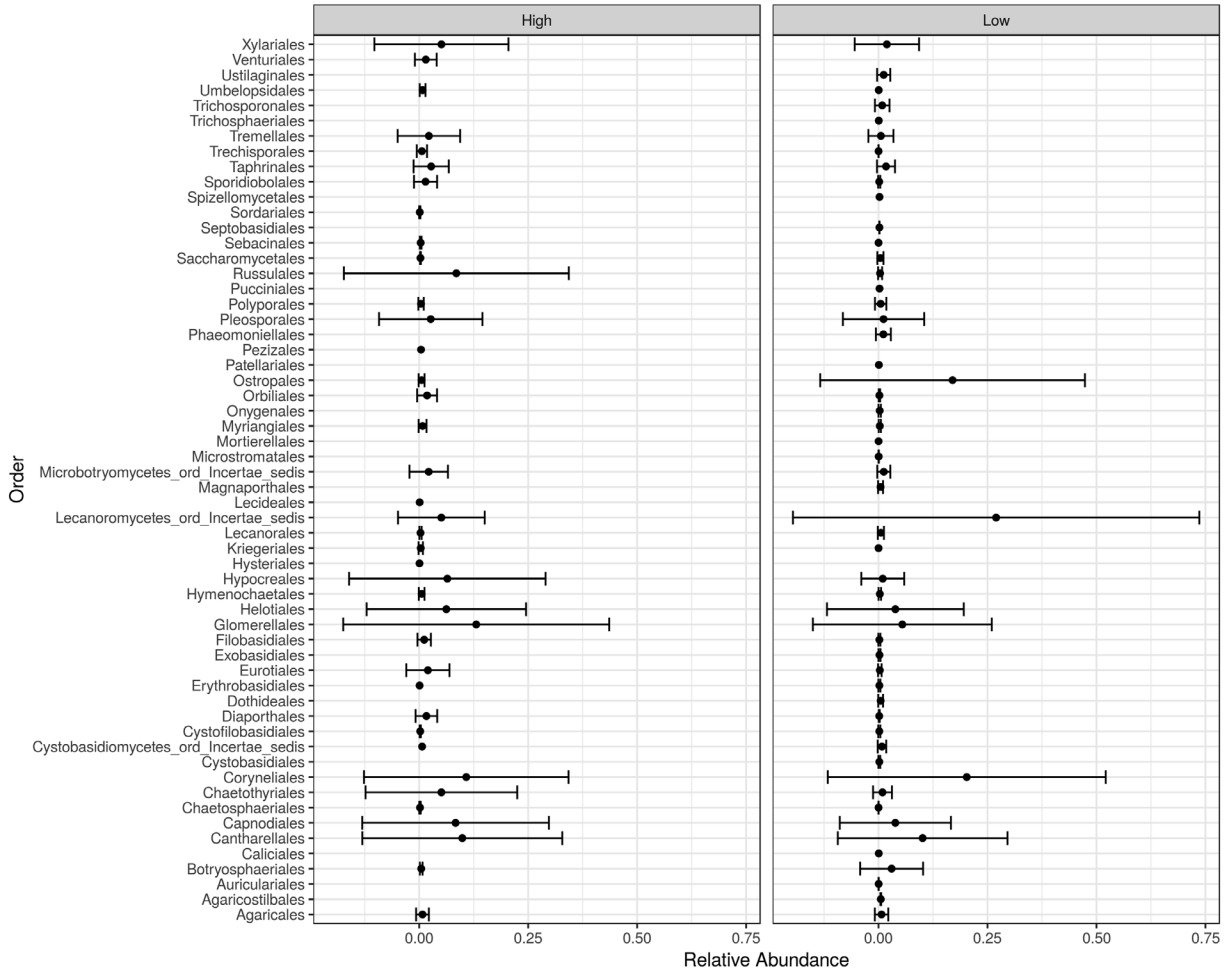

Figure 10. Relative abundance (Mean ± SD) of FE orders within relatively high-elevation and low-elevation *Metrosideros* communities sampled on four O‘ahu ridges (pooled).

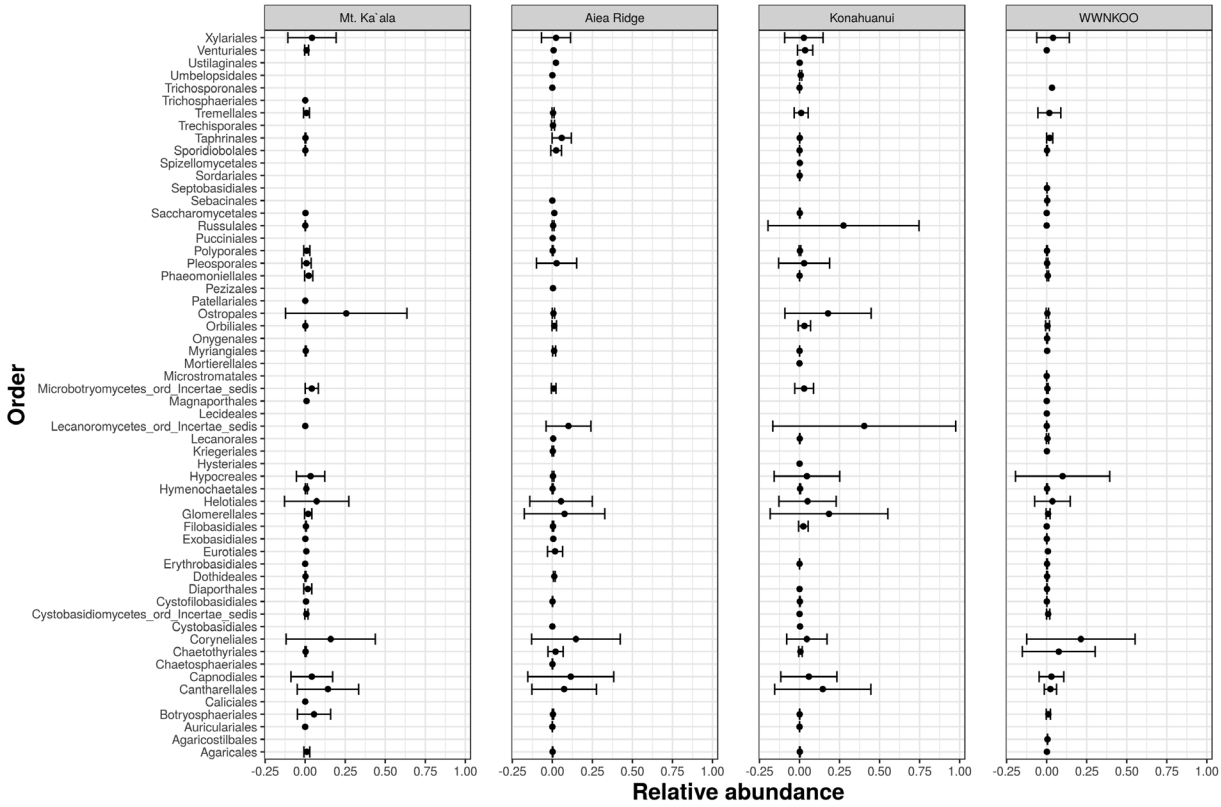

Figure 11. Relative abundance of FE orders within each of four *Metrosideros* sites: Mt. Ka‘ala, ‘Aiea Ridge, Konahuanui, and Wiliwilinui/Kuliou‘ou (WWNKOO). FEs are pooled across host taxa within sites.

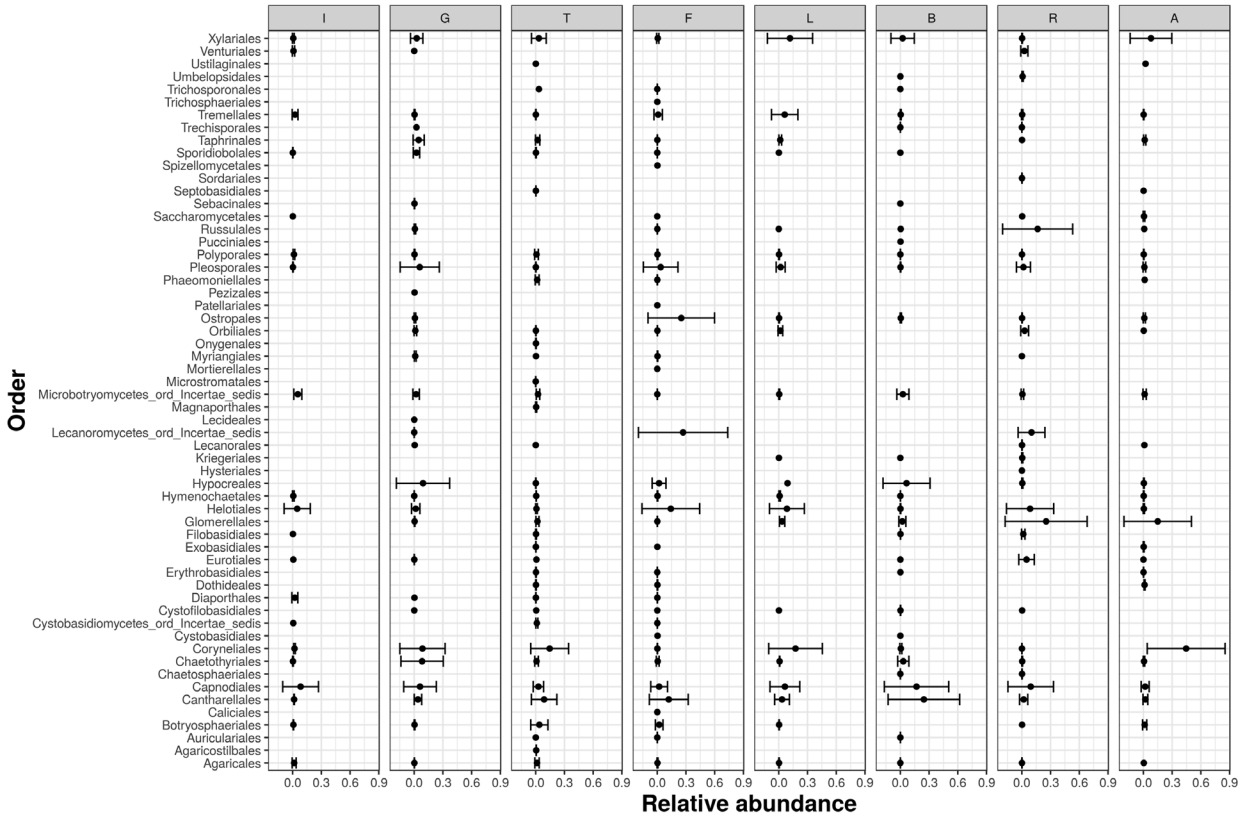

Figure 12. Relative abundance of FE orders within each of eight *Metrosideros* taxa on O‘ahu: *M. polymorpha* var. *incana* (I), *M. polymorpha* var. *glaberrima* (G), *M. tremuloides* (T), *M. polymorpha* race L (L), *M. polymorpha* race F (F), *M. polymorpha* race B (B), *M. rugosa* (R), and *M. polymorpha* race *prostrata* (A).

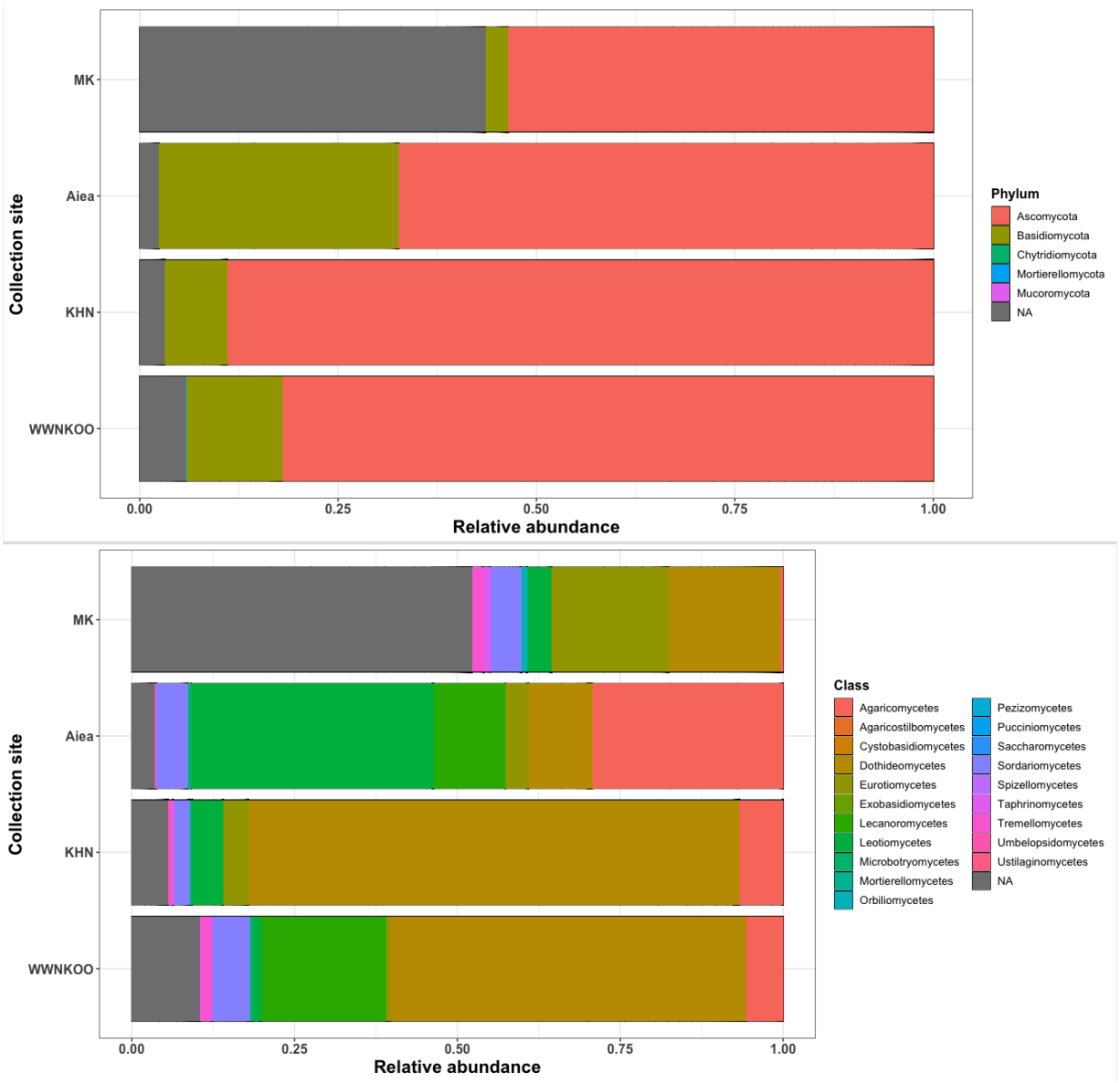

Figure 13. Relative abundance of FE phyla (Top) and classes (Bottom) among four sites (*Metrosideros* communities): Mt. Kaʻala (MK), ʻAiea Ridge (Aiea), Konahuanui (KHN), and Wiliwilinui and Kuliouʻou (WWNKOO).

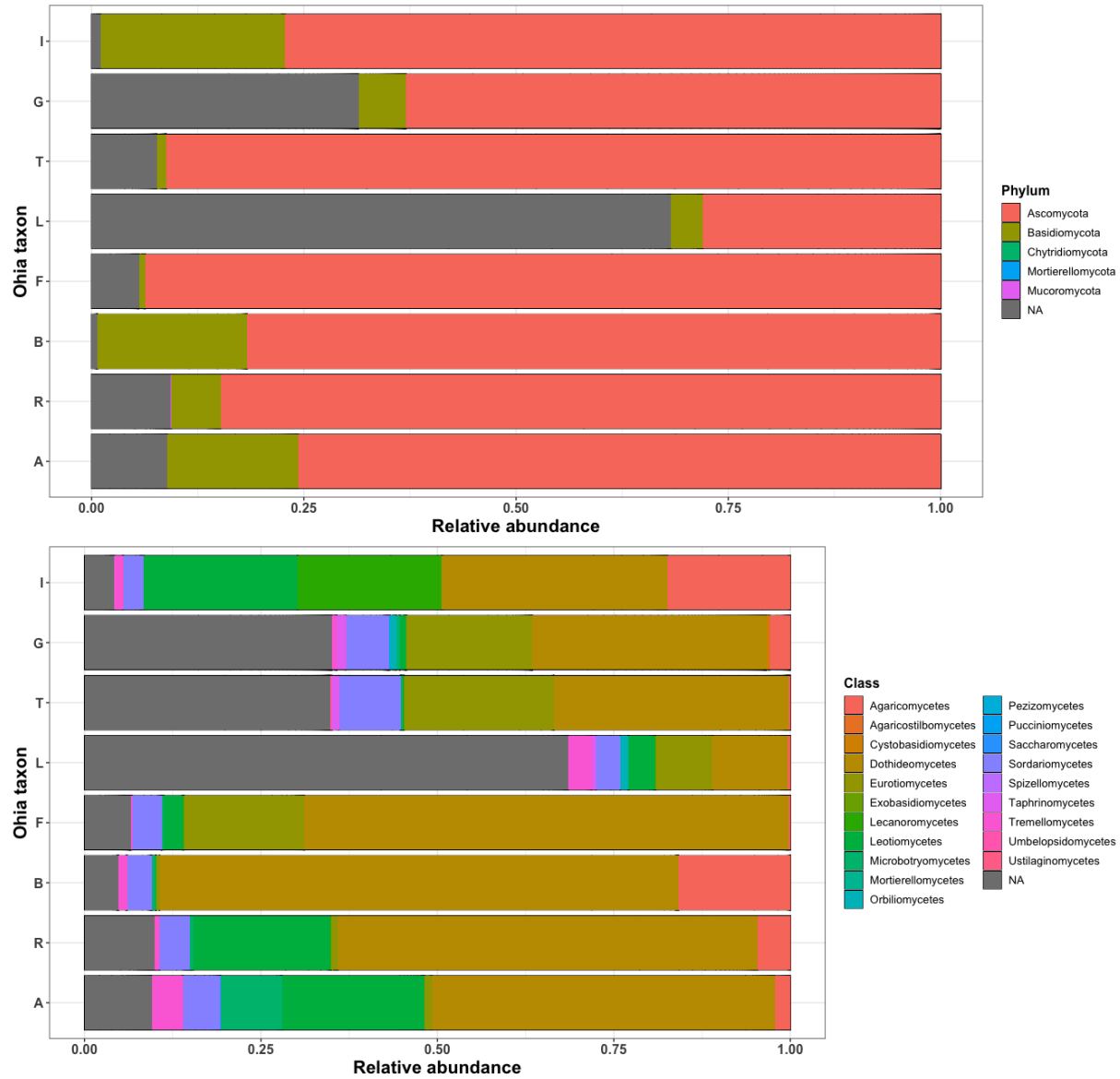

Figure 14. Relative abundance of FE phyla (Top) and classes (Bottom) within each of eight *Metrosideros* taxa: *M. polymorpha* var. *incana* (I), *M. polymorpha* var. *glaberrima* (G), *M. tremuloides* (T), *M. polymorpha* race L (L), *M. polymorpha* race F (F), *M. polymorpha* race B (B), *M. rugosa* (R), and *M. polymorpha* race *prostrata* (A).

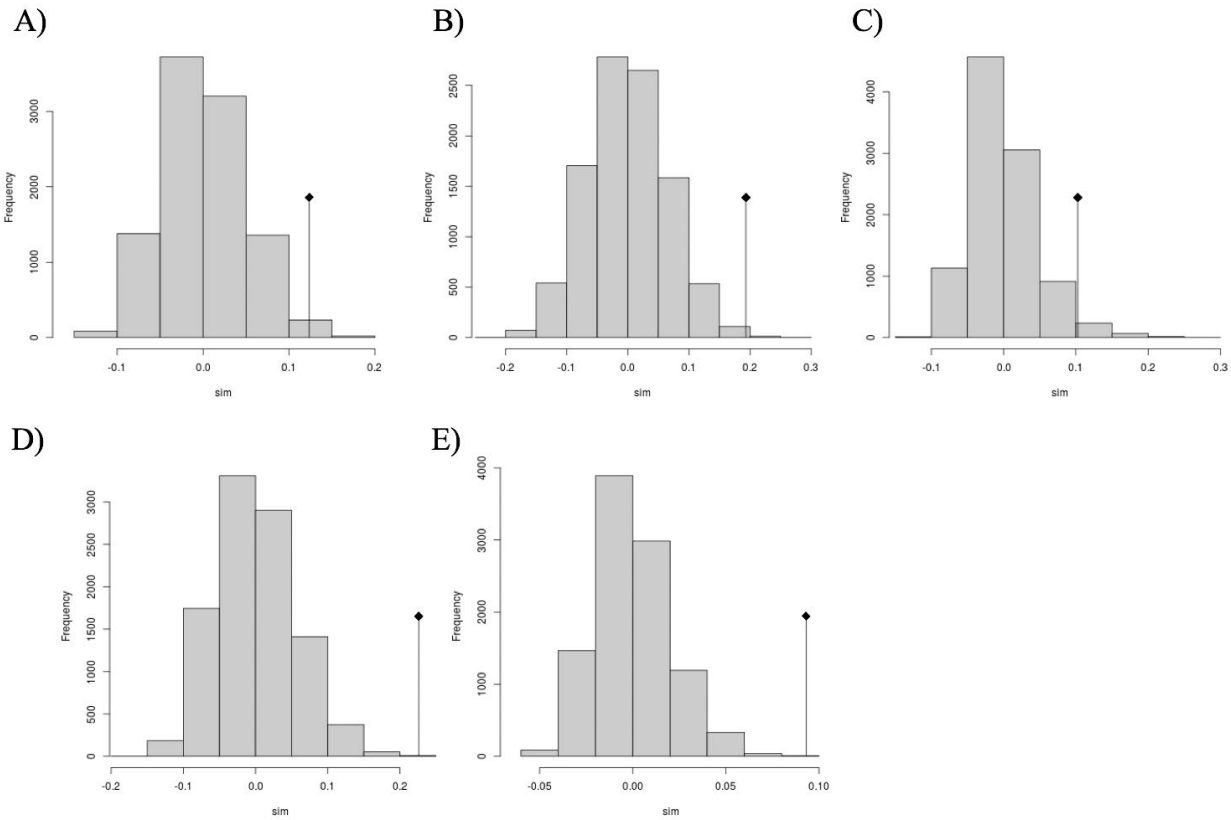

Figure 15. Mantel test histograms of Bray-Curtis distance matrix computed from FE ESV relative abundance data within each of the four *Metrosideros* communities on Oʻahu: A) Mt. Kaʻala, B) ʻAiea Ridge, C) Konahuanui, D) Kuliouʻou and Wiliwilinui, as well as E) all sites combined. The vertical diamond-tipped line marks the strength of dissimilarity correlations between FE communities and Euclidean geographic distances.

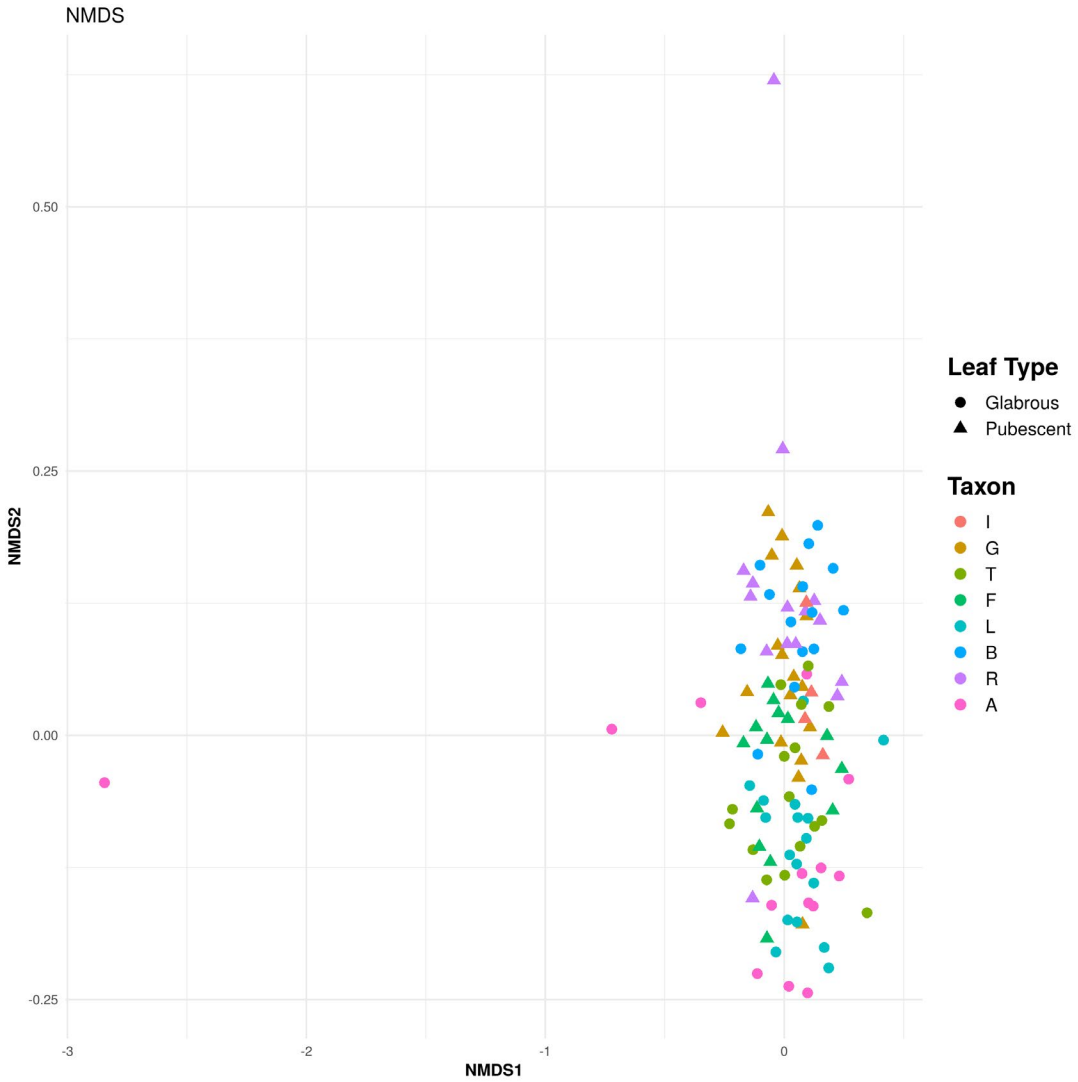

Figure 16. Non-metric dimensional scaling (NMDS) plot of the effects of leaf type and *Metrosideros* taxon on FE relative abundance. Euclidean distance is the dissimilarity measurement. The eight *Metrosideros* taxa are *M. polymorpha* var. *incana* (I), *M. polymorpha* var. *glaberrima* (G), *M. tremuloides* (T), *M. polymorpha* race L (L), *M. polymorpha* race F (F), *M. polymorpha* race B (B), *M. rugosa* (R), and *M. polymorpha* race *prostrata* (A). Each point represents one sampled adult.

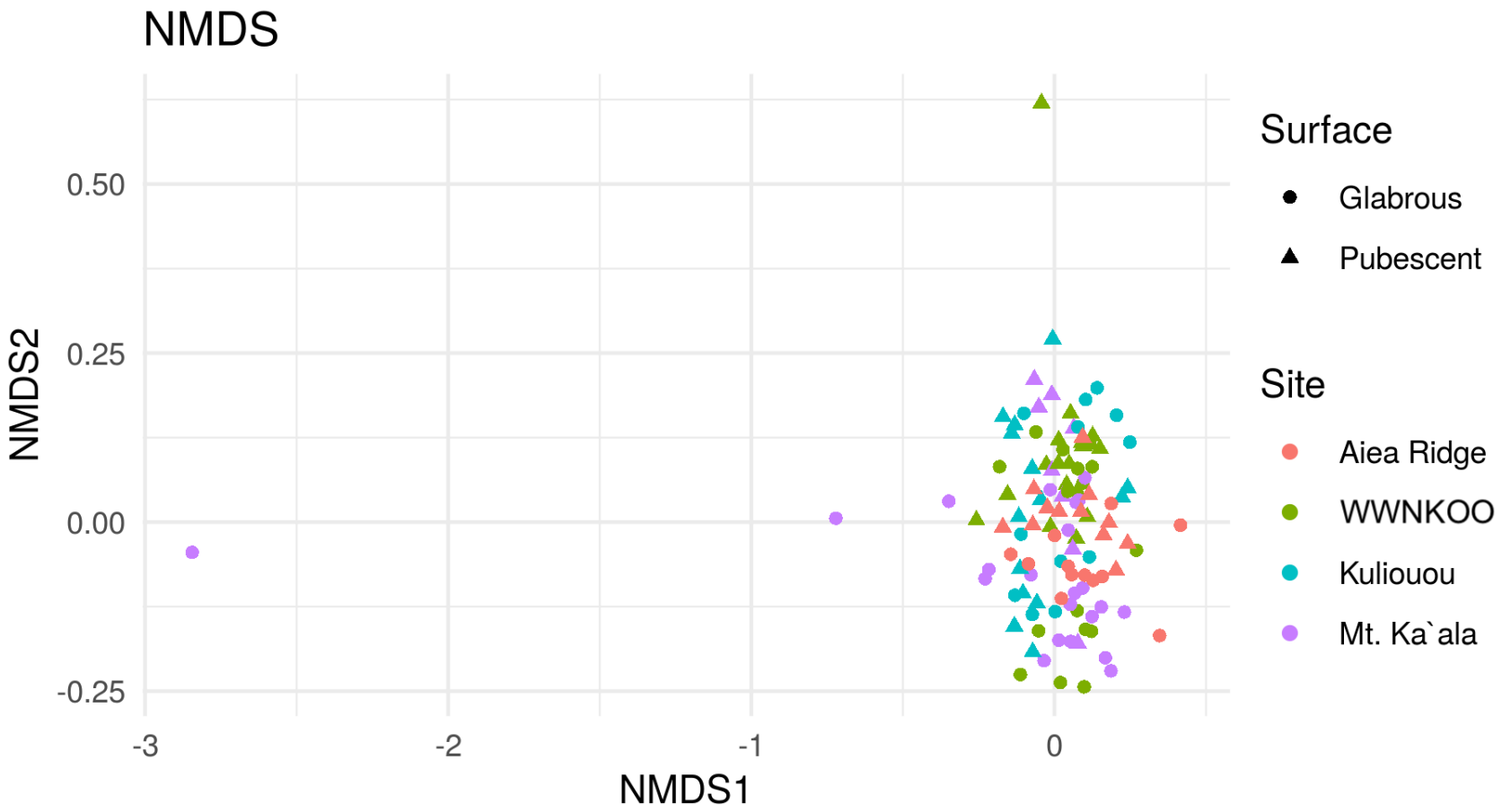

Figure 17. Non-metric dimensional scaling (NMDS) plot showing how leaf type and site influence FE relative abundance. Euclidean distance is the dissimilarity measurement for all plots. Each point represents one sampled adult.

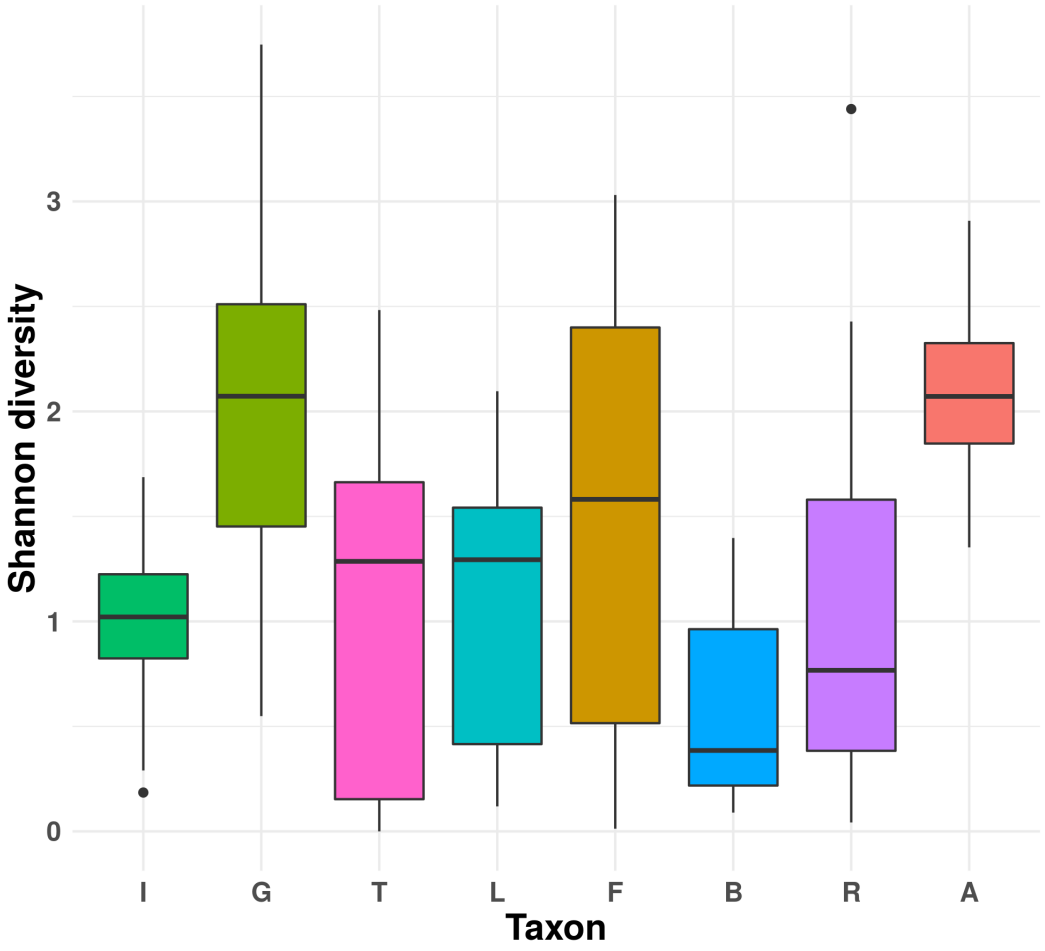

Figure 18. Shannon diversity box plots illustrating how each *Metrosideros* taxon influences FE diversity. Group of samples above 1,200 m elevation represents population at the peak of Mt. Ka‘ala. The eight *Metrosideros* taxa are *M. polymorpha* var. *incana* (I), *M. polymorpha* var. *glaberrima* (G), *M. tremuloides* (T), *M. polymorpha* race L (L), *M. polymorpha* race F (F), *M. polymorpha* race B (B), *M. rugosa* (R), and *M. polymorpha* race *prostrata* (A).

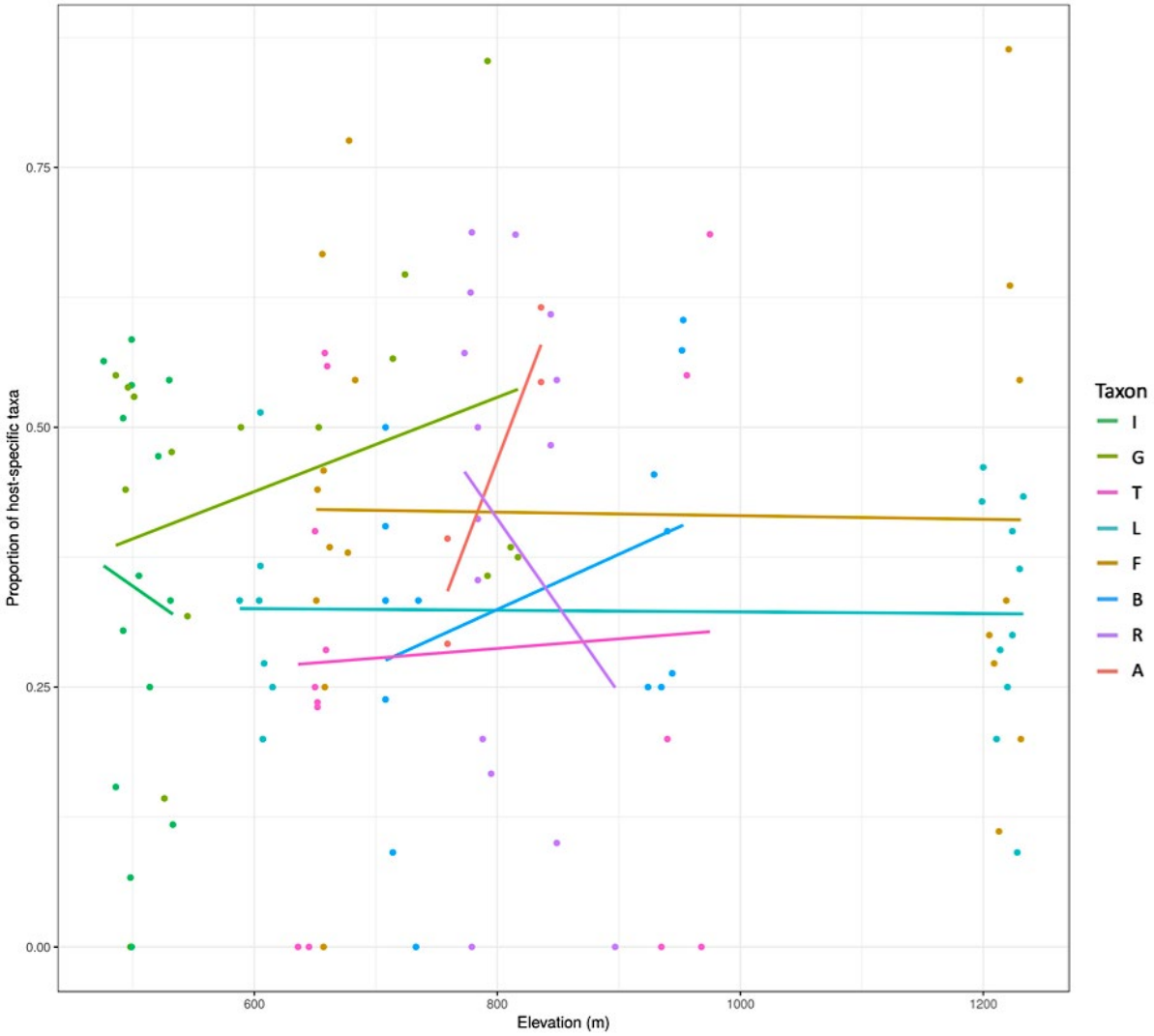

Figure 19. Proportion of host-specific FEs in individual *Metrosideros* adults occurring at different elevations. Host taxa are indicated by color, and trend lines indicate patterns of host-specificity within individual taxa across elevations. The eight *Metrosideros* taxa are *M. polymorpha* var. *incana* (I), *M. polymorpha* var. *glaberrima* (G), *M. tremuloides* (T), *M. polymorpha* race L (L), *M. polymorpha* race F (F), *M. polymorpha* race B (B), *M. rugosa* (R), and *M. polymorpha* race *prostrata* (A).

APPENDIX A: Kruskal-Wallis Test (H_{1A})

Methods

Kruskal-Wallis tests were done to compare Shannon diversity levels among three high-elevation *Metrosideros* taxa for which the highest and lowest estimates were observed. The Kruskal-Wallis test is the nonparametric equivalent of a one-way ANOVA, and does not assume normal distributions among any independent group (McDonald 2014). The null hypothesis assumes equal medians among all explanatory variables (Logan 2010).

Results

Post-hoc tests were done to compare Shannon diversity levels among the three high-elevation *Metrosideros* taxa, which showed the highest (*M. polymorpha* race *prostrata*) and lowest (*M. polymorpha* race B and *M. rugosa*) FE diversity values (Kruskal-Wallis: $H = 7.70$, $df = 2$, $p = 0.02$). Pairwise comparison Nemenyi tests (Pohlert 2014) indicated a significant difference between *M. polymorpha* race *prostrata* and *M. polymorpha* race B ($p = 0.02$), but not *M. rugosa* ($p = 0.08$).

APPENDIX B: Supplementary Figures

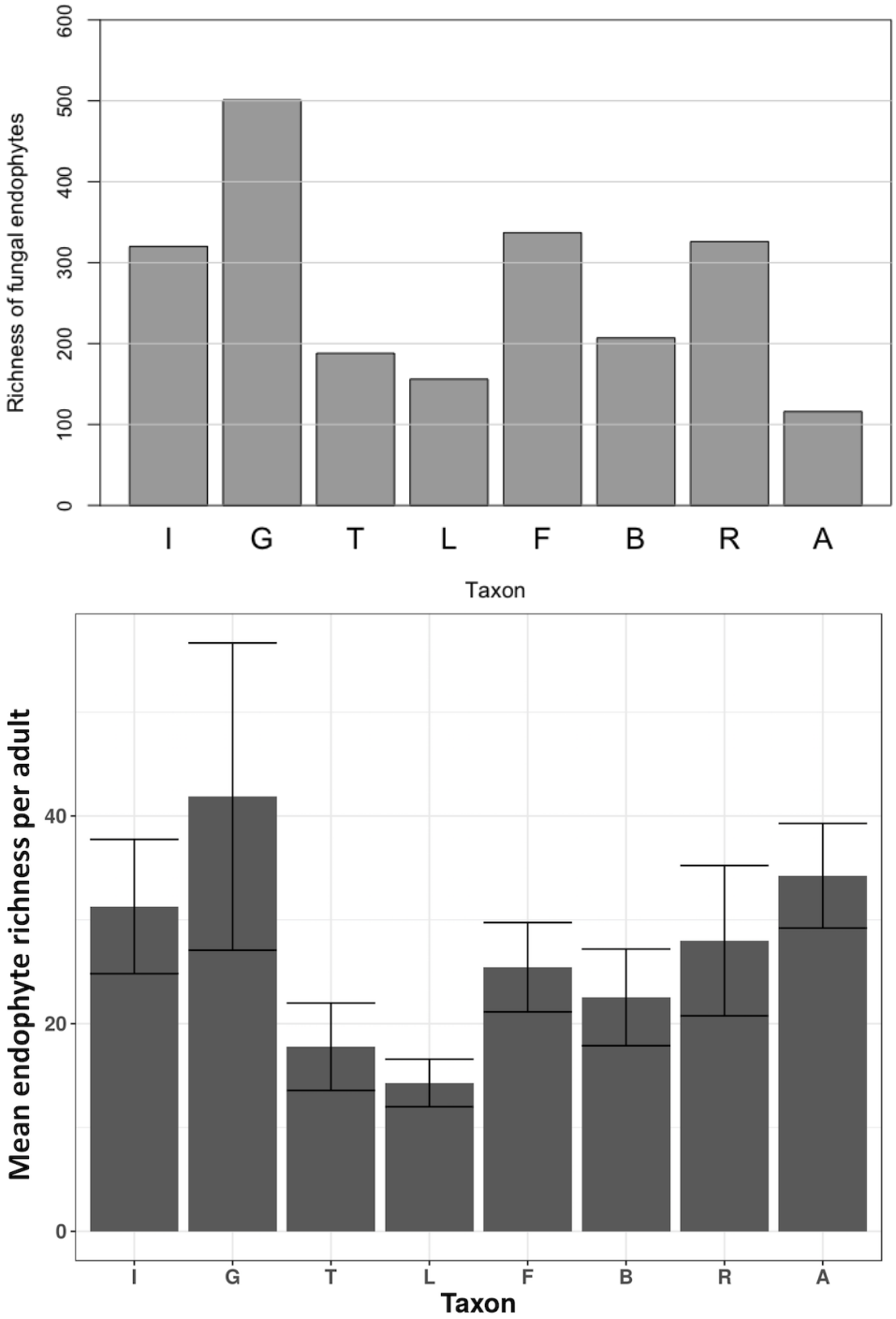

Figure S1. FE richness among eight *Metrosideros* taxa on O‘ahu: *M. polymorpha* var. *incana* (I), *M. polymorpha* var. *glaberrima* (G), *M. tremuloides* (T), *M. polymorpha* race L (L), *M. polymorpha* race F (F), *M. polymorpha* race B (B), *M. rugosa* (R), and *M. polymorpha* race *prostrata* (A). Top: FE richness per *Metrosideros* taxon. Bottom: Mean (± 1 SE) FE richness per adult per *Metrosideros* taxon.

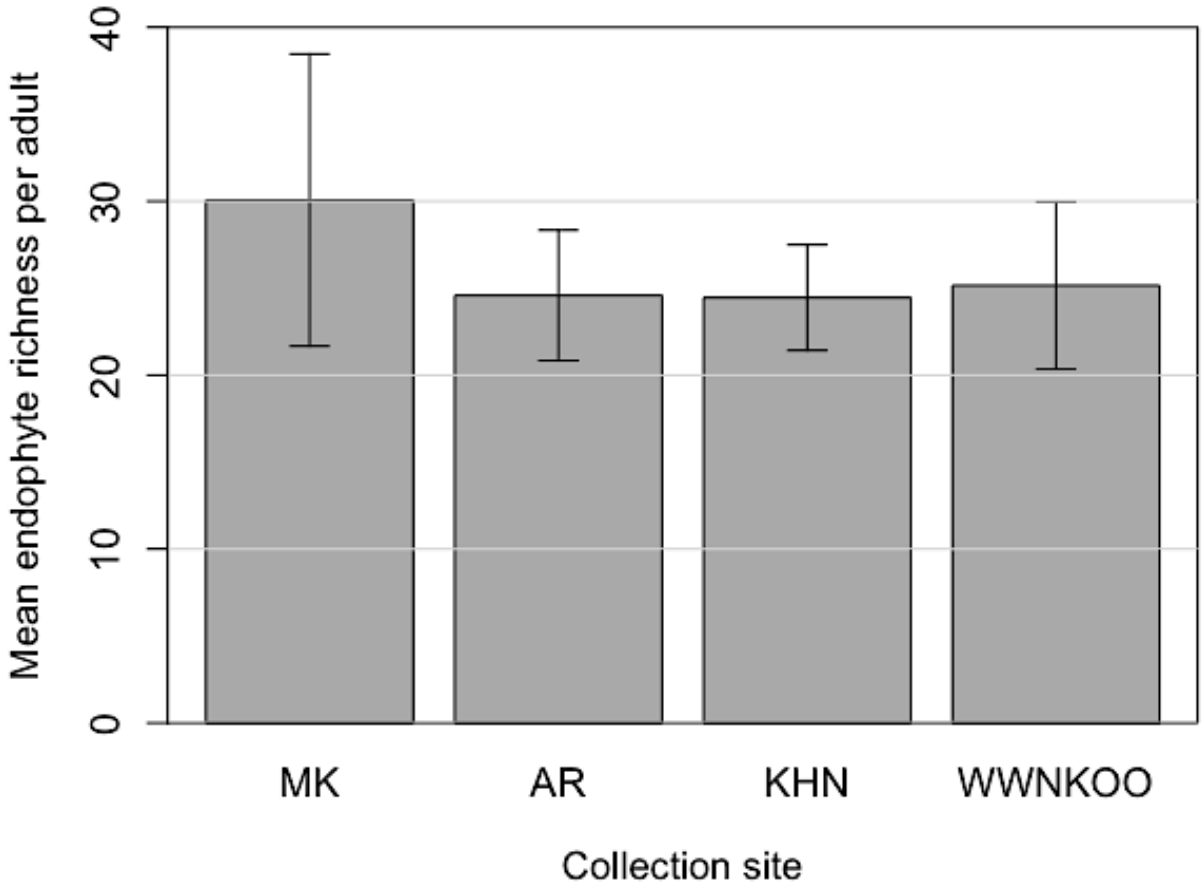

Figure S2. Mean (± 1 SE) FE richness per adult per site on O‘ahu Island: Mt. Ka‘ala (MK), ‘Aiea Ridge (AR), Konahuanui (KHN), and Wiliwilinui-Kuliou‘ou (WWNKOO).

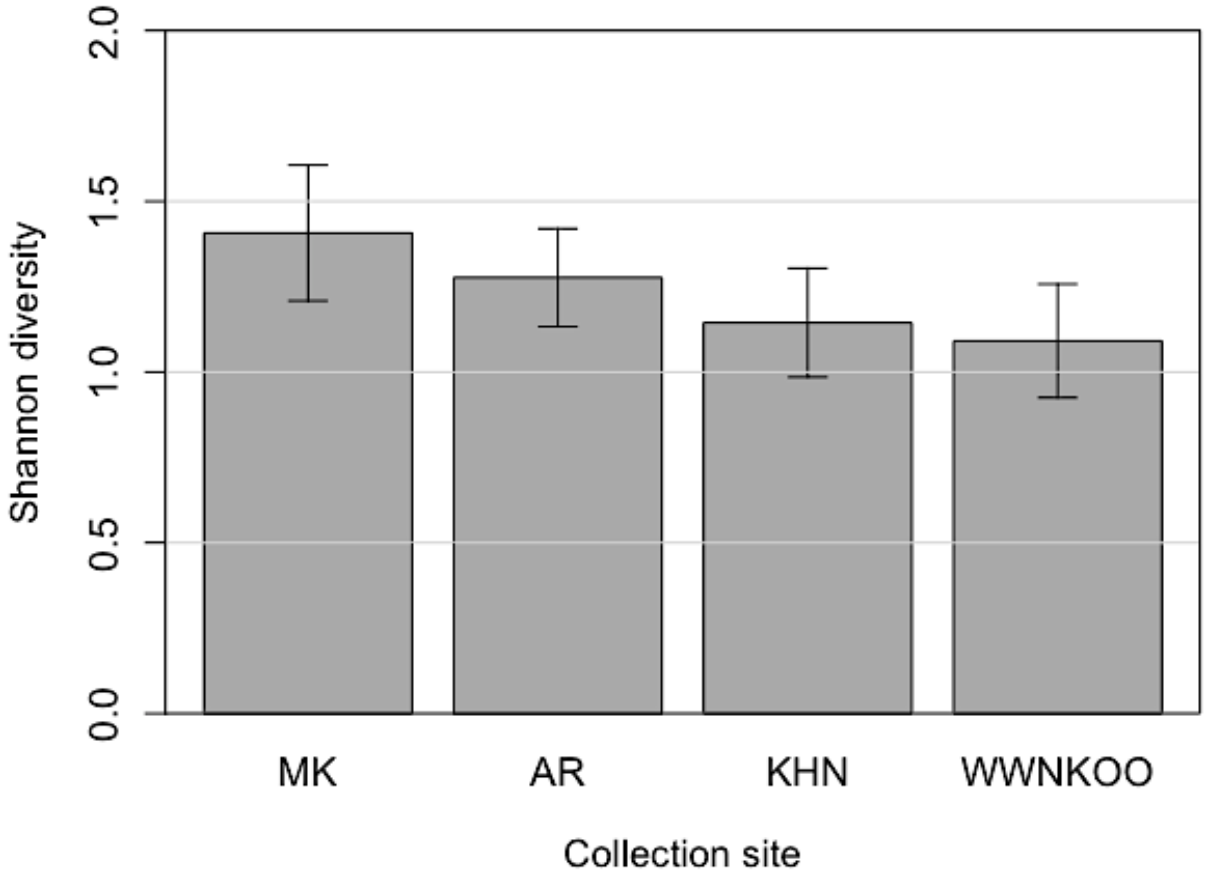

Figure S3. Mean (± 1 SE) Shannon diversity values per site. The sites are Mt. Ka‘ala (MK), ‘Aiea Ridge (AR), Konahuanui (KHN), and Wiliwilinui and Kuliou‘ou (WWNKOO).

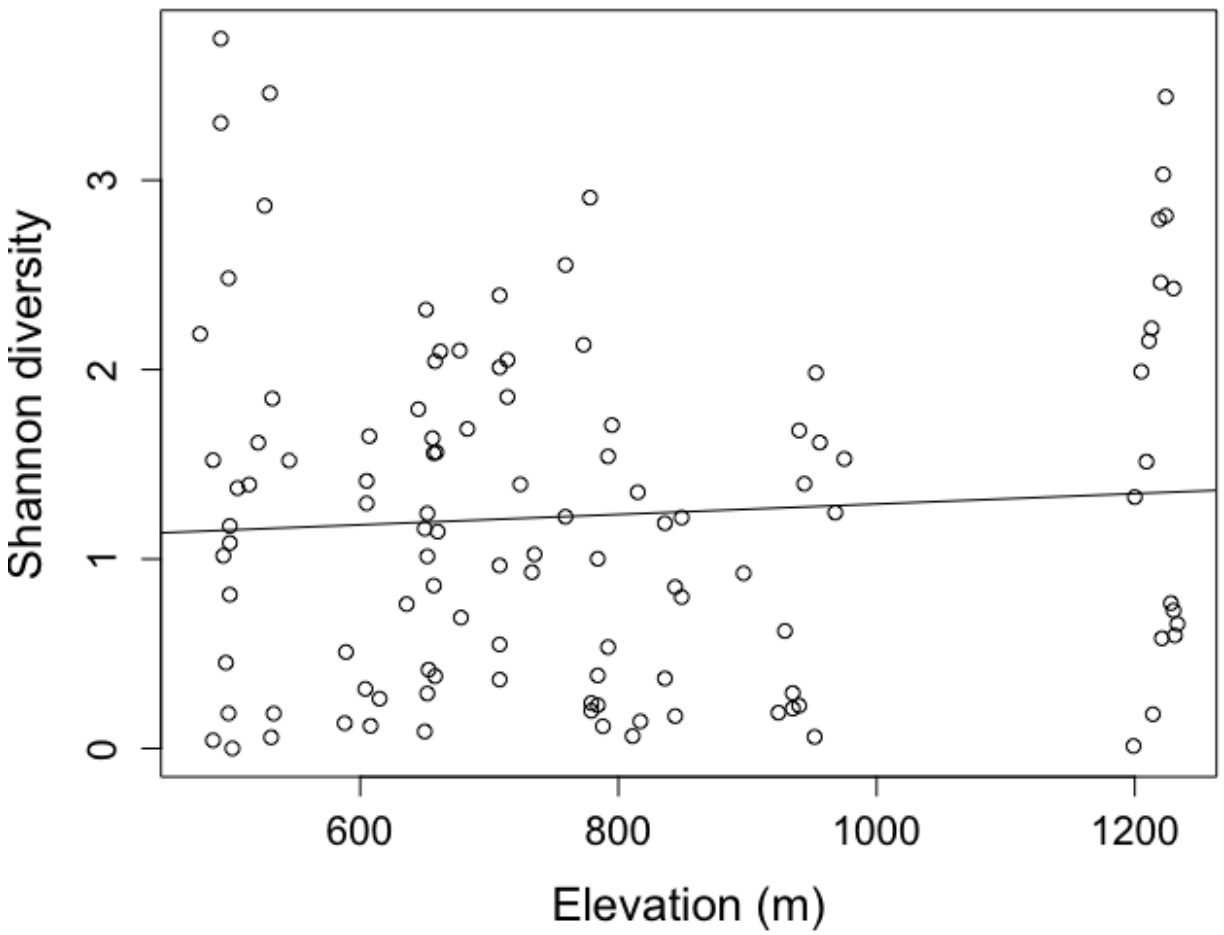

Figure S4. The relationship between elevation and Shannon diversity estimates of leaf FEs in *Metrosideros* on O‘ahu ($t = 0.74$, $df = 111$, $p = 0.48$, adj. $r^2 = 0.06$). Plots at 1,200 m represent samples from the summit of Mt. Ka‘ala.

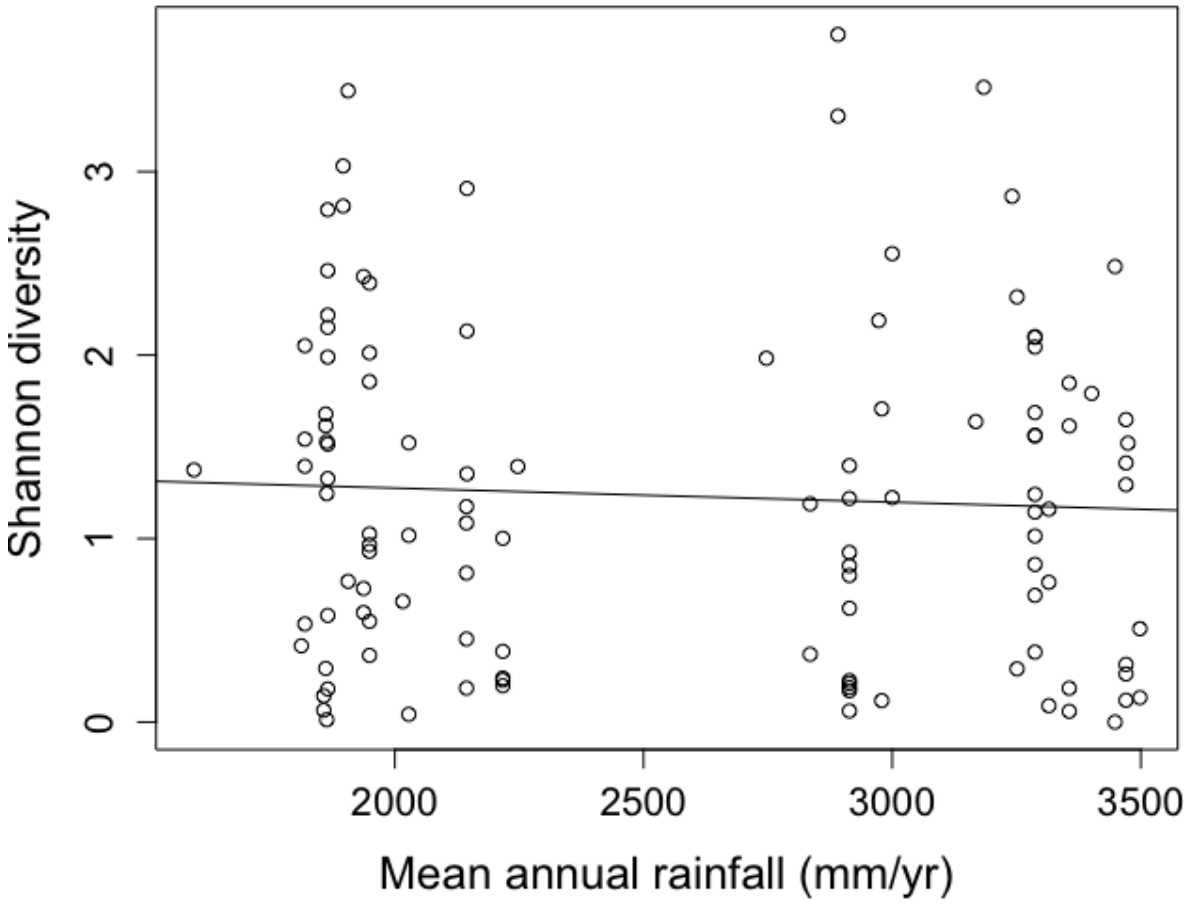

Figure S5. The relationship between mean annual rainfall and Shannon diversity estimates of leaf FEs in *Metrosideros* on O‘ahu ($t = -0.58$, $df = 111$, $p = 0.56$, adj. $r^2 = -0.04$). Rainfall data collected from Giambelluca et al. (2013).

LITERATURE CITED

Adee, K., and Conrad, C. E. 1990. *Metrosideros polymorpha* Gaud. 'Ohi'a lehua. *Silvics of North America* 2 (654): 466.

Amend, A. S., Seifert, K. A., and Bruns, T. D. 2010. Quantifying microbial communities with 454 pyrosequencing: does read abundance count? *Molecular Ecology* 19 (24): 5555-5565.

Anagnostakis, S. L., and Hillman, B. 1992. Evolution of the chestnut tree and its blight. *Arnoldia* 52 (2): 2-10.

Anderson, M. J. 2001. A new method for non-parametric multivariate analysis of variance. *Austral Ecology* 26 (1): 32–46.

Arnold, A. E. 2002. Fungal endophytes in neotropical trees: abundance, diversity, and ecological interactions. PhD dissertation thesis, University of Arizona, Tuscon, AZ

Arnold, A. E., Henk, D. A., Eells, R. L., Lutzoni, F., and Vilgalys, R. 2007. Diversity and phylogenetic affinities of foliar fungal endophytes in loblolly pine inferred by culturing and environmental PCR. *Mycologia* 99 (2): 185-206.

Arnold, A. E., and Herre, E. A. 2003. Canopy cover and leaf age affect colonization by tropical fungal endophytes: ecological pattern and process in *Theobroma cacao* (Malvaceae). *Mycologia* 95 (3): 388-398.

Arnold, A. E., and Lutzoni, F. 2007. Diversity and host range of foliar fungal endophytes: are tropical leaves biodiversity hotspots? *Ecology* 88 (3): 541-549.

Arnold, A. E., Mejía, L. C., Kyllo, D., Rojas, E. I., Maynard, Z., Robbins, N., and Herre, E. A. 2003. Fungal endophytes limit pathogen damage in a tropical tree. *Proceedings of the National Academy of Sciences* 100 (26): 15649-15654.

Arnold, A. E., Miadlikowska, J., Higgins, K. L., Sarvate, S. D., Gugger, P., Way, A., Hofstetter, V., Kauff, F., and Lutzoni, F. 2009. A phylogenetic estimation of trophic transition networks for ascomycetous fungi: are lichens cradles of symbiotrophic fungal diversification? *Systematic Biology* 58 (3): 283-297.

Bailey, J. K., Deckert, R., Schweitzer, J. A., Rehill, B. J., Lindroth, R. L., Gehring, C., and Whitham, T. G. 2005. Host plant genetics affect hidden ecological players: links among *Populus*, condensed tannins, and fungal endophyte infection. *Canadian Journal of Botany* 83 (4): 356-361.

Bálint, M., Tiffin, P., Hallström, B., O`Hara, R. B., Olson, M. S., Fankhauser, J. D., Piepenbring, M., and Schmitt, I. 2013. Host genotype shapes the foliar fungal microbiome of balsam poplar (*Populus balsamifera*). *PLOS One* 8 (1): 53987.

Barge, E. G., Leopold, D. R., Peay, K. G., Newcombe, G., and Busby, P. E. 2019. Differentiating spatial from environmental effects on foliar fungal communities of *Populus trichocarpa*. *Journal of Biogeography* 46 (9): 2001–2011.

Bazzicalupo, A. L., Bálint, M., and Schmitt, I. 2013. Comparison of ITS1 and ITS2 rDNA in 454 sequencing of hyperdiverse fungal communities. *Fungal Ecology* 6 (1): 102-109.

Begon, M., J. L. Harper, and C. R. Townsend. 1996. Ecology: Individuals, Populations, and Communities, 3rd edition. Blackwell Science Ltd., Cambridge, MA.

Bengtsson-Palme, J., Ryberg, M., Hartmann, M., Branco, S., Wang, Z., Godhe, A., De Wit, P., Sánchez-García, M., Ebersberger, I., de Sousa, F., and Amend, A. 2013. Improved software detection and extraction of ITS1 and ITS2 from ribosomal ITS sequences of fungi and other eukaryotes for analysis of environmental sequencing data. *Methods in Ecology and Evolution* 4 (10): 914-919.

Blaalid, R., Carlsen, T. O. R., Kumar, S., Halvorsen, R., Ugland, K. I., Fontana, G., and Kauserud, H. 2012. Changes in the root-associated fungal communities along a primary succession gradient analysed by 454 pyrosequencing. *Molecular Ecology* 21 (8): 1897-1908.

Blackwell, M. 2011. The Fungi: 1, 2, 3… 5.1 million species? *American Journal of Botany* 98 (3): 426-438.

Bohs, L. 2007. Phylogeny of the *Cyphomandra* clade of the genus *Solanum* (Solanaceae) based on ITS sequence data. *Taxon* 56 (4): 1012-1026.

Brown, J. K., and Hovmøller, M. S. 2002. Aerial dispersal of pathogens on the global and continental scales and its impact on plant disease. *Science* 297 (5581): 537-541.

Burgess, T. I., Gordon, T. R., Wingfield, M. J., and Wingfield, B. D. 2004. Geographic isolation of *Diplodia scrobiculata* and its association with native *Pinus radiata*. *Mycological Research* 108 (12): 1399-1406.

Callahan, B. J., McMurdie, P. J., and Holmes, S. P. 2017. Exact sequence variants should replace operational taxonomic units in marker-gene data analysis. *The ISME Journal* 11 (12): 2639.

Callahan, B. J., McMurdie, P. J., Rosen, M. J., Han, A. W., Johnson, A. J. A., and Holmes, S. P. 2016a. DADA2: High-resolution sample inference from Illumina amplicon data. *Nature Methods* 13 (7): 581-583. doi: 10.1038/nmeth.3869. URL: http://doi.org/10.1038/nmeth.3869.

Callahan, B. J., Sankaran, K., Fukuyama, J. A., McMurdie, P. J., and Holmes, S. P. 2016b. Bioconductor workflow for microbiome data analysis: from raw reads to community analyses. *F1000Research* 5.

Cannon, P. F., and C. M. Simmons. 2002. Diversity and host preference of leaf endophytic fungi in the Iwokrama Forest Reserve, Guyana. *Mycologia* 94 (2): 210–220.

Carson, H. L., and D. A. Clague. 1995. Geology and biogeography of the Hawaiian Islands. Pages 14–29 in: W. Wagner and V. Funk, eds. Hawaiian biogeography: Evolution in a hotspot archipelago. Smithsonian Institution Press, Washington, DC.

Chock, G., Peterka, J., and Yu, G. 2005. Topographic wind speed-up and directionality factors for use in the City and County of Honolulu Building Code. *Proceedings of the 10th American Conference on Wind Engineering, May*.

Christian, N., Herre, E. A., and Clay, K. 2019. Foliar endophytic fungi alter patterns of nitrogen uptake and distribution in *Theobroma cacao*. *New Phytologist* 222 (3): 1573-1583.

Cleary, M., Nguyen, D., Marčiulynienė, D., Berlin, A., Vasaitis, R., and Stenlid, J. 2016. Friend or foe? Biological and ecological traits of the European ash dieback pathogen *Hymenoscyphus fraxineus* in its native environment. *Scientific Reports* 6: 21895.

Cobian, G. M., Egan, C. P., and Amend, A. S. 2019. Plant–microbe specificity varies as a function of elevation. *The ISME Journal* 13 (11): 2778-2788.

Cordell, S., Goldstein, G., Melcher, P. J., and Meinzer, F. C. 2000. Photosynthesis and freezing avoidance in ohia (*Metrosideros polymorpha*) at treeline in Hawaii. *Arctic, Antarctic, and Alpine Research* 32 (4): 381-387.

Cordell, S., Goldstein, G., Mueller-Dombois, D., Webb, D., and Vitousek, P. M. 1998. Physiological and morphological variation in *Metrosideros polymorpha*, a dominant Hawaiian tree species, along an altitudinal gradient: the role of phenotypic plasticity. *Oecologia* 113 (2): 188-196.

Cordier, T., Robin, C., Capdevielle, X., Fabreguettes, O., Desprez-Loustau, M. L., and Vacher, C. 2012. The composition of phyllosphere fungal assemblages of European beech (*Fagus sylvatica*) varies significantly along an elevation gradient. *New Phytologist* 196 (2): 510-519.

Corn, C. A. 1979. Variation in Hawaiian *Metrosideros*. Ph.D. dissertation, University of Hawai`i at Manoa, Honolulu.

Darcy, J. L., Cobian, G. M., Swift, S. O., Zahn, G. L., Perry, B. A., and Amend, A. A. 2019. Fungal communities living within leaves of native Hawaiian dicots are structured by landscape-scale variables as well as by host plants. *BioRxiv*: 640029.

Datlof, E. M., Amend, A. S., Earl, K., Hayward, J., Morden, C. W., Wade, R., Zahn, G., and Hynson, N. A. 2017. Uncovering unseen fungal diversity from plant DNA banks. *PeerJ* 5: e3730.

Dawson, J. W. 1970. Pacific capsular Myrtaceae. II. The *Metrosideros* complex: *M. collina* group. *Blumea* 18: 441-445.

Dawson, J. W. 1984. New species and combinations in New Caledonian *Metrosideros* and *Carpolepis* (Myrtaceae) with notes on other species. *Adansonia* 4: 465–489.

Dawson, J. W., and Stemmermann, R. L. 1990. Manual of the Flowering Plants of Hawaii. Pages 964-970 in: W. L. Wagner, D. H. Herbst and S. H. Sohmer, editors. Bernice P. Bishop Museum, Honolulu, HI.

DeBoer, N., and Stacy, E. A. 2013. Divergence within and among 3 varieties of the endemic tree,`Ōhi`a Lehua (*Metrosideros polymorpha*) on the eastern slope of Hawai`i Island. *Journal of Heredity* 104 (4): 449-458.

Dickie, I. A., Martínez-García, L. B., Koele, N., Grelet, G. A., Tylianakis, J. M., Peltzer, D. A., and Richardson, S. J. 2013. Mycorrhizas and mycorrhizal fungal communities throughout ecosystem development. *Plant and Soil* 367 (1-2): 11-39.

Douanla-Meli, C., Langer, E., and Mouafo, F. T. 2013. Fungal endophyte diversity and community patterns in healthy and yellowing leaves of *Citrus limon*. *Fungal Ecology* 6 (3): 212-222.

Dreyfuss, M. M., and Chapela, I. H. 1994. Potential of fungi in the discovery of novel, low-molecular weight pharmaceuticals. In *Discovery of Novel Natural Products with Therapeutic Potential* (pp. 49-80). Newnes.

Dupuis, J. R., Pillon, Y., Sakishima, T., Gemmill, C. E., Chamala, S., Barbazuk, W. B., Geib, S. M., and Stacy, E.A. 2019. Targeted amplicon sequencing of 40 nuclear genes supports a single introduction and rapid radiation of Hawaiian *Metrosideros* (Myrtaceae). *Plant Systematics and Evolution* 305 (10): 961-974.

Durán, E. L., Ploper, L. D., Ramallo, J. C., Piccolo Grandi, R. A., Hupper Giancoli, Á. C., and Azevedo, J. L. 2005. The foliar fungal endophytes of *Citrus limon* in Argentina. *Canadian Journal of Botany* 83 (4): 350-355.

Durbin, R., Eddy, S. R., Krogh, A., and Mitchison, G. 1998. *Biological sequence analysis: probabilistic models of proteins and nucleic acids*. Cambridge University Press, Cambridge, United Kingdom.

Eddy, S. R. 1998. Profile hidden Markov models. *Bioinformatics* 14 (9): 755–763.

Ekar, J. M., Price, D. K., Johnson, M. A., and Stacy, E. A. 2019. Varieties of the highly dispersible and hypervariable tree, *Metrosideros polymorpha*, differ in response to mechanical stress and light across a sharp ecotone. *American Journal of Botany* 106 (8): 1106-1115.

Eusemann, P., Schnittler, M., Nilsson, R. H., Jumpponen, A., Dahl, M. B., Würth, D. G., Buras, A., Wilmking, M., and Unterseher, M. 2016. Habitat conditions and phenological tree traits overrule the influence of tree genotype in the needle mycobiome–*Picea glauca* system at an arctic treeline ecotone. *New Phytologist* 211 (4): 1221-1231.

Ewing, B., and Green, P. 1998. Base-calling of automated sequencer traces using phred. II. Error probabilities. *Genome Research* 8 (3): 186-194.

Fierer, N., Breitbart, M., Nulton, J., Salamon, P., Lozupone, C., Jones, R., Robeson, M., Edwards, R. A., Felts, B., Rayhawk, S., and Knight, R. 2007. Metagenomic and small-subunit rRNA analyses reveal the genetic diversity of bacteria, archaea, fungi, and viruses in soil. *Applied and Environmental Microbiology* 73 (21): 7059-7066.

Friedman, M., Henika, P. R., and Mandrell, R. E. 2002. Bactericidal activities of plant essential oils and some of their isolated constituents against *Campylobacter jejuni*, *Escherichia coli*, *Listeria monocytogenes*, and *Salmonella enterica*. *Journal of Food Protection* 65 (10): 1545-1560.

Gazis, R., Rehner, S., and Chaverri, P. 2011. Species delimitation in fungal endophyte diversity studies and its implications in ecological and biogeographic inferences. *Molecular Ecology* 20 (14): 3001-3013.

Gentry, A. H. 1988. Tree species richness of upper Amazonian forests. *Proceedings of the National Academy of Sciences* 85: 156-159.

Ghasemi, S., Khodaei, S., Karimi, K., Tavakoli, M., Pertot, I., and Arzanlou, M. 2019. Biodiversity study of endophytic fungi associated with two *Quercus* species in Iran. *Forest Systems* 28 (1): 3.

Giambelluca, T. W., Chen, Q., Frazier, A. G., Price, J. P., Chen, Y. L., Chu, P. S., Eischeid, J. K., and Delparte, D. M. 2013. Online rainfall atlas of Hawai`i. *Bulletin of the American Meteorological Society* 94 (3): 313-316.

Giambelluca, T. W., Shuai, X., Barnes, M. L., Alliss, R. J., Longman, R. J., Miura, T., Chen, Q., Frazier, A. G., Mudd, R. G., Cuo, L., and Businger, A. D. 2014. Evapotranspiration of Hawai`i. *Final report submitted to the US Army Corps of Engineers—Honolulu District, and the Commission on Water Resource Management, State of Hawai`i*.

Gilbert, G. S., and Reynolds, D. R. 2005. Nocturnal fungi: Airborne spores in the canopy and understory of a tropical rain forest. *Biotropica* 37 (3): 462-464.

Gilbert, G. S., and Webb, C. O. 2007. Phylogenetic signal in plant pathogen–host range. *Proceedings of the National Academy of Sciences* 104 (12): 4979-4983.

Google Earth 7.3. 2019a. *Oahu 21°27′ N, 158°03′ W.* Viewed 18 October 2019.<http://www.google.com/earth/index.html>.

Google Earth 7.3. 2019b. *Oahu 21°29'44.16"N, 158°09'5.76" W.* Viewed 18 October 2019.<http://www.google.com/earth/index.html>.

Google Earth 7.3. 2019c. *Oahu 21°24'59.04" N, 157°51'48.96" W*. Viewed 18 October 2019.<http://www.google.com/earth/index.html>.

Google Earth 7.3. 2019d. *Oahu 21°21'5.76" N, 157°47'55.68" W.* Viewed 18 October 2019.<http://www.google.com/earth/index.html>.

Google Earth 7.3. 2019e. *Oahu 21°19'48"N, 157°44'54.24" W.* Viewed 18 October 2019.<http://www.google.com/earth/index.html>.

Griffin, E. A., and Carson, W. P. (2018). Tree endophytes: cryptic drivers of tropical forest diversity. Pages 63-103 in: *Endophytes of Forest Trees: Biology and Applications*, eds A. M. Pirttilä, and C. Frank. Basel Springer, Basel, Switzerland.

Hawksworth, D. L. 1991. The fungal dimension of biodiversity: magnitude, significance, and conservation. *Mycological Research* 95 (6): 641–655.

Hawksworth, D. L. 2001. The magnitude of fungal diversity: the 1.5 million species estimate revisited. *Mycological Research* 105 (12): 1422-1432.

Hawksworth, D. L. 2012. Global species numbers of fungi: are tropical studies and molecular approaches contributing to a more robust estimate? *Biodiversity and Conservation* 21: 2425-2433.

Hawksworth, D. L., and Lücking, R. 2017. Fungal diversity revisited: 2.2 to 3.8 million species. *Microbiology Spectrum* 5 (4): 79-95.

Hebert, P. D., Cywinska, A., and Ball, S. L. 2003. Biological identifications through DNA barcodes. *Proceedings of the Royal Society of London B: Biological Sciences* 270 (1512): 313-321.

Helander, M., Ahlholm, J., Sieber, T. N., Hinneri, S., and Saikkonen, K. 2007. Fragmented environment affects birch leaf endophytes. *New Phytologist* 175 (3): 547-553.

Heller, W. P., Hughes, M. A., Luiz, B. C., Brill, E., Friday, J. B., Williams, A. M., and Keith, L. M. 2019. First report of *Ceratocystis huliohia* causing mortality of *Metrosideros polymorpha* trees on the Island of Kauaʻi, Hawaiʻi USA. *Forest Pathology* 49 (5): 12546.

Hudson, C. M., Kirton, E., Hutchinson, M. I., Redfern, J. L., Simmons, B., Ackerman, E., Singh, S., Williams, K. P., Natvig, D. O., and Powell, A. J. 2015. Lignin-modifying processes in the rhizosphere of arid land grasses. *Environmental Microbiology* 17 (12): 4965-4978.

Johnston, P. R., and Park, D. 2016. *Neocoleroa metrosideri* sp. nov. (Sympoventuriaceae, Venturiales). *Phytotaxa* 253 (3): 214-218.

Jones, J. D., and Dangl, J. L. 2006. The plant immune system. *Nature* 444 (7117): 323-329.

Kembel, S. W., and Mueller, R. C. 2014. Plant traits and taxonomy drive host associations in tropical phyllosphere fungal communities. *Botany* 92 (4): 303-311.

Knight, R., Vrbanac, A., Taylor, B. C., Aksenov, A., Callewaert, C., Debelius, J., Gonzalez, A., Kosciolek, T., McCall, L. I., McDonald, D., and Melnik, A.V. 2018. Best practices for analysing microbiomes. *Nature Reviews Microbiology* 16 (7): 410-422.

Kõljalg, U., Nilsson, R. H., Abarenkov, K., Tedersoo, L., Taylor, A. F., Bahram, M., Bates, S. T., Bruns, T. D., Bengtsson-Palme, J., Callaghan, T. M., and Douglas, B. 2013. Towards a unified paradigm for sequence-based identification of fungi. *Molecular Ecology* 22 (21): 5271-5277.

Kruskal, J. B. 1964. Nonmetric multidimensional scaling: a numerical method. *Psychometrika* 29 (2): 115-129.

Lanzén, A. 2013. *Analysis of sequencing data in environmental genomics. Exploring the diversity of the microbial biosphere*. The University of Bergen, Bergen, Norway.

Lear, G., Dickie, I., Banks, J., Boyer, S., Buckley, H. L., Buckley, T. R., Cruickshank, R., Dopheide, A., Handley, K. M., Hermans, S., and Kamke, J. 2018. Methods for the extraction, storage, amplification and sequencing of DNA from environmental samples. *New Zealand Journal of Ecology* 42 (1): 10-50A.

Lee, D. E., Conran, J. G., Lindqvist, J. K., Bannister, J. M., and Mildenhall, D. C. 2012. New Zealand Eocene, Oligocene and Miocene macrofossil and pollen records and modern plant distributions in the southern hemisphere. *The Botanical Review* 78 (3): 235-260.

Lefcheck, J. 2012. NMDS tutorial in R. [ONLINE] Available at: https://jonlefcheck.net/2012/10/24/nmds-tutorial-in-r/. [Accessed 14 March 2019].

Legendre, P., and Anderson, M. J. 1999. Distance-based redundancy analysis: Testing multispecies responses in multifactorial ecological experiments. *Ecological Monographs* 69 (1): 1–24.

Legendre, P., and Fortin, M. J. 1989. Spatial pattern and ecological analysis. *Vegetatio* 80 (2): 107-138.

Lentendu, G., Zinger, L., Manel, S., Coissac, E., Choler, P., Geremia, R. A., and Melodelima, C. 2011. Assessment of soil fungal diversity in different alpine tundra habitats by means of pyrosequencing. *Fungal Diversity* 49 (1): 113-123.

Lim, Y. W., Kim, B. K., Kim, C., Jung, H. S., Kim, B. S., Lee, J. H., and Chun, J. 2010. Assessment of soil fungal communities using pyrosequencing. *The Journal of Microbiology* 48 (3): 284-289.

Logan, M. 2011. *Biostatistical Design and Analysis Using R: A Practical Guide*. John Wiley & Sons, Chichester, United Kingdom.

Luiz, B. 2017. Understanding *Ceratocystis* species A: growth, morphology, and host resistance. MS thesis, University of Hawaii, Hilo, HI.

Lutzoni, F., Nowak, M. D., Alfaro, M. E., Reeb, V., Miadlikowska, J., Krug, M., Arnold, A. E., Lewis, L. A., Swofford, D. L., Hibbett, D., and Hilu, K. 2018. Contemporaneous radiations of fungi and plants linked to symbiosis. *Nature Communications* 9 (1): 5451.

Magurran, A. E. 1988. *Ecological Diversity and its Measurement*. Princeton University Press, Princeton, NJ.

Mantel, N. 1967. The detection of disease clustering and a generalized regression approach. *Cancer Research* 27 (2 Part 1): 209-220.

McArdle, B. H., and Anderson, M. J. 2001. Fitting multivariate models to community data: A comment on distance-based redundancy analysis. *Ecology* 82 (1): 290–297.

McDonald, J. H. 2014. *Handbook of Biological Statistics*, 3rd ed., Sparky House Publishing: Baltimore, MD.

McMurdie, P. J., and Holmes, S. 2013. phyloseq: an R package for reproducible interactive analysis and graphics of microbiome census data. *PLOS One* 8 (4): e61217.

McMurdie, P. J., and Holmes, S. 2014. Waste not, want not: why rarefying microbiome data is inadmissible. *PLOS Computational Biology* 10 (4): e1003531.

Mejía, L. C., Rojas, E .I., Maynard, Z., Van Bael, S., Arnold, A .E., Hebbar, P., Samuels, G. J., Robbins, N., and Herre, E. A. 2008. Endophytic fungi as biocontrol agents *of Theobroma cacao* pathogens. *Biological Control* 46 (1): 4-14.

Meyer, C. P., and Paulay, G. 2005. DNA barcoding: error rates based on comprehensive sampling. *PLOS* 3: e422.

Mmbaga, M. T., and Steadman, J. R. 1992. Effect of abaxial leaf pubescence on rust sport despostion, spore germination and uredinu density. *Bean Improvement Cooperative Annual Report (USA)* 35: 130-131.

Moricca, S., and Ragazzi, A. 2008. Fungal endophytes in Mediterranean oak forests: a lesson from Discula quercina. *Phytopathology* 98 (4): 380-386.

Morrison, K. R., and Stacy, E.A. 2014. Intraspecific divergence and evolution of a life-history trade-off along a successional gradient in Hawaii's *Metrosideros polymorpha*. *Journal of Evolutionary Biology* 27 (6): 1192-1204.

Mueller-Dombois, D. 1987. Forest dynamics in Hawaii. *Trends in Ecology & Evolution* 2 (7): 216-220.

Mueller-Dombois, D. 1992. Distributional dynamics in the Hawaiian vegetation. *Pacific Science* 46 (2): 221-231.

Nilsson, R. H., Larsson, K. H., Taylor, A. F. S., Bengtsson-Palme, J., Jeppesen, T. S., Schigel, D., Kennedy, P., Picard, K., Glöckner, F. O., Tedersoo, L., and Saar, I. 2018. The UNITE database for molecular identification of fungi: handling dark taxa and parallel taxonomic classifications. *Nucleic acids Research* 47 (D1): D259-D264.

O'Brien, H. E., Parrent, J. L., Jackson, J. A., Moncalvo, J. M., and Vilgalys, R. 2005. Fungal community analysis by large-scale sequencing of environmental samples. *Applied and Environmental Microbiology* 71 (9): 5544-5550.

Oksanen, J., Blanchet, F. G., Friendly, M., Kindt, R., Legendre, P., McGlinn, D., Minchin, P. R., O'Hara, R. B., Simpson, G. L., Solymos, P., Stevens, M. H. H., Szoecs, E., and Wagner, H. 2018. vegan: Package `vegan`. *Community Ecology Package, version*, 2.5-3. https://CRAN.R-project.org/package=vegan

Oono, R., Lutzoni, F., Arnold, A. E., Kaye, L., U`Ren, J. M., May, G., and Carbone, I. 2014. Genetic variation in horizontally transmitted fungal endophytes of pine needles reveals population structure in cryptic species. *American Journal of Botany* 101 (8): 1362-1374.

O'Rorke, R., Cobian, G. M., Holland, B. S., Price, M. R., Costello, V., and Amend, A. S. 2015. Dining local: the microbial diet of a snail that grazes microbial communities is geographically structured. *Environmental Microbiology* 17 (5): 1753-1764.

Peay, K. G., Kennedy, P. G., and Bruns, T. D. 2008. Fungal community ecology: a hybrid beast with a molecular master. *Bioscience* 58 (9): 799-810.

Peay, K. G., Kennedy, P. G., and Talbot, J. M. 2016. Dimensions of biodiversity in the Earth mycobiome. *Nature Reviews Microbiology* 14 (7): 434-447.

Percy, D. M., Garver, A. M., Wagner, W. L., James, H. F., Cunningham, C. W., Miller, S. E., and Fleischer, R. C. 2008. Progressive island colonization and ancient origin of Hawaiian *Metrosideros* (Myrtaceae*). Proceedings of the Royal Society of London B: Biological Sciences* 275 (1642): 1479-1490.

Petrini, O. 1991. Fungal endophytes of tree leaves. Pages 179-197 in: *Microbial Ecology of Leaves*. Springer Publishing, New York, NY.

Pirozynski, K. A., and Malloch, D.W. 1975. The origin of land plants: a matter of mycotrophism. *Biosystems* 6 (3): 153-164.

Pitman, N. C., Terborgh, J. W., Silman, M. R., Núñez, V., Neill, D. A., Cerón, C. E., Palacios, W. A., and Aulestia, M. 2001. Dominance and distribution of tree species in upper Amazonian terra firme forests. *Ecology* 82 (8): 2101-2117.

Porras-Alfaro, A., and Bayman, P. 2011. Hidden fungi, emergent properties: endophytes and microbiomes. *Phytopathology* 49: 291-315.

Porter, T. M., and Golding, G. B. 2011. Are similarity-or phylogeny-based methods more appropriate for classifying internal transcribed spacer (ITS) metagenomic amplicons? *New Phytologist* 192 (3): 775-782.

Poulin, R., Krasnov, B. R., and Mouillot, D. 2011. Host specificity in phylogenetic and geographic space. *Trends in Parasitology* 27 (8): 355-361.

Pumplin, N., and Voinnet, O. 2013. RNA silencing suppression by plant pathogens: defence, counter-defence and counter-counter-defence. *Nature Reviews Microbiology* 11 (11): 745-460.

Quail, M. A., Smith, M., Coupland, P., Otto, T. D., Harris, S. R., Connor, T. R., Bertoni, A., Swerdlow, H. P., and Gu, Y. 2012. A tale of three next generation sequencing platforms: comparison of Ion Torrent, Pacific Biosciences and Illumina MiSeq sequencers. *Biomed Central Genomics* 13 (1): 341.

R Core Team. 2018. R: A language and environment for statistical computing. R Foundation for Statistical Computing, Vienna, Austria. http://www.R-project.org.

Raja, H. A., Miller, A. N., Pearce, C. J., and Oberlies, N. H. 2017. Fungal identification using molecular tools: a primer for the natural products research community. *Journal of Natural*

Products 80 (3): 756-770.
Redman, R. S., Freeman, S., Clifton, D. R., Morrel, J., Brown, G., and Rodriguez, R. J. 1999. Biochemical analysis of plant protection afforded by a nonpathogenic endophytic mutant of *Colletotrichum magna*. *Plant Physiology* 119 (2): 795-804.
Reynolds, H. L., Packer, A., Bever, J. D., and Clay, K. 2003. Grassroots ecology: plant-microbe-soil interactions as drivers of plant community structure and dynamics. *Ecology* 84 (9): 2281-2291.
Rideout, J. R., He, Y., Navas-Molina, J. A., Walters, W. A., Ursell, L. K., Gibbons, S. M., Chase, J., McDonald, D., Gonzalez, A., Robbins-Pianka, A., and Clemente, J. C. 2014. Subsampled open-reference clustering creates consistent, comprehensive OTU definitions and scales to billions of sequences. *PeerJ* 2: 545.
Rivers, A. R., Weber, K. C., Gardner, T. G., Liu, S., and Armstrong, S. D. 2018. ITSxpress: Software to rapidly trim internally transcribed spacer sequences with quality scores for marker gene analysis. *F1000Research* 7: 1418.
Rodriguez, R. J., White Jr., J. F., Arnold, A. E., and Redman, R. S. 2009. Fungal endophytes: diversity and functional roles. *New Phytologist* 182 (2): 314-330.
Rondon, M. R., Goodman, R. M., and Handelsman, J. 1999. The Earth`s bounty: assessing and accessing soil microbial diversity. *Trends in Biotechnology* 17 (10): 403-409.
Rosenzweig, M. L. 1995. In *Species Diversity in Space and Time*. Cambridge University Press, Cambridge, United Kingdom.
Rousk, J., Bååth, E., Brookes, P. C., Lauber, C. L., Lozupone, C., Caporaso, J. G., Knight, R., and Fierer, N. 2010. Soil bacterial and fungal communities across a pH gradient in an arable soil. *The ISME Journal* 4 (10): 1340-1351.
Ryberg, M., Kristiansson, E., Sjökvist, E., and Nilsson, R. H. 2009. An outlook on the fungal internal transcribed spacer sequences in GenBank and the introduction of a web-based tool for the exploration of fungal diversity. *New Phytologist* 181: 471-477.
Sadeghi, F., Samsampour, D., Seyahooei, M. A., Bagheri, A., and Soltani, J. 2019. Diversity and spatiotemporal distribution of fungal endophytes associated with *Citrus reticulata* cv. siyahoo. *Current Microbiology* 76 (3): 279-289.
Saikkonen, K. 2007. Forest structure and fungal endophytes. *Fungal Biology Reviews* 21 (2-3): 67-74.
Saikkonen, K., Wäli, P., Helander, M., and Faeth, S. H. 2004. Evolution of endophyte–plant symbioses. *Trends in Plant Science* 9 (6): 275-280.
Saucedo-Garcia, A., Anaya, A. L., Espinosa-Garcia, F. J., and Gonzalez, M. C. 2014. Diversity and communities of foliar endophytic fungi from different agroecosystems of *Coffea arabica L.* in two regions of Veracruz, Mexico. *PLOS One* 9 (6): e98454.
Schloss, P. D., Westcott, S. L., Ryabin, T., Hall, J. R., Hartmann, M., Hollister, E. B., Lesniewski, R. A., Oakley, B. B., Parks, D. H., Robinson, C. J., and Sahl, J. W. 2009. Introducing mothur: open-source, platform-independent, community-supported software for describing and comparing microbial communities. *Applied and Environmental Microbiology* 75 (23): 7537-7541.
Schoch, C. L., Seifert, K. A., Huhndorf, S., Robert, V., Spouge, J. L., Levesque, C. A., Chen, W., and Fungal Barcoding Consortium. 2012. Nuclear ribosomal internal transcribed spacer (ITS) region as a universal DNA barcode marker for Fungi. *Proceedings of the National Academy of Sciences* 109 (16): 6241-6246.
Sieber, T. N. 2007. Endophytic fungi in forest trees: are they mutualists? *Fungal Biology*

Reviews 21 (2-3): 75-89.
Spatafora, J. 2007. Pezizomycotina. Version 19 December 2007. *http://tolweb.org/Pezizomycotina/29296/2007.12.19 in* The Tree of Life Web Project, *http://tolweb.org/*
Stacy, E. A., Johansen, J. B., Sakishima, T., Price, D., and Pillon Y. 2014. Incipient radiation within the dominant Hawaiian tree *Metrosideros polymorpha*. *Heredity* 113 (4): 334–342.
Stacy, E. A., and Sakishima, T. 2019. Phylogeography of the highly dispersible landscape-dominant woody species complex, *Metrosideros*, in Hawaii. *Journal of Biogeography* 46 (10): 2215-2231.
Stacy, E. A., Sakishima, T., Tharp, H., and Snow, N. 2020. Strong isolation within *Metrosideros* (`Ohi`a) on O`ahu correlates with extreme environments. *Journal of Heredity* (in press).
Staley, J. T., and Konopka, A. 1985. Measurement of in situ activities of nonphotosynthetic microorganisms in aquatic and terrestrial habitats. *Annual Review of Microbiology* 39 (1): 321-346.
Stockinger, H., Krüger, M., and Schüßler, A. 2010. DNA barcoding of arbuscular mycorrhizal fungi. *New Phytologist* 187 (2): 461-474.
Stockinger, H., Walker, C., and Schüßler, A. 2009. '*Glomus intraradices* DAOM197198', a model fungus in arbuscular mycorrhiza research, is not *Glomus intraradices*. *New Phytologist* 183 (4): 1176-1187.
Stoeckle, M. 2003. Taxonomy, DNA, and the bar code of life. *BioScience* 53: 796-797.
Sur, G. L., Keating, R., Snow, N., and Stacy, E. A. 2018. Leaf micromorphology aids taxonomic delineation within the hypervariable genus *Metrosideros* (Myrtaceae) on O'ahu. *Pacific Science* 72 (3): 345-361.
Suryanarayanan, T. 2011. Diversity of fungal endophytes in tropical trees. Pirttilä, A. M., and Frank, A. C., editors. Pages 67-80 in: *Endophytes of Forest Trees*, vol 80. Springer Publishing, Dordrecht, The Netherlands.
Suryanarayanan, T. S., Venkatesan, G., and Murali, T. S. 2003. Endophytic fungal communities in leaves of tropical forest trees: diversity and distribution patterns. *Current Science* 85: 489-493.
Tarran, M., Wilson, P. G., and Hill, R. S. 2016. Oldest record of *Metrosideros* (Myrtaceae): Fossil flowers, fruits, and leaves from Australia. *American Journal of Botany* 103 (4): 754-768.
Tarran, M., Wilson, P. G., Macphail, M. K., Jordan, G. J., and Hill, R. S. 2017. Two fossil species of *Metrosideros* (Myrtaceae) from the Oligo-Miocene Golden Fleece locality in Tasmania, Australia. *American Journal of Botany* 104 (6): 891-904.
Tedersoo, L., Nilsson, R. H., Abarenkov, K., Jairus, T., Sadam, A., Saar, I., Bahram, M., Bechem, E., Chuyong, G., and Kõljalg, U. 2010. 454 Pyrosequencing and Sanger sequencing of tropical mycorrhizal fungi provide similar results but reveal substantial methodological biases. *New Phytologist* 188 (1): 291-301.
Terhonen, E., Blumenstein, K., Kovalchuk, A., and Asiegbu, F. O. 2019. Forest tree microbiomes and associated fungal endophytes: functional roles and impact on forest health. *Forests* 10 (1): 42.
Thermo Fisher Scientific. 2016. Ion PGM™ and Ion Proton™ System Chips. [ONLINE] Available at: http://www.thermofisher.com/us/en/home/life-science/sequencing/next-generation-sequencing/ion-torrent-next-generation-sequencing-workflow/ion-torrent-next-

generation-sequencing-run-sequence/ion-pgm-ion-proton-system-chips.html. [Accessed 2016 December 02].
Thermo Fisher Scientific. 2018. Ion 520™ & Ion 530™ ExT Kit – Chef. [ONLINE] Available at: https://www.thermofisher.com/document-connect/document-connect.html?url=https%3A%2F%2Fassets.thermofisher.com%2FTFS-Assets%2FLSG%2Fmanuals%2FMAN0015806_Ion520_530ExTKit_QR.pdf&title=UXVpY2sgUmVmZXJlbmNlOiBJb24gNTIwICZhbXA7IElvbiA1MzAgRXhUIEtpdCAtIENoZWY=. [Accessed 2018 July 10].
Tsujii, Y., Onoda, Y., Izuno, A., Isagi, Y., and Kitayama, K. 2016. A quantitative analysis of phenotypic variations of *Metrosideros polymorpha* within and across populations along environmental gradients on Mauna Loa, Hawaii. *Oecologia* 180 (4): 1049-1059.
Valkama, E., Koricheva, J., Salminen, J. P., Helander, M., Saloniemi, I., Saikkonen, K., and Pihlaja, K. 2005. Leaf surface traits: overlooked determinants of birch resistance to herbivores and foliar micro-fungi? *Trees* 19 (2): 191-197.
Vandruff, S. M. 2014. *Variation of subterranean fungal community structure across substrate age and elevation in native forests on Hawai'i Island, USA* (Doctoral dissertation, University of Hawai'i at Hilo).
Vaz, A. B., Fontenla, S., Rocha, F. S., Brandão, L. R., Vieira, M. L., De Garcia, V., Góes-Neto, A., and Rosa, C. A. 2014. Fungal endophyte β-diversity associated with Myrtaceae species in an Andean Patagonian forest (Argentina) and an Atlantic forest (Brazil). *Fungal Ecology* 8: 28-36.
Vega, F. E., Simpkins, A., Aime, M. C., Posada, F., Peterson, S. W., Rehner, S. A., Infante, F., Castillo, A., and Arnold, A. E. 2010. Fungal endophyte diversity in coffee plants from Colombia, Hawai'i, Mexico and Puerto Rico. *Fungal Ecology* 3 (3): 122-138.
Westcott, S. L., and Schloss, P. D. 2015. De novo clustering methods outperform reference-based methods for assigning 16S rRNA gene sequences to operational taxonomic units. *PeerJ* 3: e1487.
Wilson, D. 1995. Endophyte: the evolution of a term, and clarification of its use and definition. *Oikos*: 274-276.
Wilson, P. G. 1996. Myrtaceae in the Pacific, with special reference to *Metrosideros*. *The Origin and Evolution of the Pacific Island Biotas, New Guinea to Eastern Polynesia: Patterns and Processes*: 233-245.
Wright, S. 1943. Isolation by distance. *Genetics* 28 (2): 114-138.
Zahn, G. 2020. *gzahn/Ohia_Fungi: Metrosideros Endophyte Fungi.* Zenodo. https://doi.org/10.5281/zenodo.3666815
Zareb, A., Smail-Saadoun, N., and Rezki-Sekhi, L. 2016. Endophytic fungi of leaf of Atlas pistachio of Dayate Aiat (Laghouat, Algeria). In *Options Méditerranéennes. Series A: Mediterranean Seminars*. ENA, École Nationale d'Agriculture de Meknès (Morocco); CIHEAM-IAMZ, Zaragoza (Spain); Ministry of Agriculture and Fisheries of the Kingdom of Morocco.
Zhou, D., and Hyde, K. D. 2001. Host-specificity, host-exclusivity, and host-recurrence in saprobic fungi. *Mycological Research* 105 (12): 1449-1457.
Zimmerman, N. B., and Vitousek, P. M. 2012. Fungal endophyte communities reflect environmental structuring across a Hawaiian landscape. *Proceedings of the National Academy of Sciences* 109 (32): 13022-13027.